Functional characterization of the three isoforms of Fbw7 (F-box and WD repeat domain containing 7) in ubiquitin dependent proteolysis

A DISSERTATION
SUBMITTED TO THE FACULTY OF THE GRADUATE SCHOOL
OF THE UNIVERSITY OF MINNESOTA
BY

Wei Zhang

IN PARTIAL FULFILLMENT OF THE REQUIREMENTS
FOR THE DEGREE OF DOCTOR OF PHILOSOPHY

Advisor:

Dr. Deanna Koepp

January 2010

ACKNOWLEDGEMENTS

My graduate study at University of Minnesota is rewarding. I would like to thank many people who have helped me to conquer the difficulties and lead me to be a scientist.

First, I would like to thank my advisor, Dr. Deanna Koepp, for her long time support and encouragement. It is her that guides me to the scientific world, so that I am able to experience the beauty of science. All of these would be impossible without her.

I also want to thank my current and previous thesis committee, Dr. Deb Ferrington, Dr. Nik Somia, Dr. Tom Neufeld, Dr. Lorene Lanier, Dr. Ross Johnson, and Dr. Kylie Walters for their continuous support for years.

I am very grateful for the help from the people of Koepp lab. Andrew Kile, my classmate, has always been a good source to talk to. Dong-Hwan Kim, a junior student in the lab, has kindly shared his remarkable scientific knowledge with me; some of communications with Dong-Hwan really inspired me to rethink my experiment from different angles. I would like to thank Chi Meng Fong, another junior student, for his unselfish contribution of the information on bakery stores and Asian restaurants. I have also learned a lot from Allison Ritter, junior scientist in the lab, on English and the American culture. I really need to thank Elithebeth Macdonald, who helped to perform a yeast two hybrid screen when she was an undergraduate student in the lab, and the protein she pulled out from the screen established the second part of my graduate study. I would also like to thank Swarna Swaminathan,

previous research associate in the lab, for her effort to make the lab like a team and I really cherish her friendship.

Many people outside the Koepp lab have also supported me for many years. Dr Sean Conner and people in his lab have been wonderful neighbors. People from Dr. Kylie Walters lab, especially my friend Fen Liu, unselfishly shared the reagents and equipments. I also want to thank my friends Shan Zhou, Erika Sorensen, Priah Nadarajan and Amaranath Govindan and people in the ubiquitin proteasome community.

I want to give my special thanks to Dr. Xuelin Wang, not only because he is always available for scientific discussion and technique support, but also because of his long time encouragement and friendship.

Finally, I want to thank my family for their endless love. They always inspire me to explore and discover the excitement of the world.

ABSTRACT

Fbw7 is the F-box protein of SCF^{Fbw7} E3 ubiquitin ligase, which specifically associates with the substrates to be ubiquitinated. Substrates of Fbw7 play important roles in cell cycle regulation, proliferation, signal transduction and metabolism, which are related to tumor formation, suggesting that Fbw7 functions as a tumor suppressor.

Fbw7 has three splicing variants α, β and γ, and the biological function of each isoform is not well understood. Our lab is interested in how the Fbw7 isoforms regulate cyclin E proteolysis and the cell cycle. By using mammalian and insect cell culture systems, I demonstrate that the three isoforms can form homo- and hetero-dimers in vivo and in vitro. The dimerization domain is located immediately upstream of the F-box motif, and it is highly conserved in all Fbw7 homologues and other related F-box proteins, indicating the dimerization may be common feature of a subset of F-box proteins. Abolishment of dimerization inhibits cyclin E proteolysis and leads to a prolonged half-life of cyclin E, although it does not affect Fbw7 binding to cyclin E or to the Cul-Rbx1-Skp1 E3 catalytic module. Cyclin E accumulation can be commonly found in many primary tumors and cancer cell lines. These results suggest a novel mechanism of how F-box proteins recognize their substrates.

Fbw7 isoforms show different protein stabilities, where the α isoform is stable, but the β and γ isoforms are not. The stability of the β and γ isoforms is largely controlled by their N- terminal unique region. In order to better understand the mechanism regulating their stability, we performed a yeast two hybrid screen and identified SLP1

(stomatin like protein 1) as an Fbw7γ isoform specific interacting protein. SLP1 binds to the unique region of γ isoform, and stabilizes γ. We find that Cdk2 promotes the degradation of both SLP1 and the γ isoform, and this function of Cdk2 is dependent on its kinase activity. SLP1 also physically interacts with Cdk2 through its membrane association domain. These results support a model in which Fbw7γ and SLP1 are coordinately targeted for ubiquitin mediated degradation by Cdk2.

TABLE OF CONTENT

LIST OF TABLES

LIST OF FIGURES

CLARIFICATION OF CONTRIBUTIONS

My thesis work includes the contribution of my advisor and colleagues. I would like to list their contributions in detail.

Chapter 2

Deanna Koepp helped me to generate Fbw7α ΔD and Fbw7ΔN constructs. Wei Zhang generated most the other constructs, virus, reagents, and preformed all the experiments.

Chapter 3

Elizabeth MacDonald performed a yeast 2 hybrid screen with the instruction from Deanna, and she identified SLP1 as an Fbw7γ specific interaction protein. Wei Zhang designed and preformed the rest of the experiments.

Chapter I:

Introduction

1. **Ubiquitin, E1 and E2**.

The ubiquitin proteasome system (UPS) is the most important proteolytic system regulating intracellular protein degradation. It is a highly conserved process found in single eukaryotic cells like *Saccharomyces Cerevisiae*, to complex organisms like humans. It functions in almost every aspect of cellular life, such as cell cycle control, apoptosis, inflammation, transcription, signal transduction, protein quality control, and many other biological processes. Although it is a complicated system, the ubiquitination process requires two major steps: 1), a polyubiquitin chain is attached to a selective protein substrate, 2) this polyubiquitinatd substrate is recognized and degraded by the 26S proteasome. The major components of UPS include ubiquitin; E1, E2, E3 enzymes and the 26S proteasome (Figure 1.1, see p41).

1.1. Ubiquitin:

Ubiquitin is a highly conserved 76 amino acid protein that exists in all eukaryotic cells. Ubiquitination is an important post translational modification. With the help from E1, E2 and E3 enzymes, one (mono ubiquitination) or more ubiquitin (polyubiquitination) molecules can be covalently attached to a lysine residue of a protein substrate. Usually, mono ubiquitination functions in protein traffic and signal transduction, and polyubiquitination functions in protein proteolysis.

1.2. E1, ubiquitin activation enzyme

There is only a single E1 in most organisms, and E1 activates the entire ubiquitination cascade [1, 2]. There may be more than one E1 in human: in addition to

the classic E1 (Ube1), another divergent E1 (Uba6) has been identified in 2007, which specifically activates ubiquitin but not other ubiquitin like proteins [3]. Chemically, the exact mechanism of how E1 works is well understood: E1 associates with ubiquitin and catalyzes the adenylation of the carboxyl terminus of ubiquitin in an ATP dependent manner. E1 forms a thioester between its conserved catalytic cysteine and the ubiquitin. This E1-ubiquitin thioester complex recruits a selective E2 and transfer the thioester-linked ubiquitin to a conserved E2 cysteine. The E1-ubiquitin complex formation is important because E2 shows very low affinity to free E1 and free ubiquitin [4, 5]. E2 in turn recruits a specific E3 to continue ubiquitin transfer. Eventually, an isopeptide linkage will be generated between the activated carboxyl terminus of ubiquitin and the amino group of a lysine residue on a substrate or the previous ubiquitin of a polyubiquitin chain [4]. The crystal structure of *S. cerevisiae* E1 was resolved in 2008, revealing that the C terminus ubiquitin fold domain and the catalytic cysteine of E1 are important for binding to E2 [6].

1.3. E2, ubiquitin conjugation enzyme:

There are 13 E2s in budding yeast and at least 38 E2s in human [7]. Since there are a large number of E3s (up to hundreds), each E2 may serve for many E3s. Therefore, their biological functions depend upon which E3 or E3s they bind. The structure of E2 family is well characterized: all E2s share a conserved ubiquitin conjugating (UBC) core domain, where the catalytic cysteine residue resides. The highly conserved residues surrounding the catalytic cysteine are either important for binding to ubiquitin or to E1 [8-10]. Recently, some studies suggest E2 has more

important functions than just as an ubiquitin carrier. It is actively involved in 1) switching from ubiquitin initiation to elongation; 2) controlling the processivity of ubiquitin chain formation; and 3) selecting the correct linkage.

2. E3 ubiquitin ligase

2.1. The basic functions of E3:

E3s provide the substrate specificity to the entire ubiquitin system, because they physically interact with their specific substrates. The basic function of an E3 is clear: it must bind to the substrate and catalyze or facilitate the covalent bond formation between substrate and ubiquitin molecule. An individual E3 may be further involved in ubiquitin chain elongation, an example of this is E3α [11]. However, in some cases, the ubiquitin chain elongation is catalyzed by separate E2/E3s, which provides for additional regulation possibilities in the ubiquitination system [12-14].

2.1.1. The selection of ubiquitination sites:

Once E3s associate with their specific substrate, how do they choose which lysine residue(s) to start the ubiquitin transfer? Studies based on the single lysine to arginine mutation of c-Jun, T-cell receptor subunit, and encephalomyocarditis (EMC) virus3C protease show that most E3s are not selective in terms of which lysine to ubiquitinate [15-17].

2.1.2. The processivity of a poly-ubiquitin chain:

Once a lysine residue of a given protein substrate is ubiquitinated by a given E3, does this E3 continue to ubiquitinate other lysines or does it stick to the same lysine to form a polyubiquitin chain? Since the polyubiquitin chain is the signal targeting the substrate to the proteasome, the processivity of subsequent polyubiquitin chain assembly is particularly important. In addition, the deubiquitination enzymes (DUBs) can disassemble ubiquitin chain from the distal end before the substrate reaches the proteasome. In order to attach a poly ubiquitin chain on a single lysine but not mono ubiquitin on numerous lysines, usually the ligation of the first ubiquitin molecule to the first lysine will inhibit the further ubiquitination of the other lysines within the same substrate.

2.1.3. The ubiquitination signal:

Most ubiquitin signals are short protein sequences in a protein substrate. The first ubiquitination signal, the Destruction box (D-box), was identified in mitotic cyclin [18]. Within the destruction box sequence, RXALGXIXN, alanine and leucine are the residues determining specificity [18, 19]. Synthetic D-box peptide can partially inhibit substrate ubiquitination, suggesting the D box need not be in a fixed conformation to be recognized by its E3. However, the optimal binding between substrate and E3s may require a specific conformation [20].

2.1.4. The different lysine linkage of polyubiquitin chain

Ubiquitin is a 76 amino acid small protein, containing 7 lysine residues (Lys6, Lys11, Lys27, Lys29, Lys33, Lys48 and Lys63). Polyubiquitin chains can be formed by using different lysine of ubiquitin. For example, K48 polyubiquitin chain is formed through

lysine on position 48 of the ubiquitin molecule. Different ubiquitin linkages result in various conformations of ubiquitin chain, providing diverse biological functions. Among these polyubiquitin linkages, K48 and K63 are most well known.

K48 polyubiquitin chain: K48 is the major form of polyubiquitin linkage that will target protein substrates for degradation.

K63 polyubiquitin chain: K63 polyubiquitin linkage is most functioning in signal transduction, especially of NF-κB pathway; receptor endocytosis; vascular sorting and DNA repair processes (reviewed by [21-23]).

More than 120 E3s had been identified in humans, and more than 700 in plants. Despite their structural and functional diversity, they can be classified into two big groups: HECT domain E3s and RING E3s[24].

3. HECT domain E3 ligase family

A key feature of the HECT ligases is a conserved Cys residue that forms an intermediate thioester bond with the ubiquitin molecule before they catalyze substrate ubiquitination. In other words, the HECT ligases are physically involved in ubiquitin transfer. By contrast, RING E3s usually hold an E2 at one end and facilitate the transfer of ubiquitin from E2 directly to substrates.

About 5% of known E3s belong to HECT E3 family [25]. The first identified HECT E3 is E6-AP (E6 Associated Protein), which functions together with human papillomavirus (HPV) gene product E6, to specifically destabilize p53[26]. The C

terminus of E6-AP shows 35-45% similarity to numerous proteins in the database [27]. This -350 amino acid long C terminal region is named HECT domain (Homologous to E6-AP Carboxyl Terminus).

Studies suggest that all HECT E3s share a similar mechanism to catalyze ubiquitination: they use their N-terminal unique region to interact with specific substrates, and C-terminal HECT domain to mediate E2 binding and ubiquitination. Since the conserved HECT domain is responsible for E2 binding, most HECT ligases work with the same E2s, UbcH7 and UbcH8 [28-30]. Based on their diverse N-terminal domains, the 28 human HECT E3s can be divided into three sub-groups: the Nedd4 family (9 members), the HERC family (6 members) and other HECTs (13 members)[31].

3.1. Nedd4 family

The N-termini of Nedd4 family proteins contain C2 domain and two or four WW domains. Nedd4 HECT E3 family includes nine proteins: Nedd4 (also known as Nedd4-1), Nedd4L (also known as Nedd4-2), Itch, WWP1, WWP2, Smurf1, Smurf2, Nedl1 (also known as Hecw1) and Nedl2 (also known as Hecw2). Seven of the Nedd4 family proteins function in regulating key signaling pathways. For example, Itch, following T cell activation, is activated by phosphorylation, and then targets transcription factors Jun-b and Jun for ubiquitin mediated degradation [32]. Smurf1 and Smurf2 antagonize TGF-β signaling by targeting either TGF-β receptor or Smads for degradation [33]. Nedd4 HECT E3s also function in protein trafficking and viral budding [34-39].

3.2. HERC family

HERC family includes 6 proteins. The-N termini of HERC family proteins contain one or more RCC1 (Regulator of Chromosome Condensation 1)-Like domains (RLD). HERC1 is localized at the Golgi apparatus and vesicular membranes, and it binds to ARF1 (ADP ribosylation factor 1) and the small G protein Rab, suggesting it functions in membrane trafficking [40].

3.3. Other HECT E3s

The 13 protein members in this family have various multiple function domains in their N termini. For example, HUWE1 processes both WWE domain and Ubiquitin association domain (UBA). HUWE1 is responsible for several substrates involved in cell proliferation and transformation. Recent study suggests that HUWE1 targets N-Myc for degradation [41]. Moreover, a recent report proposed that small specific mutations in HUWE1 are associated with X-linked mental retardation [42]. The well known HECT E3 E6-AP binds to HPV gene product E6, and E6/E6-AP complex will target tumor suppressor p53 for degradation HPV infection [26].

4. RING E3 ligase family

Most E3 ligases belong to the RING E3 ligase family. The key feature of RING finger E3s is a series of histidine and cysteine residues with a characteristic space that allows 2 zinc ions to form a “cross-brace” structure, and this structure is called RING (Really Interesting New Gene) finger. Based on sequence homology research, there

are potentially 616 RING finger proteins in humans. However, it is still unclear if all of the RING finger proteins function as E3s. The canonical RING sequence is Cys-X_2-Cys-$X_{(9-39)}$-Cys-$X_{(1-3)}$-His-$X_{(2-3)}$-Cys-X_2-Cys-$X_{(4-48)}$-Cys-X_2-Cys (where X is any amino acid, and number indicates how many amino acids could be in between the key cysteine and histidine residues). It is well accepted that RING fingers function as scaffolds to bring other proteins spatially close, because 1) the zinc ions and their ligands are catalytically inactive; 2) it is the spacing of zinc ligands but not any primary sequence that is highly conserved in this family [43]. Although there are hundreds of RING finger E3s, they can be grouped in two families: 1) single subunit RING E3s, the single RING E3 functions together with E2 is sufficient to ubiquitinate substrates; 2) multiple subunits RING E3s, in which case the RING protein is a subunit of a protein complex, but it needs adaptor protein to bind substrates [44-47].

4.1 The basic function of RING finger

RING finger proteins bind to E2 and perhaps activate E2, just like HECT E3s use their HECT domain to bind E2s. This key principle was first identified from RING finger protein Rbx1 and its E2 UbcH7 [48, 49]. However, E2-E3 binding affinity shows poor correlation with its ubiquitination activity. Some active E2-E3 pairs have a relatively low binding affinity. On the other hand, some E3s are inactive when they stably bind to E2 [50, 51]. This can be explained by the dynamic interaction between E2 and E3. Since E2s use the overlapping sequence to bind E1 and E3, they have to disassociate from E3s in order to bind E1 to recharge with new ubiquitin molecule. Therefore, it can be difficult to detect by conventional method such as co-immuno-

precipitation which includes many washing steps. As to the ubiquitin transfer, it is thought that RING E3s catalyze ubiquitin transfer directly from E2-ub to their substrates, ubiquitin need not to form a transient bond with RING E3s. But how does this happen exactly? Although they are still in debate, some independent studies suggest that RING E3s can induce a critical conformational change of E2-ub, and largely accelerate the E2-ub disassociation. For example, when E2 Cdc34 is fused with its substrate Sic1, the basal autoubiquitination rate is low. However, when Cdc34 binds to RING containing SCF E3, the autoubiquitination of Sic1 is largely increased [52].

As discussed above in the E2 part, the initial ubiquitination and ubiquitin chain elongation are separate steps. The ubiquitin chain initiation, attaching the first ubiquitin to one of the lysine residues on substrate, is sequence non selective and slow. Which lysine on the substrate will be ubiquitinated is largely dependent on the accessibility rather than primary sequence [53, 54]. The ubiquitin chain elongation step, which more ubiquitin molecules will attached to one the first ubiquitin, is faster and selective. In the case of Cdc34, this step is up to 30 times faster than the first initiation step, and it is highly specific for lysine 48, but not the other 6 lysines, on ubiquitin [54]. Emerging evidence suggests that ubiquitin chain initiation and elongation could be the result of separate E2s [51].

4.2 Regulation of RING E3s:

Substrate phosphorylation: substrate phosphorylation is the most common and best understood mechanism. The first evidence of substrate phosphorylation emerged

from cell cycle regulator, Sic1. At late G1 phase of the cell cycle, Sic1 is phosphorylated by cyclin/Cdk complex at multiple sites, followed by ubiquitination and degradation. Only the phosphorylated form of Sic1, but not the unmodified form, is able to bind the E3 (SCF^{cdc4}) [55-58]. It is also true for Cdc4's human counterpart of SCF^{Fbw7} and its substrate cyclin E [59]. Indeed, the majority of cullin-RING E3 substrates are targeted to their respective ligase by phosphorylation.

E3 phosphorylation, The first example came from APC/C E3 ligase, which activity can be regulated by the phosphorylation of one of the core subunits complex. APC/C has two activators, cdh1 and cdc20. Phosphorylation dependent recruitment of cdc20 can increase the ligase activity, whereas cdh1 phosphorylation by mitotic cyclin/Cdk can inhibit the kinase activity [60-64].

E3 autoubiquitination, Many RING E3s (especially the multiple subunits E3s) can be regulated by an autoubiquitination mechanism. When these E3s bind to E2, ubiquitin can be transferred to E3s, and in turn, E3s are down-regulated because they are then destroyed by the proteasome. Autoubiquitination can serve as a homeostatic mechanism to keep E3 activity low and shield their substrates from inappropriate degradation [65, 66]. Interestingly, sometimes autoubiquitination may turn the ligase activity on, although the exact mechanism is unclear [67, 68].

Ubiquitin like modifiers: some ubiquitin like modifiers like Nedd8 can modify the cullin subunit of RING E3s. Based on the structural evidence of Cul5/Rbx1 complex, neddylation of cullin dramatically changes its conformation, and E2-ub is spatially closer to the substrate [69].

CAND1 regulation: CAND1 is a small protein that is able to bind cullins and

inhibit ubiquitin ligase activity (detail see cullin-RING E3).

Substrate competition, An unorthodox hypothesis was first proposed by Rape et al [70]. It was based on the observation that at metaphase/anaphase transition, APC/C substrates securin and cyclin B must be degraded before Aurora and polo like kinase 1. This particular temporal order is critical for ensuring the chromosome segregation and alignment in order. In an *in vitro* system, Rape et al demonstrate that the substrate with highest processivity will be degraded first, whereas the substrates with low processivity will have to shuttle on and off APC/C several times before they acquire a ubiquitin chain long enough to target them to the proteasome.

Small co-substrates, A novel RING E3 regulation mechanism was revealed by a recent study on the plant hormone auxin. Auxin fills in the small cavity between the F-box protein Tir1 and Tir1 substrates to ensure a stable binding [71]. The ability of an F-box protein to use a small molecule as a co-receptor to stabilize binding with substrates could be a general mechanism in signaling by plant hormones.

Accessory protein for substrate binding, Most F-box components in cullin-RING E3s are able to directly bind to their phosphorylated substrates. However, there are exceptions, such as F-box protein Skp2. The ubiquitination of Skp2 substrate p27 requires an accessory protein Cks1, which binds to Skp2. Phosphorylated p27 side chain can be recognized by Cks1, therefore the binding between F-box protein Skp2 and its substrate p27 is enhanced [72].

5. 26S proteasome

The proteasome is a 2.5 mega-Dalton multiple subunit protein complex existing in all eukaryotes. The name of 26S comes from the estimated sedimentation coefficient of the entire complex. 26S can be found in both cytoplasm and nucleus [73]. Its major function is to degrade unneeded proteins tagged with polyubiquitin chain. The 26S proteasome contains two major parts: the 28 subunit core particle (CP, 20S) and 19 subunit regulatory particle (RP, 19S, PA700). These two particles do not always associate with each other.

5.1 The 20S

20S is a cylinder or barrel like structure, whose 28 subunits are arranged in 4 stacked rings [74-76]. Both prokaryotes and eukaryotes contain 28 subunits in the 20S with different complexity: prokaryotes have 14 copies of two distinct polypeptides, whereas eukaryotes have 2 copies each of 7 distinct α type and 7 distinct β type polypeptides. The α subunits comprise the outer rings, and the β subunits the inner rings of the 20s proteasome [73, 77, 78]. The α subunits have some clear functions: 1) they help to construct the barrel like structure [79], 2) they control the access to the 20S chamber and [76] 3) they are the sites binding to the 19S, which regulates the proteolytic activities of the proteasome [80, 81]. The inner rings consist of the β subunits are the major proteolysis sites. 3 (β1, β2, β5) out of 7 β subunits contain active proteolytic sites. The proteolytic β subunits belong to the unusual N-terminal nucleophile (Ntn) hydrolase family. Each active site can cleave a broad range of peptide sequences. β1 prefers to cleave on the C-terminal side of acidic residues

(caspase-like); β2 after tryptic residues (trypsin-like), and β5 after hydrophobic residues (chymotrypsin-like) [82]. They carry out successive cleavage reactions to break the protein substrates into small peptides [83]. The proteasome does not degrade proteins to amino acids[84], but rather a mixture of small peptides with an average length of 8-11 amino acids [85]. In mammals, these peptides may be recycled as raw material for adaptive cell-mediated immunity.

5.2 The 19S

It is well accepted that free 20S itself cannot degrade ubiquitinated protein substrates without its regulatory partner, the 19S. The 19S regulatory particle is critical for substrate recognition, substrate unfolding and substrate translocation. The 19S contains about 19 subunits, which can be further divided into lid and base subassemblies [86]. The base includes 10 subunits and resides in between the 20S and the lid. 6 of 10 subunits are ATPases (Rpt proteins), facing the α subunits of the 20s. Upon activation, they will insert into the cavity of α subunits to form a holoenzyme [87-89]. The remaining 4 subunits are scaffolding proteins Rpn1, Rpn2, Rpn10 and Rpn13.

The regulatory function of the 19S resides in three aspects.

First, the 19S is controlling the substrate entry [87-93]. Since the proteolytic sites face the interior of the 20S, substrates must be able to access to this interior space of the 20S. The 19S first binds to the cylinder end of the 20S through the interaction between α subunits and Rpt proteins [94] and then opens a channel located at the cylinder end of the 20S. Next, the 19S is, in turn, opens its own substrate translocation

channel, which is connected to the channel opened earlier on the 20S.

Second, the 19S is unfolding substrates to facilitate their entry. The substrate translocation channel, even when open, is too narrow for the bulk substrates to get in [87, 90, 92, 95]. The size of the channel opening restricts the mistaken entry of cytoplasmic proteins, and imposes another constraint on true substrates: they must be unfolded before their translocation to the 20S. The protein-unfolding activity of the 19S is largely mediated by its six ATPase subunits (Rpt proteins), which are members of the AAA protease family [96-101].

Third, the 19S is mediating substrate recognition. Rpn10 and Rpn13 are two 19S subunits function in recognizing ubiquitin tagged substrates.

The lid subassembly of the 19S: Of the nine lid subunits, only Rpn11 has a known function. It is a deubiquitination enzyme (DUB), and this activity is critical for proteasome function in yeast and humans [102-105]. Proteasome substrates, before being degraded, are first separated from some or all attached ubiquitin molecules and this early step of degradation is mediated primarily by Rpn11.

6. The Cullin-RING finger ubiquitin ligase

RING E3s ligases are classified into two groups: the single subunit RING E3s, and the multiple subunits RING E3. Most of the multiple subunit RING E3s contain one cullin subunit, therefore they are named cullin dependent ligase (CDL). This model, that multiple subunit RINGs are assembled on Cullin scaffold was first

established by two groups in 1997 [55, 56]. So far, there are seven cullin proteins have been identified, they are Cul1, 2, 3, 4A, 4B, 5 and 7.

6.1 Structure of cullin-RING ligases:

Cul1 and presumably all other cullin proteins function as molecular scaffold. In the case of Cul1, it simultaneously interact with adaptor protein Skp1 (S-phase kinase associated protein 1) at its N-terminus and with the RING finger protein Rbx1 (also known as Roc1 or Roc2) at its C-terminus. Rbx1 recruits the E2 conjugation enzyme, and Skp1 binds to the F-box protein, which presents specific substrates to be ubiquitinated. The rigidity of the Cul1 N-terminus is critical for ubiquitin transfer, because a mutation increasing its flexibility destroys ligase activity in vitro [106].

Substrate adaptor for cullin-RING E3s: in the canonical example of SCF complex, Skp1 is the adaptor protein for Cul1[107], and Skp1 also interacts with Cul7 [108]. Other cullins may associate with different adaptor proteins: Cul2 and Cul5 associate with elongin C [109], Cul3 associates with BTB domain proteins [110-113]. Both elongin and BTB proteins show considerable homology to Skp1. However, it is not the case for Cul4A adapter DDB1 (DNA-damage binding protein1). It is not yet clear how DDB1 links substrate adaptor proteins to Cul4A [114-116] (Figure 1.2, p43).

Substrate receptors for Cullin-RING E3s: the key feature of Cullin-RING ligase is that one cullin-RING-adaptor catalytic core is able to associate with a large number of substrate receptor proteins. These receptor proteins refers to F-box containing proteins [117] or SOCS box (suppressor of cytokine signaling/elongin-BC) containing proteins, which specifically bind to Cul2 or Cul5 through adaptor protein elongin C

[118].

6.2 Special regulation of cullin-RING E3 ligases-Neddylation

Most mechanisms regulating other RING E3s are also applicable to Cullin-RING E3. Post translational modifications, especially phosphorylation, seem extend the spatial and temporal regulation to ubiquitin process.

However, the reversible cullin neddylation is unique to cullin-E3s. All the 7 cullin proteins identified so far can be modified by an ubiquitin-like protein, nedd8[119]. At least in Cul1, neddylation does not seem to need a nedd8 ligase, but nedd8 conjugation enzyme and the RING subunit are required [48]. Neddylation enhances cullin-RING E3 ubiquitination activity presumably by facilitating the recruitment of E2-ub [120]. Neddylation is reversible process, and the nedd8 attached to cullins can be removed by COP9 signalosome [121]. Neddylation is also negatively regulated by CAND1. CAND1 competes with Skp1 for binding to Cul1, and it can bind only to the unneddylated form of Cul1. The crystal structure of Nedd8-Cul5-Rbx1 solved last year provided new insights of how nedd8, CAND1 and cullin-RING assembly: the neddylation of cullin dramatically re-arranges the RIND domain on Rbx1 and WHB domain on Cul5, which result in the elimination of a CAND1-binding site and exposition of multiple potential catalytic sites to the E2-ubi. Therefore, neddylation positively regulates cullin-RING E3 ligase activity by functioning as a conformational switch, which is able to activate CAND1-bound closed architectures of cullins to dynamic, open forms to facilitate ubiquitin transfer [69].

7. SCF^{Fbw7} ubiquitin ligase and its substrates

SCF^{Fbw7} (Skp1-Cul1-F box protein, Fbw7) is a multiple subunit E3 ubiquitin ligase, which belongs to cullin-RING E3 family. It is one of the most extensively studied SCF complexes, and the elucidation of the composition, regulation and functions of SCF^{Fbw7} has really shed new light on understanding the entire ubiquitin proteasome system.

7.1 The structural architecture of SCF^{Fbw7}:

Among the 4 major subunits of SCF^{Fbw7}, Cul1 functions as a scaffold, simultaneously interacts with Skp1, and Rbx1 [55]. Adaptor protein Skp1, in turn interacts with substrate bind protein Fbw7 [117]. RING finger component Rbx1 recruits E2-ub to transfer ubiquitin to the substrates presented by Fbw7 [48]. Skp1, Cul1 and Rbx1 form the catalytic core of the complex [56] (Figure1.3, see p45). Since the catalytic core can recruit different F-box proteins, the F-box component is clarified by labeling its name via superscript. For example, Fbw7 is the F-box protein for SCF^{Fbw7} complex. This section will focus on the substrates of SCF^{Fbw7}.

7.2 The substrates of SCF^{Fbw7}:

Since the F-box protein is the component that physically interacts with substrates, the substrate specificity is determined by F-box protein. There are many critical substrates have been identified for SCF^{Fbw7}, including cyclin E, c-Myc, Notch (intracellular domain), c-Jun, c-Myb, SREBP1, mTOR, PGC-1α.

Cyclin E: in 1997, two groups reported that Cdc4p, together with Skp1 and Cdc53p, ubiquitinated Sic1 for degradation in a phosphorylation dependent manner [55, 122]. Sic1 is a cyclin dependent kinase inhibitor for B-type cyclins, and it prevents premature S phase entry [123]. It turns out that Fbw7 is the yeast homologue of Cdc4p, and it also functions in cell cycle regulation by degrading cyclin E at early S phase upon phosphorylation [59]. Cyclin E is a key cell cycle regulator, which is often mis-regulated in cancer [124]. Upon the association with cyclin E, Cdk2 (cyclin dependent kinase 2) is activated to trigger the downstream phosphorylation cascade, which is critical for G1 to S phase transition. Thus, cyclin E protein accumulation should be strictly restricted at this particular point of cell cycle to prevent Cdk2 mis-activation [125, 126]. The protein level of cyclin E is controlled by cell cycle regulated transcription and ubiquitination.

The study on cyclin E protein degradation had been intense. It was first solved by three independent groups in 2001[59, 127, 128]. Cyclin E-SCF^{Fbw7} association is controlled by multiple phosphorylations of cyclin E. Initial study suggested that Cyclin E is phosphorylated by Cdk2 at its C terminal threonine 380 (T380) by an autophosphorylation mechanism, then phosphorylated cyclin E binds to Fbw7 to be ubiquitinated. In addition to Cdk2, cyclin E also can be phosphorylated by another kinase, GSK3β (glycogen synthase kinase 3β), at this T380 site [129]. Moreover, within this T380 phospho-degron, there is another phosphorylation site has been identified at serine 384 (S384), which can only be phosphorylated by Cdk2 [129, 130]. S384 is critical for phospho-degron function, because it provides a negative charge at the +4 position to the central T380 residue. It is this +4 negative charge that directly

interacts with the WD40 domain of Fbw7, and it is conserved through all known Fbw7 substrates [58] (Table 1.1) However, mutation of Thr380 to alanine greatly reduced but did not eliminate Fbw7 binding, suggesting the existence of more phosphorylation sites within cyclin E. Subsequent study reveals that cyclin E also contains an N terminal phospho-degron, which is centered at threonine 62 (T62). Mutation of T62 abolishes the residual binding of T380A, but its role in Fbw7 binding seems secondary to T380 degron [128].

c-MYC: MYC protein belongs to MYC family of transcription factor, which has critical functions in mitogenic and cell growth responses[131]. SCF^{Fbw7} mediated ubiquitination of MYC starts from the phosphorylation of its N-terminal threonine (T58) by GSK3β, and its phosphorylation event is required for +4 serine (S62) phosphorylation of MYC mediated by MAPK (mitogen activated protein kinase) [132, 133]. Although MYC T58 degron is similar to cyclin E T380 degron, the +4 position negative charge may have a different meaning for MYC: S384 of cyclin E facilitate its binding to Fbw7, whereas S62 of MYC inhibits its binding [134]. Thus, except for priming T58 phosphorylation, the exact role of S62 for MYC degradation is still unclear.

JUN: JUN is another transcription factor, which can also be activated by many mitogens. As part of the AP1(activator protein1) transcription factor, JUN has a positive role in cell proliferation [135]. It is quite clear that $SCF^{Fbw7}$is the E3 ubiquitin ligase targeting phosphorylated JUN for degradation, but how JUN gets phosphorylated is still in debate. Early studies suggest that JNK (c-Jun NH2- terminal kinase) mediated phosphorylation of JUN protects it from degradation [136, 137].

However, more recent study suggests that JNK is the kinase that phosphorylates and enhances JUN degradation at least in neurons [138].

SREBP1: The sterol regulatory element binding protein (SREBP) family of transcription factors functions in cholesterol and lipid metabolism. This family contains three proteins: SREBP1a, SREBP1c and SREBP2. The nuclear forms of these proteins are highly unstable, and SCF^{Fbw7} is the E3 ligase that targets them for proteasome dependent degradation. The phosphorylation of SREBP1a is mediated by GSK3β at its C terminal degron, T436 and S430, which is consistent with the +4 negative charge pattern. The abolishment of Fbw7 can stabilize SREBP1 and result in increased expression of SREBP1 regulated genes [139, 140]. Interestingly, the association of SREBP1 to its target gene will enhance GSK binding to T436 and S430, suggesting that DNA binding could provide a trigger to phosphorylation and ubiquitination of transcription factors [140].

Notch: the Notch signaling regulates cell differentiation processes during embryonic and adult life. Proteins from Notch family (Notch 1-4 in mammals) are single transmembrane proteins localized at the cell membrane with a large extracellular domain and small intracellular domain. Upon ligand activation, the intracellular domain of Notch is cleaved by γ-secretase and then translocates to the nucleus to regulate downstream gene expression [141]. In 1997, Hubbard et al reported Sel-10 negatively regulated Lin12/Notch signaling pathway in *C. elegans* [142]. It turns out Sel-10 is the *C. elegans* homologue of Fbw7, and Fbw7 regulates the degradation of notch intracellular domain [143]. In Fbw7 deficient mice, the protein level of the intracellular domain of notch4 and notch1 is increased [144, 145].

The phospho- degron of notch1 was recently identified at T2512 at the C terminus [146, 147]. It is interesting that SCF^{Fbw7} has more than one substrate in the Notch signaling pathway. In addition to notch, MYC is a downstream target of notch1, and it has a key role in notch mediated leukemia [148-150]. Moreover, some studies also linked Fbw7 to the proteolysis of γ-secretase (presenilin), which is another important regulator of Notch signaling [151, 152].

Myb: myb is a transcription factor that activates the expression of more than eighty target genes. Thus, myb plays important roles in many aspects, including development, cell proliferation [153]. SCF^{Fbw7} has been identified as the E3 ligase that targeted myb for degradation. The phosphorylation of myb is mediated by GSK3β at T572, and the substitution of T572 to alanine largely stabilizes myb protein [154].

mTOR: mTOR (mammalian target of rapamycin) is an evolutionarily conserved kinase, which has emerged as a central mediator of cell growth and proliferation via the regulation of protein synthesis, and it is becoming a major target of therapeutic intervention [155]. Recently, Mao et al used Cdc4 phospho-degron sequence I/L-I/L/P-T-P-xxxx (where positive charged lysine and arginine are unfavorable in the x location) to search the mouse genome and they found that mTOR showed a strong match. In line with this finding, biochemical studies confirm that SCF^{Fbw7} is the E3 that targets mTOR for degradation. Since PTEN also regulates the mTOR pathway, they propose that Fbw7 cooperates with PTEN to regulate mTOR [156].

PGC-1α: Peroxisome proliferators-activated receptor γ (PPAR γ) co-activator-1α is a highly regulated transcription co-activator that functions in energy metabolism in mammals. Misregulation of PGC-1α is linked to the pathogenesis of diabetes, obesity

and neurological disorders [157]. Olsen et al reported that SCF^{Fbw7} regulates PGC-1α through ubiquitin pathway. PGC-1α needs to be phosphorylated by GSK3β and MAPK at each of its two phospho-degrons in order to bind Fbw7. Interestingly, they found in response to oxidative stress, Fbw7 protein in the neurons was decreased. It in turn leads to PGC-1α accumulation, which is important to activate the downstream genes to antagonize the stress. However, the underlying mechanism of Fbw7 down regulation under stress condition is still unclear [158]. It will be interesting to determine if Fbw7 protein level is high in the patients with Parkinson's disease, which is partially resulted from stress accumulation.

8. F-box protein: Fbw7 (F-box protein with WD40 repeats)

8.1 F-box proteins

The F-box sequence homology was initially identified in proteins which contain β-transducin repeats, such as Cdc4, β-TrCP, Met30 [159]. However, the sequence was not further characterized until the discovery of a novel Cdc4 suppressor protein, Skp1 [117]. At the same time, a yeast 2-hybrid screen searching for cyclin F-binding proteins identified the human Skp1 counterpart [160, 161]. Skp1 was found to be important for the stability of certain cell cycle-related proteins. Alignment of Skp1 interacting protein sequences by Elledge et al lead to the finding of this 40 amino acid motif, which is required for Skp1 binding. The term "F-box" was named after cyclin F, the first identified F box protein [117]. To date, there are at least 69 F-box proteins have been identified in humans, 74 in mouse, 26 in *Saccharomyces cerevisiae,* about

30 in *Drosophila*; more than 300 in *C. elegans* and more than 600 in *Arabidopsis*. In addition to F-box motif, F-box proteins contain separate protein interaction motif for substrate binding, such as WD40 repeat and Leucine rich repeats. Based on the different substrate binding motifs, F-box proteins can be classified into three major groups: 1) Fbws, containing F box and WD40 repeats; 2) Fbls, containing F-box and Leucine rich repeats; 3) Fbxs, containing F-box and other unclassified motifs [162] (Figure1.4, see 47).

8.2 Fbw7 homologues and their substrates

Among the 68 human F-box proteins, Fbw7 is one of the best characterized. It is the substrate specificity determining component of SCF^{Fbw7} E3 ligase. In other words, the proteolysis of its substrates, including cyclin E and many key transcription factors (see above), is dependent on Fbw7. It is also a highly conserved protein, and its homologues show very similar regulatory functions, which further supports its critical function in biological processes.

8.2.1 Cdc4 (*S. Cerevisiae* counterpart):

Cdc4 is the first known member of FBW7 gene family. It was identified by a screen for cell division mutants in budding yeast, and named Cdc4 (cell division cycle 4) there after [163]. It turns out that Cdc4 regulates cell cycle by targeting a cyclin-dependent kinase inhibitor, Sic1, for degradation in a phosphorylation dependent manner. Sic1 inhibits the cyclin dependent kinase Cdc28, which is critical for the G1 to S-phase transition of budding yeast. Mutation of Cdc4 or other components of the

ubiquitination pathway, such as Cdc34 (E2), results in Sic1 accumulation and in turn Cdc28 inhibition, thus cells are arrested in G1 [55, 122, 123]. Later, more Cdc4 substrates were identified, such as the transcription factor Gcn4[164], another CKI called Far1[165] , and the DNA replication initiation factor Cdc6[166, 167].

More importantly, the study of Cdc4 identified the Cdc4 phospho-degron, which is a conserved phospho-epitope residing in the Cdc4 substrates [59, 168]. Since this phospho-degron is highly conserved in all Cdc4/ Fbw7 substrates, it makes genome-wide screening for potential substrates possible.

8.2.2 **Sel-10** (*C. elegans* counterpart):

Sel-10 was initially identified as a negative regulator of Lin-12/Notch signaling pathway in *C. elegans*, because of its function of targeting Lin-12 for ubiquitin mediated degradation. Then sequence analysis suggested that that Sel-10 was Cdc4 homologue, and it could potentially have human and mouse homologues, which leads to the finding of Fbw7 and mouse Fbw7 [169]. Recently, Sel-10 was found to regulating synapse elimination of certain neurons in *C. elegans* [170].

8.2.3 **Ago** (*Drosophila* counterpart):

Ago is the *Drosophila* counterpart of Fbw7, and it also regulates cyclin E, as Fbw7 does in human, in *Drosophila*. Ago depleted cells had high level of cyclin E protein, which leads to over proliferation [127]. Since then, there are two more Ago substrates have been identified: Trh and Gcm. Trh (Trachealess) is a transcription factor has many known targets in tracheal development. By targeting Trh for ubiquitin mediated degradation, ago shows a novel function in trachea morphogenesis [171].

Gcm (glial cell missing) is a glial regulatory protein, which promotes glial differentiation at early embryonic development. Gcm can be targeted for degradation by two F-box proteins, ago and slimb. In the two F-box proteins double knockout strain, Gcm protein level increases, leading to excess glial progenies [172].

8.3 Mouse model:

Fbw7-deficient mice die around day 11 of gestation with manifest defects in vascular and hematopoietic development [144, 145]. These phenotypes could mainly be due to increased Notch protein and Notch signaling. Surprisingly, cyclin E levels in Fbw7 null embryos are not significantly increased, partially because of the negative feedback mechanism down regulating the mRNA level. Recently, conditional Fbw7 null mice have been generated, in which Fbw7 is deleted in only T cell lineages. Fbw7 deletion in haematopoietic stem cells resulted in hyperproliferation of immature T cells. Marrow transplant experiments revealed that Fbw7 null stem cells are defective in their long-term repopulation ability. Thus, Fbw7 may play a critical role in stem cell self-renewal. Interestingly, most of Fbw7 null mice developed leukemia, which cannot be explained by just the misregulation of MYC protein [173]. These results suggest that Fbw7 may have tissue specific substrates or it is regulated in a tissue specific manner.

8.4 Fbw7 and cancer

Fbw7 is located at position 4q32 in the human genome, which is found to be commonly absent in many human cancers [128, 174]. Because of the linkage between

excess cyclin E protein and cancer development, it was assumed that Fbw7 may function as a tumor suppressor through regulating cyclin E degradation. Since then, FBW7 has been intensively examined in primary tumors: around 6% of these tumors carry mutations in FBW7 gene [175-181]. Interestingly, the frequency of FBW7 mutation is variable depending on the tumor type. It is most frequently mutated in cholangiocarcinoma and T cell acute lymphoblastic leukemia (T-ALL) with a rate of about 30% [182], whereas in gastrointestinal and prostate and endometrial cancers its mutation rate is in range of 4-15%. Moreover, in many cancers FBW7 gene is intact or only shows very rare mutations. These cancers include the other kinds of leukemia other than T-ALL, cancers from the breast, lung, bladder, liver, ovary and bone [183-187]. The molecular basis that underlies this variation is still not clear. It is possible that the functions of Fbw7 are tissue specific, or Fbw7 itself is differentially regulated in tissues, or Fbw7 plays a more profound role in regulating early stage of development.

Since most Fbw7 abnormal tumors carry heterozygous Fbw7 mutations or deletions, Fbw7 was considered as a haploinsufficient tumor suppressor, which means loss of a single allele promotes tumorigenesis. This idea was supported by studies in Fbw7 heterozygous mice in p53+/- background. These mice showed greater susceptibility to radiation induced tumorigenesis, but most tumors still retained and expressed the wild type allele [188]. However, in wild type background, Fbw7 heterozygous mice seemed relatively normal and the conditional deletion of one allele in T cells did not induce lymphomagenesis [144, 145, 173]. Recent finding on Fbw7 dimerization suggests that Fbw7 may have dominant negative effect rather than

simple loss of function (for detail see discussion)

8.5 Mechanisms of FBW7 associated oncogenesis

FBW7 has been established as a tumor suppressor, but the clear mechanisms that link loss of FBW7 to tumor development is still under study, partially because Fbw7 has more than one oncogenic substrates. Among these oncogenic substrates, increased cyclin E activity receives more attention in Fbw7 associated tumors [189, 190]. Indeed, targeted disruption of FBW7 in cultured cells was found to induce genetic instability, and that can be suppressed when cyclin E was knocked down by RNAi, suggesting cyclin E as an effector of FBW7 associated genomic instability in this system. Moreover, cyclin E T380 mutant, which binds Fbw7 less efficiently, causes more severe genetic instability than the wildtype cyclin E, further indicating that Fbw7 restrains cyclin E induced genetic instability in this cell line [191].

9. Ubiquitin proteasome system and cell cycle

9.1. Cell cycle

Cell cycle is a process of division allowing the duplication of cells, and it is an essential mechanism by which all living organism reproduce. The most basic function of cell cycle is to duplicate the large amount of DNA, located in the chromosomes, and then precisely segregate the copies into two identical daughter cells. Cell cycle consists of four phases: G1, S, G2 and M. DNA synthesis occurs in S phase (synthesis), and chromosome segregation and cell division happens in M phase

(Mitosis). The two gap phases, G1 and G2, provide extra time for cell to check if the environment is suitable or the synthesis is complete before cell get into M phase or S phase.

Cell cycle is a uni-directional process, which means the transitions between cell cycle phases must be irreversible in order to generate this forward progression. This driving force largely depends on the strict regulation on activation and deactivation or proteolysis of the cell cycle regulators.

In general, the cell cycle regulator refers to Cyclin Dependent Kinase (Cdk) and their activating subunits cyclins or their inhibiting subunits CKIs (Cyclin dependent Kinase Inhibitor). Upon the cyclin activation, the activated Cdks will initiate phosphorylation cascades, which are required for the cell cycle transition. Since most Cdk proteins remain stable through the cell cycle, therefore, the regulation of cyclins and CKIs are essential for maintaining the cell cycle.

Cell cycle phase transitions tend to be rapid and concerted in order to prevent cells from straddling two distinct phases. Since the transitions are based on the rapid activation of Cdks, the processes of cyclin accumulation and CKI proteolysis must be coincident and rapid as well. In addition to transcriptional regulation, ubiquitin mediated proteolysis plays a central role in deactivating these regulators at proper time and place.

Cyclin B was the first cell cycle regulator that was found to be targeted for degradation by the UPS in 1991 [18]. Since then, many new players have been added to the list over time. Although the number of these regulators is adding up, all of them are ubiquitinated and degraded by two types of ubiquitin ligases: the SCF E3 ligases

and the APC/C E3 ligases. However, the strategies they use for substrate ubiquitination is different. As discussed above, the SCF E3 ligases use “activating the substrate strategy”, which requires proper phosphorylation to activate the substrate. The APC/C E3 ligases, on the other hand, use “activating the ligase strategy”, which means the ubiquitinaiton of the substrates is largely depending on the E3 activation.

9.2. APC/C (anaphase promoting complex/cyclosome)

APC is a large multiple subunits E3 ligase, which also belongs to cullin-RING E3 family. APC is composed of at least 13 core subunits and is activated by either of two weakly associating subunits Cdc20 or Cdh1[192]. Just like F box proteins in the SCF complexes, Cdc20 and Cdh1 are also determining the substrate specificity of APC by physically interacting with their substrates through the C-terminal WD40 repeat domain [193, 194]. Thus, the activity of APC is largely regulated by Cdc20 and Cdh1.

Cdc20 is synthesized in M phase and mainly functions in promoting metaphase-anaphase transition. Cdc20 itself is targeted for degradation by APC at the end of anaphase after its function has been carried out [195]. Cdh1, on the other hand, is expressed constantly and its activity is negatively regulated by Cdk mediated phosphorylation. It is activated at the end of mitosis and remains active during G1 phase when Cdks activity is low [62, 196, 197]. The alternative activation of APC by Cdc20 and Cdh1constitutes a relay system, in which some cell cycle regulators are first degraded by APC^{Cdc20} to promote metaphase-anaphase transition, and then the same substrates and many others are continually degraded by APC^{Cdh1} to allow

mitotic exit as well as no accumulation in G1 phase.

9.3. The cell cycle regulators targeted by the UPS

There are numerous cell cycle regulators that are degraded by the UPS (Figure1.5, see p49), I will only highlight two here, which are most relevant to my graduate research. Cyclin E is a positive cell cycle regulator that promotes G1-S phase transition by activating Cdk2. In the contrast, P27 is a negative regulator that arrests cell cycle by inhibiting Cdk2.

Cyclin E: progression through cell cycle needs a large number of proteins to function together. Many of these proteins are needed on a temporal base: once they finish their tasks, they need to be degraded. Cyclins are activating subunits of the cyclin/Cdk complex. Cyclin E promotes G1-S phase transition by binding and activating its catalytic partner Cdk2. Upon on the activation, Cdk2 triggers a phosphorylation cascade, which is required for chromosomal replication [126, 198]. Thus, the accumulation of cyclin E needs to be restricted at this time window of the cell cycle. Its restriction of cyclin E/Cdk2 complex is accomplished by periodic transcription [199] and degradation of cyclin E subunit, because Cdk2 protein constantly presents throughout the cell cycle [200, 201]. As discussed above, the proteolysis of cyclin E is mediated by SCF^{Fbw7} E3 ligase, which is triggered by cyclin E phosphorylation by Cdk2 and GSK3β. The persistence of cyclin E, which is due to either increased cyclin E transcription or SCF^{Fbw7} misregulation, will interfere with the processes that are essential for genomic integrity [190]. Many primary tumors that

carry FBW7 mutations show increased cyclin E level.

P27 (Kip1): is one of the best characterized CKIs. It regulates G0-S phase transition by binding to and regulating the activity of Cdk2 [202, 203]. In the presence of p27, Cdk2 is inactive even when it binds to cyclin E. P27 protein accumulates at G0 and early G1, when it tightly binds and inhibits Cdk2/cyclin E activity. As cell cycle progress, p27 gets phosphorylated by oncogenic kinase Src, and this phosphorylation largely reduces p27's ability of Cdk2 inhibition. More importantly, it triggers the transformation of p27 from Cdk2/cyclin E inhibitor to their substrate [204]. The phosphorylation of p27 at threonine 187 by Cdk2/cyclin E leads to its ubiquitin mediated degradation by $SCF^{\beta\text{-}TrCP}$ [205]. Moreover, the ubiquitination of p27 requires an accessory protein Cks1 (Cdk subunit 1), which binds to Skp2 and enhances the affinity between phosphorylated p27 and Skp2 [206, 207].

10. The three isoforms of Fbw7

Human Fbw7 has three isoforms α, β, and γ, which result from differential mRNA splicing. The mRNA of each isoform has distinct first exon, but the rest of the sequence is identical [174] (Figure 1.6, see p51). Each isoform has a distinct promoter, allowing differential expression pattern. Earlier studies found that the three isoforms of Fbw7 had some interesting difference in terms of tissue and subcellular localization, expression pattern, protein levels [208, 209].

10.1 The expression pattern of Fbw7 isoforms

The 5.5Kb mRNA of α isoform can be detected in all the tissues analyzed, with a relatively high abundance compared to the other two isoforms, and the mRNA level of α isoform is stable through the cell cycle. The 4Kb mRNA representing β and γ isoforms is less abundant in most tissues except for muscle, brain and heart [174]. Recently, more precise quantitative measurement of the mRNA suggests that the mRNA of α isoform is between 8 and 50 fold more abundant than β isoform and 67-135 fold more abundant than γ [210].

10.2 Subcellular localization of Fbw7 isoforms

The first report of the localization of Fbw7 isoforms came from the Harper group, and they observed that α and γ isoforms were localized to the nucleus whereas β isoform was cytoplasmic, when tagged versions of the three isoforms were overexpressed in 293T cells [130]. Later, the Clurman group observed a distinct subcellular localization pattern of the three isoforms; α is nuclear, β is cytoplasmic, which is consistent with the previous report. However, they observed a predominantly nucleolar localization of γ, by using an adenovirus overexpressing system in U2OS cells[209]. Our observation of the localization is consistent with the Harper group; we detect minimal exclusive nucleolar localization of γ isoform. The discrepancy among the observations could be due to protein overexpression or differences in cell lines. Since there is no isoform specific antibody available, the subcellular localization of the isoform is still inconclusive. The study of subcellular localization of each isoform is critical for understanding its function. For example, if γ isoform is exclusively localized to the nucleolus, it may suggest the γ isoform has nucleolar substrates.

10.3 The known function of Fbw7 isoforms

10.3.1 Fbw7-α isoform

Since it is the most abundant and stable isoform of Fbw7, it is thought that α isoform contributes the most to the substrate degradation. A paper published on 2006 suggests that α and γ isoforms function together to target cyclin E for degradation [211]. Cyclin E is stabilized by siRNA knockdown of these two isoforms. In both *in vitro* and *in vivo* systems, cyclin E can only be efficiently ubiquitinated in presence of both isoforms. Interestingly, they find that the γ isoform is the major isoform to target cyclin E for ubiquitination, whereas the α isoform is required for Pin1 dependent isomerization of cyclin E prior to its ubiquitination. This Pin1 dependent isomerization of cyclin E P382 is required for its multiubiquitination by SCF^{Fbw7}. In the context of human cells, α isoform is responsible for potentiating Pin1 isomerase activity, but cannot efficiently ubiquitinate cyclin E itself. The strong evidence supporting this hypothesis comes from a mutated form of Fbw7-α (Fbw7D124Y), which is derived from a cancer where cyclin E level is increased. Fbw7-αD124Y specifically cannot bind Pin1, but can still form a functional SCF complex and ubiquitinate cyclin E P382I, a mutated form of cyclin E which does not need isomerization by α. These data suggest that major function of the α isoform is to bind the Pin1/cyclin E complex and potentiate Pin1 to isomerize cyclin E at proline 382. Isomerization of cyclin E is required for its subsequent multiple phosphorylation, whereas the γ isoform is mainly functioning as an ubiquitin ligase. Therefore, efficient ubiquitination of cyclin E requires both Fbw7-α and Fbw7-γ isoforms [212].

Recently, the Clurman group generated Fbw7 isoform deficient cell lines by specific gene targeting. The unique exon of each isoform was disrupted and the protein levels of cyclin E, c-Myc and SREBP1 were individually measured [210]. They observed that the α isoform accounts for almost all Fbw7 activity in terms of promoting the degradation of cyclin E, c-Myc and SREBP1, although these results are not very well consistent with the previous ones [210]. The discrepancy on the requirement of γ isoform that the two groups observed could be due to the difference of cyclin E protein levels in these cell lines. It has been reported that in cell lines with high level of cyclin E the α isoform is sufficient for cyclin E proteolysis; however, and in cell lines with normal cyclin E level, both α and γ are required [213].

10.3.2 Fbw7-β isoform:

Fewer studies have been carried out on the β isoform, but it seems not very capable of facilitating the degradation of cyclin E and other substrates compared to the other two isoforms. It has been reported that the β isoform is dramatically up-regulated by the tumor suppressor p53 [214]. There is a potential p53 binding site upstream of the β isoform unique exon, and p53 is able to bind to this site [214]. Finally, the expression of β (but not α) isoform can be specifically induced in a p53-dependent manner [214]. These results suggest that the β isoform is a transcription target of p53, and p53 may negatively regulate cyclin E by affecting the β isoform [214]. However, since β is not the major isoform in terms of targeting cyclin E, why and how p53 regulates the β isoform is still unclear.

10.3.3 Fbw7-γ isoform:

In addition to its important function of targeting cyclin E for degradation, together with the α isoform (put in references), the γ isoform also has its own specific substrates and functions. Given it potentially nucleolar localization, the γ isoform may regulate some substrates in that particular compartment and c-Myc has been identified as one of these. In the condition of proteasome inhibition, nucleolar c-Myc is accumulated and specifically co-localized with the γ isoform [209]. Likewise, siRNA mediated γ inhibition leads to accumulation of endogenous c-Myc, and importantly, increases cell size, which is may be c-Myc dependent [209].

Recently, a paper has reported that nucleophosmin (NPM) a molecular chaperone, regulates Fbw7-γ isoform stability in the nucleolus [215]. Nucleophosmin is nucleolar protein that shuttles between the nucleus and cytoplasm [216]. Mutations in the NPM gene occur in 35% of acute myelogenous leukemias (ALL) [217]. In NPM deletion cells, c-Myc protein is markedly increased without conspicuous change of its mRNA [215]. NPM specifically interacts with the γ isoform, and it is required for the nucleolar localization and stability of the γ isoform [215]. Interestingly, a ALL derived NPM mutant can no longer stabilize the γ isoform and leads to c-Myc accumulation, suggesting that NPM regulates c-Myc through regulating the stability of Fbw7-γ [215]. However the exact mechanism of how Fbw7 γ is regulated by NPM is still unclear.

SUMMARY

Given that Fbw7 plays such an important role in regulating cell cycle, transcription, cell proliferation, and all of which is related to tumor formation, it is critical to further dissect its function. My graduate research has been focused on the three splicing variants of Fbw7 and they show some interesting difference in terms of expression pattern, subcellular localization, whereas they do exist at the same cell lines. Although some studies have been carried out on these isoforms, there are many questions remain unanswered. We are interested in studying the function of these three isoforms, if they work cooperatively to degrade the same substrate at a time or if they have unique functions, such as specific substrates. We also interested in the regulation of the each isoforms and look forward to identify their upstream regulators.

In chapter 2, I will focus on how the three isoform function cooperatively targeting cyclin E for degradation. I found that the three isoforms can form either homo- or hetero- dimers *in vitro* and *in vivo* through the dimerization domain upstream of the F-box motif. Dimer formation showed no effect on Fbw7 interaction with the SCF catalytic core or wild-type cyclin E, and dimerization does not affect Fbw7 localization. However, abolishment of the dimerization could stabilize cyclin E, which suggests that F-box protein dimerization is another mechanism to regulate SCF E3 ligases and their substrates.

In chapter 3, I will focus on a novel Fbw7 γ isoform specific interacting protein, SLP1. SLP1 was pulled down from a yeast 2 hybrid screen using unique region as bait. SLP1 interacts with γ isoform in both nuclear and cytoplasm, and interestingly stabilizes γ isoform. We find that Cdk2 activity influences the turnover of both Fbw7-

γ and SLP1. Our studies support a model in which Fbw7-γ and SLP1 are coordinately targeted for ubiquitin-mediated degradation by Cdk2 kinase activity.

Table 1.1 Cdc4/Fbw7 phosphodegron

Protein name	Phosphorylation site	CPD
Mammals		
Cyclin E	T380	LL**T**PPQ**S**GK
	T62	IP**T**PDK**E**DD
MYC	T58	LP**T**PPL**S**PS
JUN	T239	GE**T**PPL**S**PI
SREBP 1	T456*	TL**T**PPP**S**DA
SV40 large T antigen	T701	PP**T**PPP**E**PE
Notch 1	T2512*	FL**T**PSP**E**SP
Presenilin 1	T116	IY**T**PFT**E**DT
Yeast		
Gcn4	T165	LP**T**PVL**E**DA
Far1	S87	PI**S**PPP**S**LK
Cdc6	T39	DV**T**PES**S**PE
	T368	PL**T**PTT**S**PV
Clb6	S6	IP**S**PIS**E**RK
	T39	NL**T**PHS**T**NE
Rum1	T58	PP**T**PAK**T**PK
Rcn1	S113	LI**S**PPA**S**PP

Human and most yeast CPDs (Cdc4 phospho-degrons) provide a negative charge in the +4 position, either through phosphorylation or glutamate. This position makes direct contacts with a conserved pocket in the WD40 repeats of Fbw7 and Cdc4. Exceptions to the +4 negative charge rule are most CPDs of Sic1 and those of Tec1, Hap1, Cdc18 and Cig2, all of which contain multiple low-affinity degrons (not shown). *Indicates the amino acid position in full-length proteins before processing.

Ref: Markus Welcker and Bruce E. Clurman, *Nat. Rev. Cancer*, 2007 Vol. 8: 83-93

Figure 1.1The ubiquitin system.

(a) Ubiquitin (Ub) and ubiquitin-like proteins are activated for transfer by E1(ubiquitin-activating enzyme).

(b) Activated ubiquitin is transferred in thioester linkage from the active-site cysteine of E1 to the active-site cysteine of an E2 ubiquitin-conjugating enzyme.

(c) The E2∼Ub thioester next interacts with an E3 ubiquitin ligase, which effects transfer of Ub from E2∼Ub to a lysine residue of a substrate. Mono-ubiquitinated substrate can either dissociate from E3

(d) or can acquire additional Ub modifications in the form of multiple single attachments (not shown) or a ubiquitin chain

(e) The chain can be knit together via different lysine residues of ubiquitin. Whereas mono-ubiquitin and some types of chains (e.g., those assembled via Lys63 of ubiquitin) serve mainly to alter the function of the modified protein

(f) (by changing its structure, binding partners, cellular localization, etc.), polyubiquitin chains assembled via the Lys48 residue of ubiquitin typically direct the appended substrate to the proteasome for degradation

(g). The biological outcome of ubiquitination−be it degradation or signaling−is normally dictated by ubiquitin receptors (UbR) that bind and interpret the ubiquitin signal.

Ref: Raymond J. Deshaies and Claudio AP Joazeiro. *Annu. Rev. Biochem*. 2009. 78:399–434

Fig1.1 the ubiquitin system

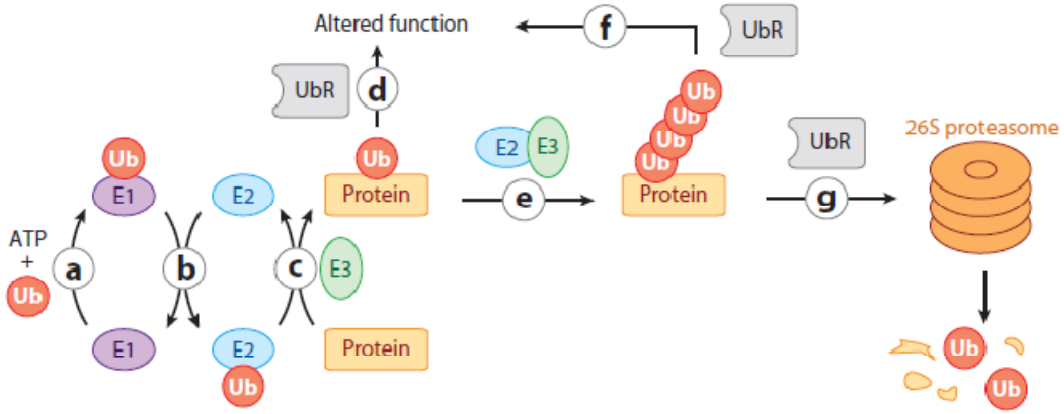

Ref: Raymond J. Deshaies and Claudio AP Joazeiro. *Annu. Rev. Biochem*. 2009. 78:399–434

Figure 1.2 The modularity of cullin–RING ligases

The common catalytic core of cullin–RING ligases (CRLs), which consists of a RING protein and a cullin-family member, defines this modular class of ubiquitin ligase. By analogy to the structure of the RING-H2 ubiquitin ligase CBL, the RING subunit of CRL enzymes is thought to function as the docking site for E2s.

a) CUL1 CRLs, which are known commonly as SKP1, CUL1, F-box (SCF) proteins, recruit substrates through the adaptor protein SKP1 and an F-box-protein substrate receptor.

b) CUL2 and CUL5 CRLs recruit substrates through an elongin-BC adaptor and a suppressor of cytokine signaling/elongin BC (SOCS/BC)-box-protein substrate receptor (labeled SOCS in the figure).

c) CUL3 CRLs recruit substrates through BTB-domain-containing substrate receptor proteins.

d) CUL4A CRLs might recruit substrates through the adaptor protein DNA damage-binding protein-1 (DDB1), which interacts with CUL4A using an unknown motif (highlighted by '?'), and through putative substrate-receptor complexes such as DET1–COP1.

Ref, Matthew D. Petroski and Raymond J.Deshaies. *Nat. Rev. Mol. Cell Biol.* 2005 Vol 6, 9-20

Figure 1.2 The modularity of cullin–RING ligases

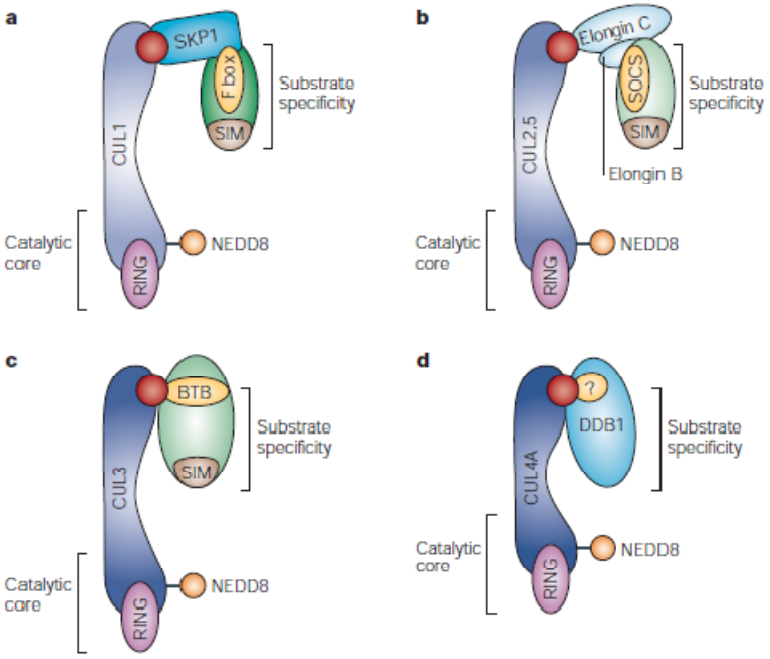

Ref, Matthew D. Petroski and Raymond J.Deshaies. *Nat. Rev. Mol. Cell Biol.* 2005 Vol 6, 9-20

Figure 1.3 the schematic of an SCF (Skp1, Cul1, Rbx1 and F box protein) ligase

The SKP1(S-phase kinase-associated protein 1)-CUL1 (cullin 1)-RBX1 (RING box 1) core complex recruits substrates through interchangeable substrate-specific F-box proteins. RBX1 binds to the E2 (UBC) that was previously charged with ubiquitin (Ub) by an E1 ubiquitin-activating enzyme (UBA). Polyubiquitinated substrates are then targeted for destruction by the proteasome.

Ref, Markus Welcker and Bruce E. Clurman, *Nat. Rev. Cancer*, 2007 Vol. 8: 83-93

Figure 1.3 the schematic of an SCF (Skp1, Cul1, Rbx1 and F box protein) ligase

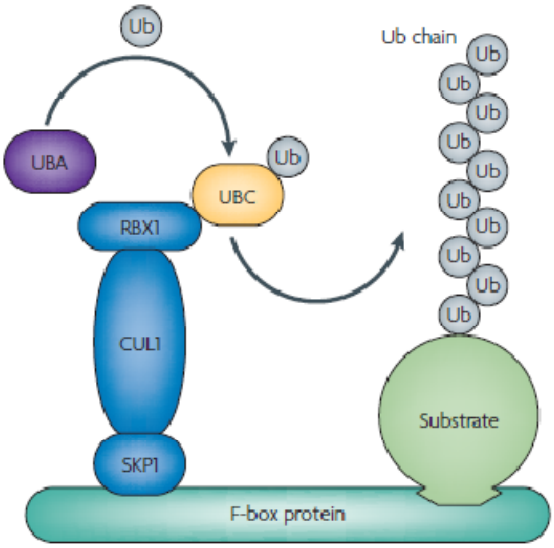

Ref, Markus Welcker and Bruce E. Clurman, *Nat. Rev. Cancer*, 2007 Vol. 8: 83-93

Figure 1.4 Domain structures of mammalian F-box proteins.

Domains identified by the Hidden Markov Model algorithms of SMART or PFam include F-box motif (F), WD40 repeat (WD), leucine-rich repeat (L), transmembrane domain (T), F-box-associated domain (FBA), between-ring domain (IBR), domain in carbohydrate binding proteins and sugar hydrolases (CASH), kelch repeat (K), calponin homology domain (CH), domain found in cupin metalloenzyme family (Jmjc), domain present in PSD-95, Dlg, and O-1 (PDZ), zinc-binding domain found in Lin-11, Isl-1, and Mec-3 (Lim), HNH nuclease family (HNHc), novel eukaryotic zinc-binding domain(CHORD), and tetratrico peptide repeat (TPR). The following domains were found via the Structural Classification of Proteins (SCOP) database, which can be used to predict protein sequences that can adopt known protein folds: ApaG-like, which is structurally similar to bacterial ApaG; Apolipophorin, the apolipophorin-III-like fold; Ubl, the ubiquitin-like fold; TDL, which is Traf-domain like; RNI-like, which may form structure similar to that of leucine-rich repeats in placental RNase inhibitor; and RCC1, which is a possible regulator of chromatin condensation-1 fold.

Ref. Jin et al. *Genes & Development*. 2004, 18:2573–2580

Figure 1.4 Domain structures of mammalian F-box proteins.

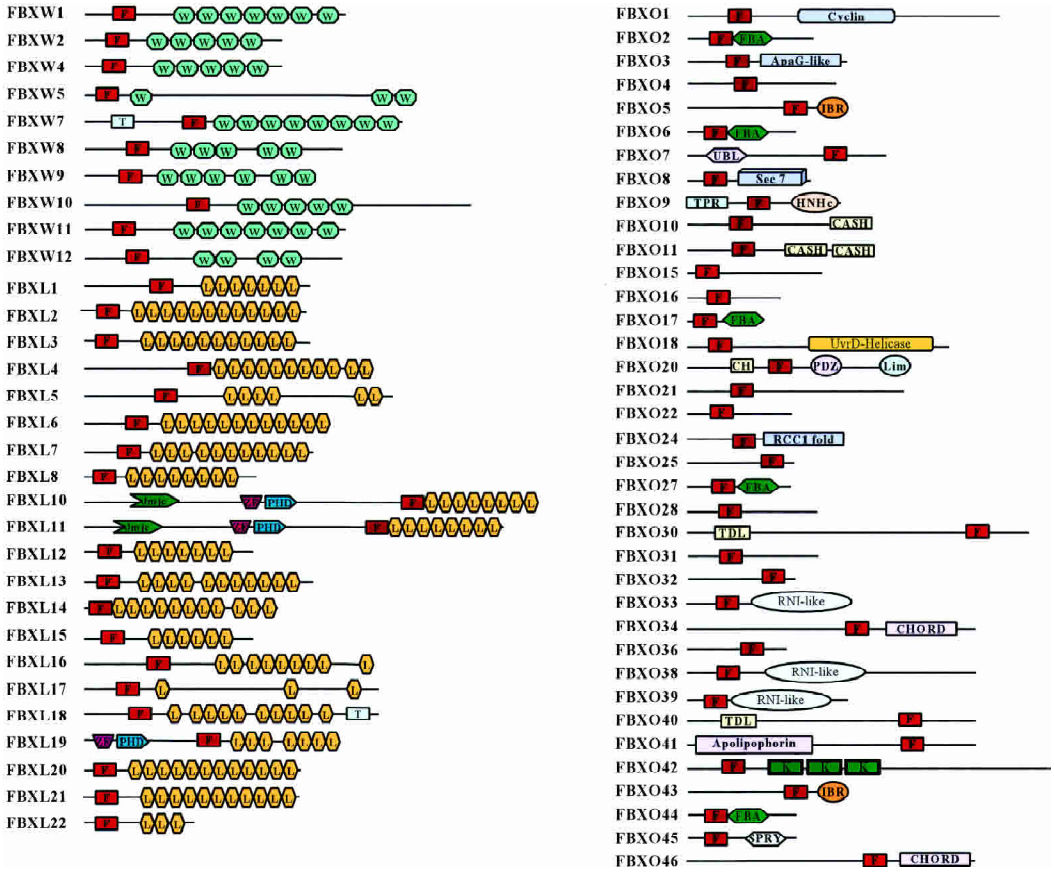

Ref. Jin et al. *Genes & Development*. 2004, 18:2573–2580

Figure 1.5 Key cell cycle regulatory proteins targeted by ubiquitin-mediated proteolysis.

a) shows yeast cells, and b) shows mammalian cells.

The class of protein-ubiquitin ligase that is responsible for ubiquitination of the respective proteins is indicated. Positive cell cycle regulators are shown as rectangles, whereas negative regulators are depicted as circles. Note that cyclin-B-Clb2 is both a positive and negative cell-cycle regulator.

APC/C, anaphase-promoting complex/cyclosome;

G1 and G2, Gap phases 1 and 2; M, Mitosis; S, DNA synthesis;

SCF, Skp1-Cullin-F-box protein.

Ref, Steven I. Reed. *Nat. Rev. Mol. Cell Biol.* 2003. Vol. 4: 855-864

Figure 1.5 Key cell cycle regulatory proteins targeted by ubiquitin-mediated proteolysis.

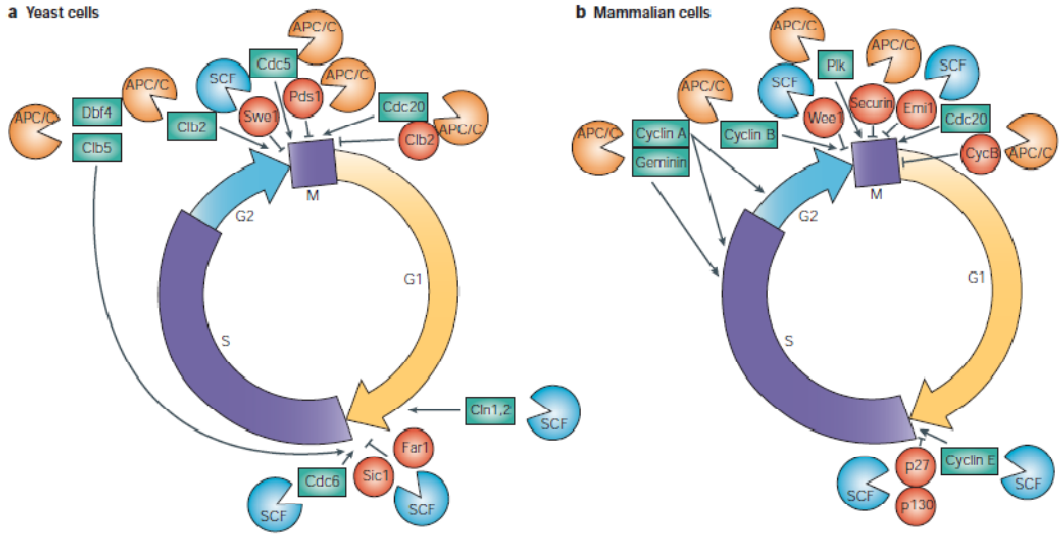

Ref, Steven I. Reed. *Nat. Rev. Mol. Cell Biol.* 2003. Vol. 4: 855-864

Figure 1.6 The organization of the *FBW7* gene and its protein isoforms.

Alternative splicing generates three distinct Fbw7 transcripts and proteins. The protein isoforms share all known functional domains: the eight WD40 repeats that mediate substrate recognition; the F-box that recruits the remainder of the SCF (complex of SKP1, CUL1 and F-box protein) ubiquitin ligase; and the dimerization domain (DD). The isoforms differ in their N termini.

NLS, nuclear localization signal;

TMD, trans-membrane domain.

Ref, Markus Welcker and Bruce E. Clurman, *Nat. Rev. Cancer*, 2007 Vol. 8: 83-93

Figure 1.6 The organization of the *FBW7* gene and its protein isoforms.

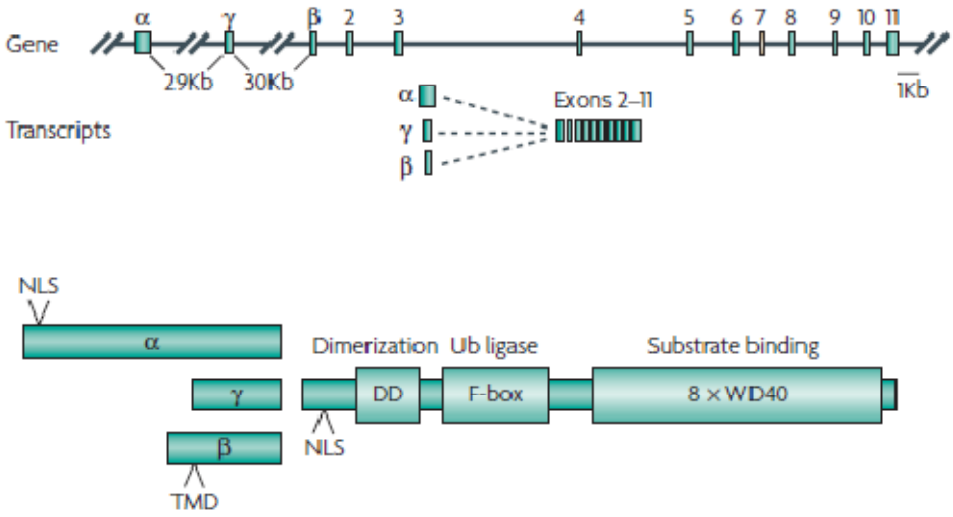

Ref, Markus Welcker and Bruce E. Clurman, *Nat. Rev. Cancer*, 2007 Vol. 8: 83-93

Chapter II:

Fbw7 Isoform Interaction Contributes to Cyclin E Proteolysis

Wei Zhang and Deanna Koepp

Department of Genetics, Cell Biology and Development,
University of Minnesota -Twin Cities, Minneapolis, Minnesota

University of Minnesota
6-160 Jackson Hall
321 Church St. SE
Minneapolis, MN 55455

Running Title: Fbw7 isoform interaction and cyclin E proteolysis

Key Words: cyclin, ubiquitin, proteolysis, F-box protein, cell cycle

(This material has appeared as “Fbw7 isoform interaction contributes to cyclin E proteolysis” by Wei Zhang and Deanna Koepp 2006 in *Molecular Cancer Research* 2006, Dec; 4; (12): 935-943. It is used here by permission)

Summary

The ubiquitin proteasome system plays important roles in regulating cell growth and proliferation. Many proteins that function in ubiquitin-mediated destruction have been linked to tumorigenesis. The putative tumor suppressor protein Fbw7 (hAgo/hCdc4) is a specificity factor for the Skp1-Cul1-F-box protein (SCF) ubiquitin ligase complex and targets a number of proto-oncogene products for ubiquitin-mediated destruction, including the cell cycle regulator cyclin E. In mammals, there are three splice variants of Fbw7, which use distinct first exons, resulting in proteins that have unique N-termini but are otherwise identical. Here we demonstrate that the Fbw7 splice variants interact with each other through an N-terminal region common to all of the Fbw7 isoforms. Other F-box proteins have been shown to regulate substrate binding or turnover by forming homo- or hetero-dimeric complexes, which are dependent on a sequence motif called the D domain. Fbw7 and its orthologs exhibit significant sequence similarity to such F-box proteins, including the D domain. Fbw7 mutants that lack the region encompassing the D domain fail to bind other Fbw7 isoforms, despite being properly localized and binding both cyclin E and Skp1. Finally, we demonstrate functional significance for this region as mutants lacking the N-terminal region involved in Fbw7 binding exhibit reduced rates of cyclin E protein turnover, indicating that Fbw7 isoform interaction is important for the efficiency of cyclin E turnover. Overall, this study contributes to the current understanding of the regulation of the Fbw7 tumor suppressor protein.

Introduction

Ubiquitin-mediated proteolysis plays an important role in regulating cell cycle transitions and thus, proteins that function in these pathways are often found mutated in cancer cells. The WD40-repeat containing F-box protein Fbw7 (hAgo/hCdc4) functions as a specificity factor for the modular Skp1-Cul1-F-box protein (SCF) ubiquitin ligase complex [59, 127, 128]. Fbw7 is proposed to function as a tumor suppressor; mutations have been identified in the Fbw7 locus in a number of breast, endometrial, ovarian and pancreatic cell lines and primary tumors [127, 128, 174, 177, 180, 183, 208, 218, 219]. In mice, $Fbw7^{+/-}$ heterozygotes exhibit increased incidence of tumor formation relative to wildtype animals [188].

The SCF^{Fbw7} complex is associated with the ubiquitination, and subsequent destruction via the proteasome, of at least four proto-oncogene protein products: cyclin E, c-Jun, c-Myc and Notch [59, 127, 128, 133, 138, 143, 220-222]. The interaction of Fbw7 with several of its substrates has been linked to a phosphodegron motif first identified in cyclin E [200, 201]. Conserved arginine residues in the WD40 repeat region are important for binding to the phosphodegron motif [59] and have been shown to contact the phosphate group in a crystal structure of Cdc4, the yeast ortholog of Fbw7, bound to an idealized consensus phosphopeptide [57]. Many of the Fbw7 mutations found in tumors are in regions that disrupt binding to this phosphodegron motif, including changes at the conserved arginine residues [127, 174, 183, 212]. Recent evidence suggests that proline isomerization may also be important in the recognition of cyclin E by Fbw7 [212, 223].

In humans, there are three splice variants of Fbw7, α, β, and γ, which arise

from the use of independent first exons [174]. While expression of individual Fbw7 isoform mRNAs do show some tissue specificity, there are examples of tissues and cell lines in which all three are expressed [174]. Interestingly, some of the Fbw7 tumor mutations are found in isoform-specific sequences, suggesting that individual isoforms may have distinct roles in preventing tumorigenesis [174, 183, 212]. Differential localization of the Fbw7 isoforms may also regulate the function of each. Fbw7-α is largely nuclear whereas Fbw7-β is primarily cytoplasmic and Fbw7-γ is reported to accumulate in the nucleolus [130, 133].The nucleolar-localized fraction of Fbw7-γ has been suggested to be responsible for the ubiquitination of c-Myc [133]. However, the precise role and contribution of each isoform to the ubiquitination of most Fbw7 substrates remains to be established.

For other WD40 repeat containing F-box proteins, there is evidence that the formation of homo-dimeric complexes, or hetero-dimeric complexes with highly related F-box proteins, can regulate substrate recognition and ubiquitination. In *Schizosaccharomyces pombe*, the F-box proteins Pop1 and Pop2 form hetero-dimeric complexes that regulate the ubiquitination and subsequent destruction of the cyclin-dependent kinase inhibitor Rum1, the S-phase regulator Cdc18 and the S phase cyclin Cig2 [224-227]. In humans, βTrCP1 and βTrCP2 homo-dimers are reported to bind and be responsible for the ubiquitination of the $SCF^{\beta TrCP}$ substrate IκB whereas heterodimers fail to bind IκB [228]. Dimerization of the βTrCP proteins occurs through a region upstream of the F-box domain called the D domain. Fbw7 and its orthologs show significant sequence similarity to βTrCP homologs, including the D

domain, but the existence of homo- or hetero-oligomeric complex formation among Fbw7 isoforms has not been previously reported.

In this study, we demonstrate that the Fbw7 splice variants can interact with each other in both mammalian and insect cells. We also identify an N-terminal region common to all the Fbw7 isoforms that is required for the interaction. This finding is similar to studies of βTrCP1/2 as the region required for the interaction includes the D domain. Furthermore, this region has functional implications for the Fbw7 protein as cells expressing Fbw7 mutants that fail to interact exhibit a reduced rate of cyclin E protein turnover. Our results broaden the current understanding of Fbw7 protein regulation and may have implications for investigating the tumor suppressor function of Fbw7.

Results

Fbw7 splice variants interact with each other

As an initial experiment to determine whether the Fbw7 splice variants might interact with each other, we used the baculovirus expression system. Using GST and Flag-tagged baculoviruses for each Fbw7 isoform, we examined their ability to co-immunoprecipitate with each other using insect cells infected with each pair-wise combination of Fbw7 isoforms. We also tested for the ability of each variant to form homo-interactions. In each case, when any Flag-tagged Fbw7 isoform is immunoprecipitated, the co-expressed GST-tagged isoform is also precipitated (Figure 2.1A, lanes 1-6, p69). None of the GST-tagged isoforms are able to interact with the anti-Flag agarose in the absence of expression of a Flag-tagged isoform, indicating

that the interaction we observe is specific (Figure2.1A, lanes 7-9, see p72). Reciprocal co-precipitation experiments confirm that the Fbw7 isoforms interact with each other (data not shown).

To test whether this interaction also occurs in mammalian cells, we co-expressed myc-tagged and Flag-tagged Fbw7 variants in 293T cells. As shown in Figure 2.1B, myc-tagged Fbw7-α co-immunoprecipitates with Flag-tagged Fbw7-α, β and γ (lanes 1-3). Similar results are observed with myc-tagged Fbw7-γ (Figure 2.1C, lanes 1-3, see p72). As a negative control, we co-transfected cells with empty Flag vector and either myc-tagged Fbw7-α or -γ (Figure2.1B, lane 4 and Figure2.1C, lane 4, see p72) and we do not observe any non-specific interaction in these samples. Reciprocal co-immunoprecipitation experiments confirm that the Fbw7 isoforms interact with each other (data not shown). We conclude that the Fbw7 isoforms can immunoprecipitate with each other in mammalian cells in the following combinations: α/α, α/β, α/γ, β/γ and γ/γ. We have been unable to generate a myc-tagged version of Fbw7-β that expresses at levels comparable to Fbw7-α and Fbw7-γ and thus have been unable to determine whether the Fbw7-β homo-oligomeric interaction occurs in mammalian cells. However, based on the results observed in insect cells, it seems likely that such an interaction occurs.

A conserved domain is necessary for Fbw7 splice variant interaction

We used deletion analysis to map the region necessary for the interaction between Fbw7 isoforms (Figure2. 2A, see p74). The interaction of other F-box proteins, most notably β-TrCP1 and β-TrCP2, has been shown to be dependent on the “D domain”, a

motif located immediately upstream of the F-box domain in these proteins [228]. We compared the amino acid sequence of Fbw7 to its homologs in yeast, worms and flies and human Fbw2 as well as βTrCP1 and its respective homologs. We find that there is significant homology among these proteins in the D domain, particularly at the C-terminal end of the domain (Figure 2B, see p74). Interestingly, only a subset of F-box proteins appears to contain the D domain. For example, a search of several F-box proteins bearing leucine rich repeats, including human Skp2 and budding yeast Dia2, shows no significant homology to the D domain (data not shown).

We generated Flag-tagged versions of Fbw7-α, β and γ in which the D domain and the N-terminal common region are deleted in frame such that the unique N-terminus for each isoform is immediately followed by the F-box domain (ΔDC, D domain plus common N-terminal region) as well as a form that deletes all residues upstream of the F-box domain (ΔN) (Figure2. 2A, p74). The deletion mutants were then co-transfected into 293T cells with myc-tagged full-length Fbw7-α and used for co-immunoprecipitation experiments. Each of these mutants is expressed and shows comparable abundance to the full-length Fbw7-α protein (Figures 3A and 3B, top panels, p76). While the Flag-tagged Fbw7-α co-immunoprecipitates myc-tagged Fbw7-α, none of the ΔDC or ΔN mutants are able to immunoprecipitate myc-tagged Fbw7-α (Figures 2.3A and 2.3B, p76).

We anticipated that the region required for the Fbw7 isoform interaction would not interfere with recognized domains of the protein, such as the WD40 repeat region or the F-box motif. To test this, we examined the ability of the ΔDC and ΔN mutants

to bind cyclin E and Skp1. The WD40 repeat region of Fbw7 has been implicated in binding cyclin E whereas the F-box domain has been shown to be important for binding Skp1 [59, 117]. Our deletion mutants were distinct from these domains and therefore we predicted binding to cyclin E and Skp1 would be retained. To test this, we co-transfected 293T cells with each mutant and either an HA-tagged Skp1 expression vector or a cyclin E expression vector. As shown in Figure 3C, the Fbw7-α, β, and γ ΔDC mutants as well as the ΔN mutant are each able to co-immunoprecipitate with HA-tagged Skp1 in a manner comparable to the respective wildtype isoforms. Likewise, in Figure 3D, each mutant also co-immunoprecipitates with cyclin E. The interactions that we observe appear to be specific for Skp1 and cyclin E as we do not observe any binding in mock immunoprecipitations (lanes 8-14, Figure2.3C and lane 8, Figure2.3D, p78). These results suggest that the deletion mutants we generated do not interfere with the F-box or WD40 domains and are not grossly misfolded. We therefore conclude that the N-terminal region of Fbw7 that contains the D domain is independent of the F-box and WD40 domains. Furthermore, this region is required for the interaction we observe between the Fbw7 isoforms.

The Fbw7 interaction domain is important for cyclin E proteolysis

We assessed the functional contribution of the region required for the interaction using a cyclin E stability assay. For these experiments, we focused on the Fbw7-α isoform as it exhibited the most robust response in the assay (data not shown). For the stability assay, we co-transfected 293T cells with equal amounts of the Flag-tagged

Fbw7-α, Fbw7-α ΔDC, Fbw7-ΔN or the empty Flag vector with a cyclin E expression vector. Cycloheximide was added to the cells 36 hours after transfection and samples were collected at 30, 90 and 180 minutes to assess cyclin E protein abundance by immunoblotting. The same blots were probed with anti-GAPDH antibodies as a loading control. A typical cyclin E stability assay for each Fbw7-α form is shown in Figure 4A and the quantification of the assay is shown in Figure 2.4B (p80). We quantified the amount of cyclin E signal relative to the GAPDH signal for this experiment and used the ratio for each timepoint, where the ratio for the zero time point is arbitrarily set to 1, to plot the amount of cyclin E signal remaining on a logarithmic scale versus time (Figure 2.4B, see p80). Even though they are expressed at approximately equivalent levels as wildtype and retain their ability to bind cyclin E and Skp1, the Fbw7-α ΔDC and ΔN mutants show a reduced rate of cyclin E turnover compared to the full-length Fbw7-α. We performed these experiments three times and each time the ΔDC and ΔN mutants exhibited reduced cyclin E turnover rates, indicating that the trends we observe are reproducible.

To determine whether this reduced rate of turnover is due to mislocalization of the mutant proteins or the loss of the ability to bind other Fbw7 molecules, we performed indirect immunofluorescence of 293T cells transfected with each Flag-tagged expression vector (Figure 2.4C, p77). We find that the ΔDC mutant localizes to the nucleus like the wildtype Fbw7-α protein, thus the effect of the ΔDC mutant on cyclin E stability cannot be due to localization differences. The ΔN mutant exhibits both nuclear and cytoplasmic staining, consistent with previous work indicating that

the Fbw7-α nuclear localization signal is in the N-terminus [133]. However, the ΔN mutant and the ΔDC mutant exhibited similar effects on cyclin E stability, thus we do not observe a significant correlation between cytoplasmic localization and reduced cyclin E turnover in this assay.

If the Fbw7ΔN and ΔDC mutants were unstable, that might explain the decreased rate of cyclin E turnover we observe. To test this possibility, we performed stability assays with 293T cells expressing Flag-tagged Fbw7 mutants. Cycloheximide was added to cells 36 hours after transfection with Fbw7-α, Fbw7α-ΔDC or Fbw7-ΔN and samples were collected at 45, 120 and 210 minutes to assess Fbw7 abundance by immunoblotting with anti-Flag antibodies. The same blots were probed with anti-GAPDH antibodies as a loading control (Figure 2.4D, p80). We observed no change in the stability of the Fbw7 mutants compared to the full-length protein, indicating that the reduced rate of cyclin E turnover in the Fbw7-αΔDC and Fbw7-ΔN mutants is not due to changes in the stability of the Fbw7 protein itself. Instead, our results strongly suggest that it is the failure of the Fbw7-α mutants to interact with other Fbw7-α molecules that has a deleterious effect on the degradation of the cyclin E protein.

Discussion

The results of this study indicate that the Fbw7 splice variants can form both homo- and heterotypic complexes with each other and suggest that at least the homotypic interactions are important for the efficient proteolysis of the SCF^{Fbw7}

substrate, cyclin E. An N-terminal domain common to all three Fbw7 splice variants is required for the isoforms to interact with each other, but it does not interfere with protein abundance or binding to Skp1 and cyclin E. It is possible that the reduced rate of cyclin E protein turnover caused by the inability of Fbw7 mutants to interact with each other, may have deleterious effects on cells that could contribute to tumor initiation, as misregulated cyclin E levels have been linked to chromosome instability and tumorigenesis [190]. Interestingly, a recent study of primary ovarian tumors with elevated levels of cyclin E protein identified a mutation, S245T (Fbw7-α residue number), in the region of Fbw7 required for its interaction with other isoforms [183]. This serine is conserved in Fbw7 homologs from multicellular organisms. Additional studies will be necessary to determine if there is a link between the defect in the S245T mutant and the interaction of Fbw7 with other isoforms.

The precise mechanism by which an Fbw7 homo-oligomeric interaction promotes cyclin E degradation remains to be determined. Since Fbw7 is the specificity factor for an SCF complex that ubiquitinates cyclin E, presumably the Fbw7-Fbw7 interaction promotes the rate of ubiquitination of cyclin E. One possibility is that the processivity of the reaction is enhanced, perhaps by reducing lag time between ubiquitination of individual cyclin E molecules. For example, it is possible that an Fbw7-Fbw7 dimer, bound through the interaction domain upstream of the F-box domain, could potentially dock with the SCF complex via the binding of one F-box domain. In this way, two cyclin E molecules would be available for ubiquitination by the same complex.

Alternatively, dimerization or oligomerization of F-box proteins might influence

the neddylation-deneddylation cycle proposed for Cul1 [229]. In this cycle, deneddylation of Cul1 by the Cop9 Signalosome (CSN) releases Cul1 from the SCF complex, upon which it is bound by the CAND1 protein and held inactive. Neddylation of Cul1 leads to its release from CAND1 and subsequent binding by a new F-box protein [230, 231]. There is evidence that cyclin E turnover is regulated by the CSN in both *Drosophila* and mice [232, 233]. Intriguingly, recent work on the SCF^{Skp2} complex indicates that increasing the amount of the Skp1-Skp2 subcomplex enhances Cul1 dissociation from CAND1 and that increased Skp2-substrate subcomplex inhibits Cul1 deneddylation [234]. Likewise, perhaps Fbw7 dimers are more efficient than monomers at dissociation of Cul1 from CAND1 or an Fbw7-Fbw7 dimer bound to cyclin E might prevent Cul1 from being deneddylated by the CSN for a longer period of time. In either case, the result would be an increase in the active pool of Cul1 and a decrease in the inactive pool of Cul1.

Recent results indicate that blocking the activity of the CSN leads to enhanced turnover of a subset of F-box proteins, including Fbw7, presumably via increased autoubiquitination as the F-box protein remains bound to the catalytic core of the SCF complex since it cannot be dissociated by deneddylation of Cul1 [235]. If the Fbw7 ΔDC mutant were to prevent the activity of the CSN on neddylated Cul1, perhaps by altering the conformation of the catalytic complex, that might explain the decreased rate of cyclin E turnover that we observe with this mutant. This explanation predicts that the Fbw7ΔDC mutant should be less stable than wildtype Fbw7. However, as we find that this mutant shows no appreciable difference in protein stability than wildtype Fbw7, we think this possibility is unlikely.

Finally, it is possible that the ΔDC mutant has a reduced binding affinity for cyclin E that our assay is not sufficiently sensitive to detect, although how the N-terminus might affect the substrate-binding domain in the WD40 region is unclear. Crystal structures of SCF complexes indicate that several α-helices of the F-box domain and Skp1 are interdigitated, but unfortunately no structural information for the N-terminus of any Fbw7 homolog that includes the D domain is available [106, 236].

Further work will be required to determine the stoichiometry of the Fbw7 complexes and to determine the extent of interaction among endogenously expressed Fbw7 isoforms. Other F-box proteins have been shown to form dimers; indeed the D domain derives its name from its role in βTrCP dimerization [228]. Fbw7 and its homologs in model organisms exhibit significant homology to the D domain and it is interesting that this domain appears in only a subset of F-box proteins. The region required for the interaction encompasses the D domain. However we still observe substantial interaction among the Fbw7 isoforms when just the D domain is deleted in frame (Supplemental Figure). Therefore, at least for the Fbw7 isoforms, residues in addition to the D domain are important for the formation of oligomeric complexes.

A functional role for the heterotypic interaction among the Fbw7 isoforms remains to be established. For βTrCP1 and βTrCP2, it has been reported that the heterodimers are unable to bind substrate protein and in this way, dimerization might regulate substrate ubiquitination [228]. The role of the heterotypic interaction with Fbw7 variants is complicated by the differential localization of each [133]. For example, Fbw7-α is localized to the nucleus whereas Fbw7-β is cytoplasmic. Our co-

immunoprecipitation results suggest that the hetero-oligomeric interactions can occur with the mammalian proteins, but if they do so in intact cells, it must either mean that only a small fraction of each population interacts or that Fbw7-α or -β can shuttle between the nucleus and the cytoplasm.

In conclusion, we have shown that alternative splice variants of the F-box protein Fbw7 interact with each other and we have identified the region of the protein necessary for this interaction. This observation broadens the current understanding of F-box protein regulation and it will be important to determine in the future if Fbw7 isoform interaction represents a common regulatory mechanism for other SCF^{Fbw7} substrates. In the case of the Fbw7α/α complex, our results may link F-box protein complex formation with tumorigenesis, as the cyclin E turnover rate is reduced in Fbw7-α mutants that fail to bind each other.

Materials and Methods

Cell culture and reagents

HEK293T cells were maintained in Dulbecco's Modified Eagle's Medium (HyClone) with 10% newborn Bovine Serum. Sf9 insect cells were grown in Insect Xpress with L-Glutamine (BioWhittaker) medium supplemented with 10% heat-inactivated newborn Bovine Serum. Hi5 insect cells were grown in ExCell 405 (JRH Biosciences) without serum.

Cell Transfection and infection

HEK293T cells were transfected with Lipofectamine2000 (Invitrogen) according

to the standard procedure provided by the manufacturer. 40 hours after transfection, cells were collected and washed with PBS (137 mM NaCl, 2.7 mM KCl, 10 mM Na_2HPO_4, 2 mM KH_2PO_4). Baculovirus expressing GST- or Flag-tagged Fbw7 isoforms were generated in Sf9 cells using BD BaculoGold Linearized Baculovirus DNA (BD Biosciences). For expression of recombinant proteins, Hi5 insect cells were infected with recombinant baculovirus and incubated for 40 hours before collection.

Generation of expression constructs

To generate either GST- or Flag-tagged Fbw7 expressing baculovirus, we used the Cre recombinase-based univector plasmid fusion system [237]. Generation of Fbw7-β baculovirus has been described[59]. Fbw7-α was amplified in two overlapping fragments using oligos DK396, DK398, DK399 and DK376. The N-terminus of the Fbw7-γ isoform was cloned using three overlapping primers DK373, DK373 and DK374 that were annealed and a full-length product generated with primers DK373 and DK376. To generate Myc-tagged Fbw7-α and ΔN plasmids, these fragments were amplified using primer pairs DK397/DK400 and DK355/DK400, respectively. PCR products were digested with EcoRI and XbaI and cloned into pcDNA3.1-MycHis vector (Invitrogen). We also made 6X Myc-tagged Fbw7-γ plasmids (in pCS2+MT) by amplifying Fbw7-γ using primers DK221 and DK375 and cloning the PCR product into the EcoRI and XbaI sites.

The ΔDC deletion mutants of Fbw7-α, β, γ were cloned into p3X FLAG-CMV 7.1 expression vector (Sigma) by two-step PCR. To delete the DC region of each isoform, we first amplified the unique region of each isoform (α primers: WZ1, WZ2;

β primers: WZ4, WZ5; γ primers: WZ7, WZ8) and the fragments starting from the F-box motif to the 3' end by PCR (α primers WZ3/DK376; β primers: WZ6/DK376; γ primers: WZ9/DK376). The sequence at the 3' of the each unique fragment and at the 5' of the C terminal fragment was complementary to each other. The two fragments of each isoform were annealed and the annealed fragment was used as the template for the next PCR. The final PCR products were digested by EcoRI and SalI, and ligated into the p3X FLAG-CMV7.1 vector. A complete list of the constructs and primers used in this study are shown Table 1 and Table 2, respectively.

Western Blot Analysis and reagents

Cell lysates were prepared in NETN buffer (20mM Tris pH 8.0, 100mM NaCl, 1mM EDTA, 0.5% NP-40) containing 1mM NaF, 2.5 mM β-glycerophosphate and protease inhibitor cocktail (Roche Applied Science). Protein concentrations were determined by the Bio-Rad protein assay (Bio-Rad Laboratories, Inc). Cell lysates were resolved by SDS-PAGE and electrophoretically transferred to nitrocellulose membrane. Membranes were blocked in PBST (137 mM NaCl, 2.7 mM KCl, 10 mM Na_2HPO_4, 2 mM KH_2PO_4, 0.1% Tween-20) containing 5% milk for at least 40 minutes. Blots were probed with primary antibodies followed by labeling with horseradish peroxidase conjugated anti-mouse or anti-rabbit secondary antibody (Jackson Immunoresearch). Following antibody incubation, blots were developed on film using an Enhanced Chemiluminescence kit (PIERCE) according to the manufacturer's instructions. Densitometry of immunoblot bands was measured by using NIH ImageJ. The primary antibodies used included: anti-Flag M2 antibody

(Sigma), anti-GST antibody (Z5, Santa Cruz), anti-HA (HA.11, Covance Research), anti-Myc (9E10, Covance Research), anti-cyclin E (HE-12, Santa Cruz), anti-GAPDH (Abcam).

Co-immunoprecipitation assays

200-500μl of cell lysate was incubated with NETN buffer containing antibody at 4°C for 4 hours, then 20μl of protein A/G beads (Santa Cruz Biotechnology) was added for another 2 hours or overnight. The beads were washed three times with NETN lysis buffer. Anti-Flag M2 (Sigma) agarose affinity gel was used to purify Flag-tagged proteins.

Protein stability assays

The cyclin E construct together with Fbw7 isoform or deletion mutant constructs were transfected into HEK293T cells. 36 to 40 hours after transfection, cycloheximide (Sigma) was added to a final concentration of 30μg/ml to stop the protein synthesis (time 0). Cell extracts from each time point were analyzed by Western blotting.

Immunofluorescence microscopy

HEK293T cells transfected with Flag tagged Fbw7 or deletion mutants were grown on cover slides for 40 hours. Cells were fixed with 3% paraformaldehyde and 2% sucrose solution for 10 minutes at room temperature. Cells were permeabilized in ice-cold 0.5% Triton X-100 solution (0.5% Triton X-100, 20mM HEPES, pH 7.4, 50 mM NaCl, 3mM $MgCl_2$, 300mM sucrose) on ice for 5 minutes and blocked with 1% bovine serum albumin in PBS (137 mM NaCl, 2.7 mM KCl, 10 mM Na_2HPO_4, 2 mM KH_2PO_4) at 37° C for 30 minutes. Cells were incubated with anti-Flag antibody

(1:2000) at 37°C for 30 minutes followed by incubation with anti-mouse FITC (1:5000) for 20 minutes at 37°C. Images were collected on a Zeiss Axioskop 2 microscope equipped with a Zeiss Axiocam R2 digital camera using Zeiss Axiovision software release 3.1 (Carl Zeiss, Thornwood, NY).

Table 1. Plasmids used in this study

Name	Description	Source
p1212-Fbw7-α	GST-Fbw7-α for baculovirus production	This study
p1212-Fbw7-β	GST-Fbw7-β for baculovirus production	Koepp et al., 2001
p1212-Fbw7-γ	GST-Fbw7-γ for baculovirus production	This study
p1214-Fbw7-α	Flag-Fbw7-α for baculovirus production	This study
p1214-Fbw7-β	Flag-Fbw7-β for baculovirus production	Koepp et al., 2001
p1214-Fbw7-γ	Flag-Fbw7-γ for baculovirus production	This study
pcDNA3.1 Fbw7-α	CMV promoter, myc, his-tagged Fbw7-α	This study
p3XFlag-Fbw7-α	CMV promoter, Flag-tagged Fbw7-α	Welcker et al., 2002
p3XFlag-Fbw7-β	CMV promoter, Flag-tagged Fbw7-β	Welcker et al., 2002
p3XFlag-Fbw7-γ	CMV promoter, Flag-tagged Fbw7-γ	Welcker et al., 2002
Myc-Fbw7-γ	CMV promoter, Myc-tagged Fbw7-γ	This study
pcDNA3.1 Fbw7ΔN	CMV promoter, myc, his-tagged Fbw7ΔN	This study
p3XFlag-Fbw7-α ΔDC	CMV promoter, Flag-tagged Fbw7-α ΔDC	This study
p3XFlag-Fbw7-β ΔDC	CMV promoter, Flag-tagged Fbw7-β ΔDC	This study
p3XFlag-Fbw7-γ ΔDC	CMV promoter, Flag-tagged Fbw7-γ ΔDC	This study
pRc-CycE	CMV promoter, cyclin E	J.W. Harper

Table 2. Oligonucleotides used in this study

Name	Sequence (5’ to 3’)
α-specific	
WZ1	CGGAATTCCACCATGAATCAGGAACAGCTCTC
WZ2	CTCTTTAGGGAGTTTTGTTTTTGTATAGAATGG
WZ3	AAAACAAAACTCCCTAAAGAGTTGGCACTC
DK396	CGGAATTCCCACCATGAATCAGGAACTGCTCTC
DK397	CGGAATTCCACCATGAATCAGGAACTGCTCTC
DK398	GGTCCAACTTTCTTTTCATTTTTGTTGTTTTTGTATAGAATGGGGAGG
DK399	CCTCCCCATTCTATACAAAAACAACAAAAATGAAAAGAAAGTTGGACC
β-specific	
WZ4	TAATTGAATTCCATGTGTGTCCCGAGAAGC
WZ5	CTCTTTAGGGAGTTTGTAAAAAATCATTTTTAATG
WZ6	ATTTTTTACAAACTCCCTAAAGAGTTGGCACTC
γ-specific	
WZ7	CGGAATTCCACCATGTCAAAACCGGGAAAACCT
WZ8	CTCTTTAGGGAGCCGTCTTCGACAAAAAGGGAGG
WZ9	TGTCGAAGACGGCTCCCTAAAGAGTTGGCACTC
DK372	CGGAATTCCCACCATGTCAAAACCGGGAAAACCTACTCTAAACCATGG CTTGGTTCCTGTTGATCTTAAAAG
DK373	AAGATATTTAGCATTAGCATCATTGCCCAAGGCCTCCCTTTTTGTCGAAG ACGGATGAAAAGAAAGTTGGAC
DK374	GCTAATGCTAAATATCTTCATCACGGTTTGATGTGGTAGAGGCTCTTTTG CACTTTTAAGATCAACAGGAA
DK375	CGGAATTCCACCATGTCAAAACCGGGAAAACCT
Common region	
DK221	TCTAGACACTTCATGTCCACATC
DK376	ACGGGGTCGACTCACTTCATGTCCACATCAAG
DK400	ACGCCGTCGACCACTTCATGTCCACATC
ΔN	
DK355	CCGAATTCCGCCACCATGCAAGTGATAGAACCCCA

Figure 2.1. **The splice variants of Fbw7 interact with each other *in vitro* and *in vivo***.

A) The three isoforms of Fbw7 interact in insect cells. Individual isoforms of Fbw7 tagged with either GST or Flag were overexpressed in Hi5 insect cells. The upper 2 panels show the expression of GST-tagged and Flag-tagged isoforms tested by Western blot, and the bottom panel shows the co-immunoprecipitation results of pairwise combinations of the isoforms. Hi5 insect cells were infected with baculovirus for 40 hours and cells harvested for lysis. Equal amounts of total protein extracted from each insect cell lysate were incubated with 20μl of anti-Flag M2 affinity agarose beads at 4°C for 2 hours followed by Western blot analysis with anti-GST antibodies. Cells of lane 7-9 were only infected with GST-tagged baculovirus and used to exclude the possibility that GST-tagged proteins non-specifically bound to the anti-Flag agarose. The asterisks indicate non-specific bands recognized by the anti-Flag antibodies.

B) and C) The Fbw7 isoforms interact in mammalian cells. Myc-tagged Fbw7-α (B) or Fbw7-γ (C) was co-transfected with the indicated Flag-tagged isoforms in 293T cells. Equal amounts of total protein extracted from cell lysates were incubated with 20 μl of anti-Flag M2 agarose for 2 hours followed by Western blot analysis with anti-Myc antibodies. Lane 4 in both (B) and (C) are controls for non-specific binding to the beads.

Figure 2.1. **The splice variants of Fbw7 interact with each other *in vitro* and *in vivo*.**

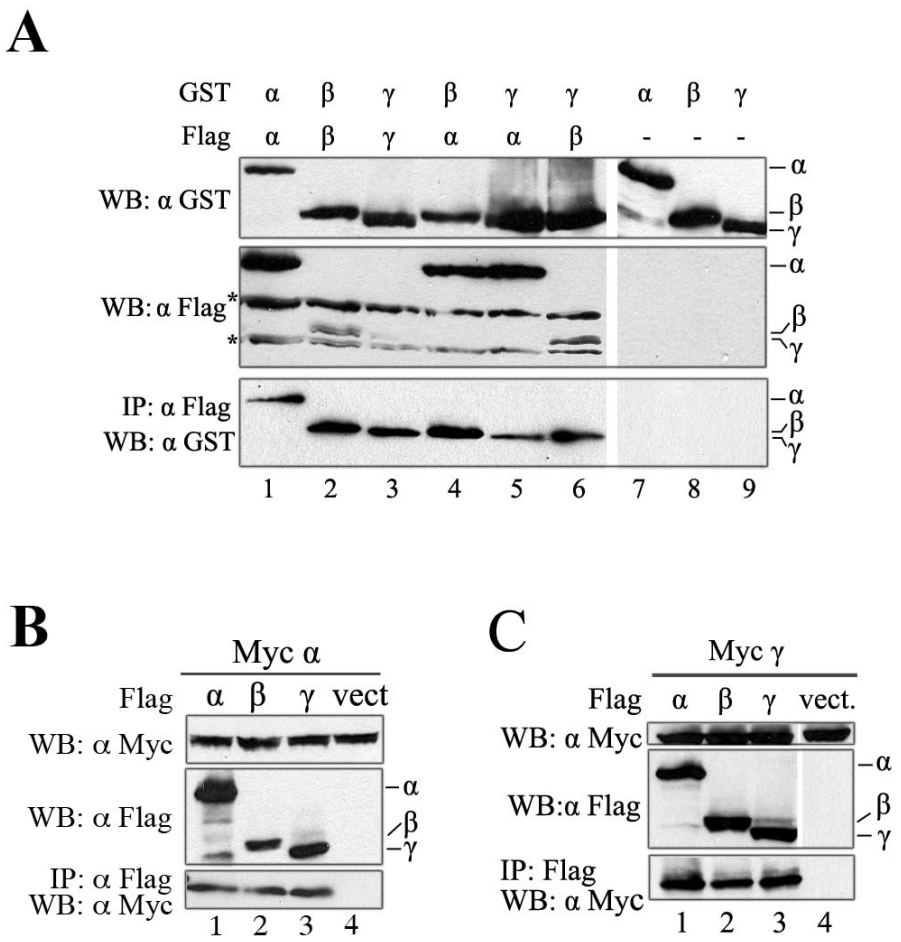

Figure2.2

A) Schematic diagram of Fbw7 domains in each splice variant and the deletion mutants used in this study.

B) Alignment of the D domain sequences from Fbw7 and its homologs and a number of other WD40-repeat containing F-box proteins, including βTrCP1 and its homologs. A consensus sequence is shown above the alignment. Black boxes indicate identical residues while gray shading indicates residues of similar functional groups. The alignment was generated using Clustal W and the Megalign program of the Lasergene Navigator Suite.

Figure2.2

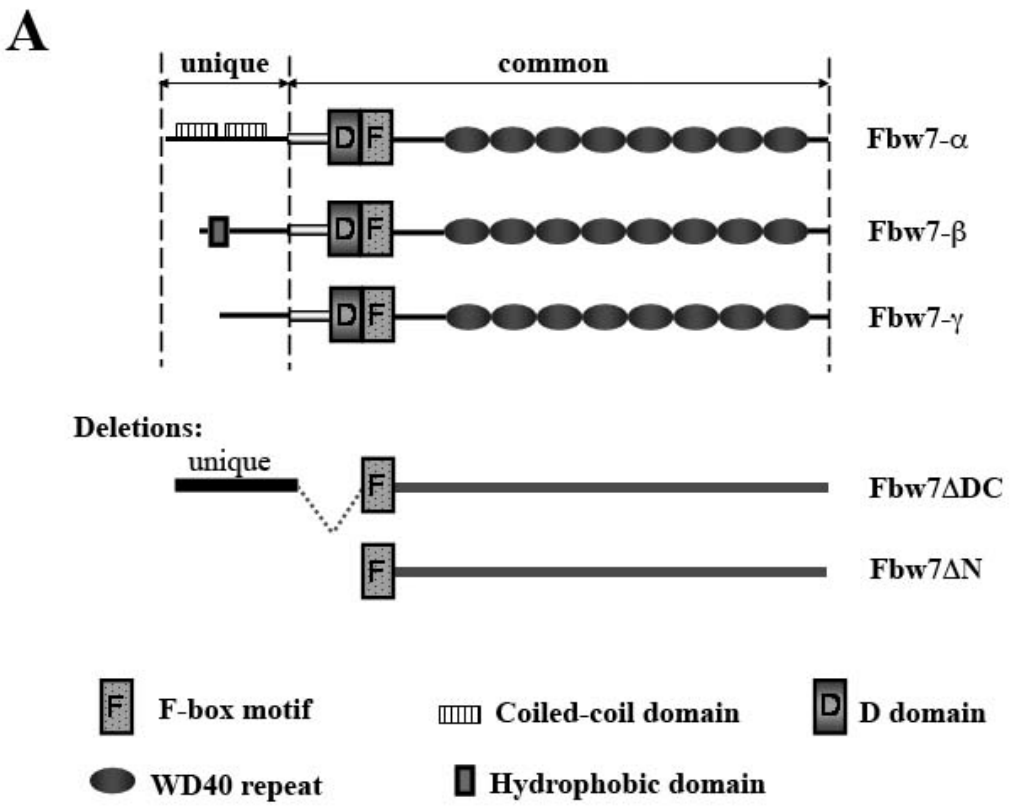
A
unique
common
D F
Fbw7-α
Fbw7-β
Fbw7-γ
Deletions:
unique
F
Fbw7ΔDC
Fbw7ΔN
F F-box motif
Coiled-coil domain
D D domain
WD40 repeat
Hydrophobic domain


B
F . . L S E . E Q . . A L D b L L S . C p . p Q L . . f . p . L E P f L Q R D F I S L Consensus
Fbw7 H. sapiens
Ago D. melanogaster
Sel-10 C. elegans
βTRCP1 H. sapiens
Slimb D. melanogaster
Lin-23 C. elegans
Fbw2 H. sapiens
Cdc4 S. cerevisiae
Pof1 S. pombe
Met30 S. cerevisiae
Pop1 S. pombe
Pop2 S. pombe

Figure2.3. The domain required for Fbw7 isoform interaction encompasses the D domain.

A) The N-terminus is required for the Fbw7 isoform interaction. 293T cells were co-transfected with vectors expressing Flag-tagged full-length Fbw7 isoforms and either Myc-tagged Fbw7-α or Myc-tagged Fbw7-ΔN. The upper two panels are the Western blot analyzing the expression of the proteins, and the bottom panel is the immunoprecipitation result. Equal amounts of total protein extracted from each lysate were incubated with 20 μl of anti-Flag agarose beads prior to SDS-PAGE and Western blot analysis using anti-Myc antibodies. In lanes 7 and 8, empty Flag vector was transfected as a negative control. The asterisk indicates a non-specific band recognized by the anti-Myc antibodies.

B) Fbw7-ΔDC no longer binds Fbw7 isoforms. 293T cells were transfected with full length Flag-tagged Fbw7-α or the Fbw7-ΔDC mutant of each isoform together with Myc-tagged Fbw7-α. The upper two panels are the Western blot analyzing the expression of the proteins, and the bottom panel is the immunoprecipitation result. Equal amounts of total protein extracted from each lysate were incubated with 20 μl of anti-Flag agarose beads prior to SDS-PAGE and Western blot analysis.

Figure2.3. The domain required for Fbw7 isoform interaction encompasses the D domain.

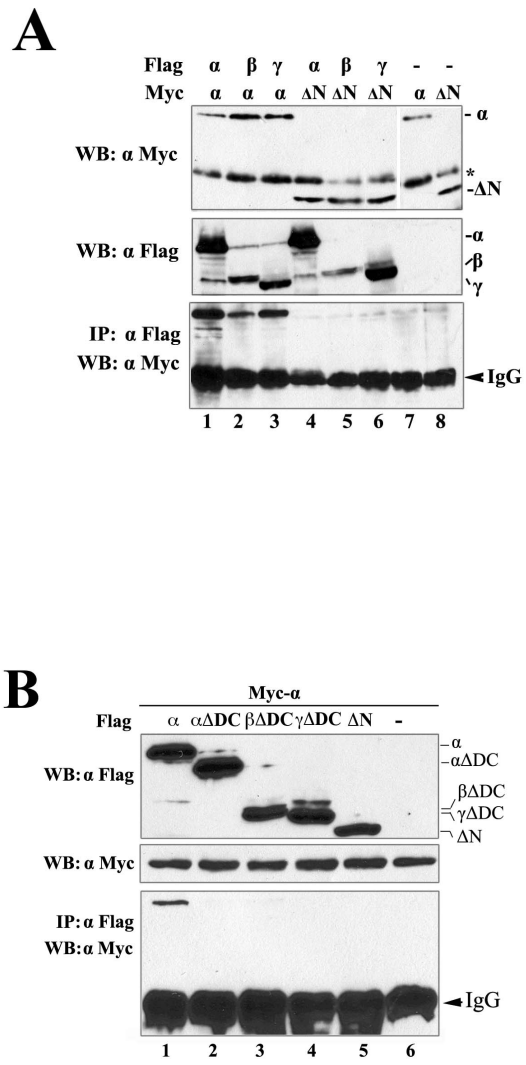

Figure 2.3 continue

C) The deletion mutants of Fbw7 co-immunoprecipitate Skp1. 293T cells were transfected with the Fbw7 deletion mutants and HA-tagged Skp1. The upper two panels show the expression of Flag-tagged full length Fbw7 isoforms and the ΔDC deletion mutants and HA-tagged Skp1. The bottom panel shows the IP (immunoprecipitation) result. Equal amounts of total protein extracted from each cell lysate were incubated with anti-HA antibody for 2 hours followed by incubation with 20 μl pre-washed protein A/G agarose beads. Lanes 8-14 show control experiments in which no HA-Skp1 was transfected. The asterisk indicates the Fbw7-ΔN band, which runs just above the IgG heavy chain.

D) The Fbw7 deletion mutants co-immunoprecipitate cyclin E. 293T cells were transfected with Flag-tagged full-length Fbw7 isoforms, ΔDC deletion mutants or Flag vector together with equal quantities of the cyclin E expression construct. The upper two panels show the expression of the indicated forms of Fbw7 and cyclin E. The bottom panel shows the IP result. Equal amounts of total protein from each cell lysate were incubated with 20 μl of pre-washed anti-Flag M2 agarose beads at 4°C overnight.

Figure 2.3 continue

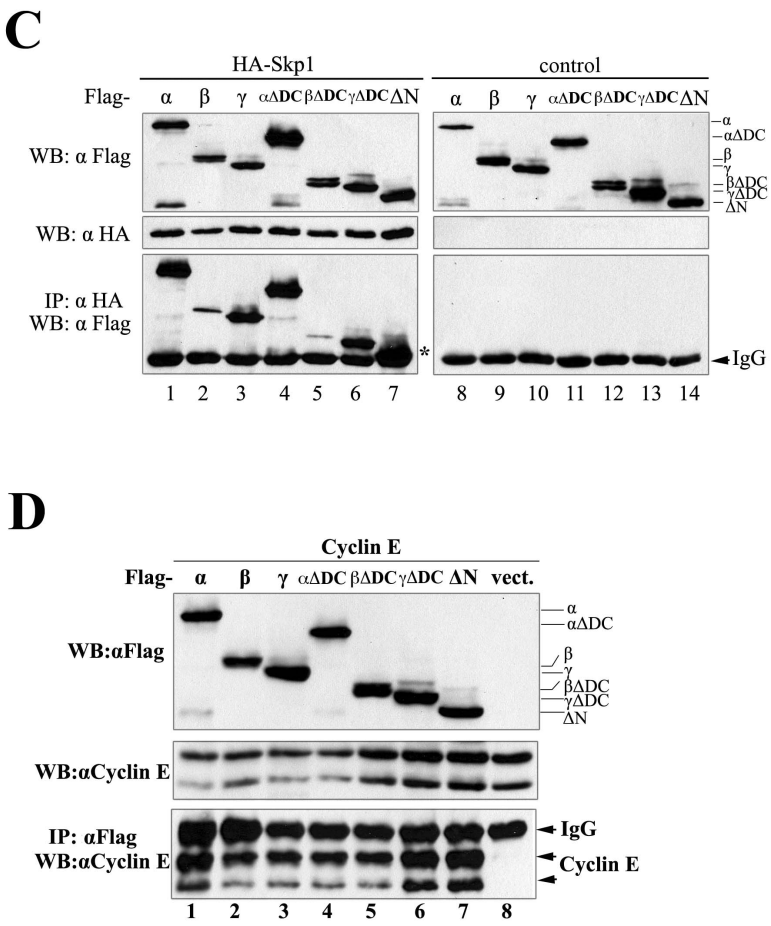

Figure2.4. The homo-oligomeric interaction of Fbw7 isoforms is important for cyclin E proteolysis.

A) Examples of cyclin E stability assays. 293T cells were co-transfected with the same amount of cyclin E expression construct together with Flag-tagged Fbw7-α, Fbw7-αΔDC, the Fbw7-ΔN or empty vector. 36 hours after transfection, cycloheximide (final concentration, 30μg/ml) was added to stop protein synthesis (time point 0). Cells were collected at the indicated time points and cyclin E protein abundance was analyzed by Western blot. Anti-GAPDH antibodies were used as a loading control.

B) Quantitation of cyclin E stability. The results the cyclin E stability experiments in (A) were analyzed by Image J software. The log of the ratio of cyclin E (both bands) to the loading control is plotted versus time.

C) The Fbw7-α ΔDC mutant shows similar localization to the full-length protein. 293T cells were grown on coverslips and transfected with Fbw7-α, -αΔDC, and -ΔN. 36 hours after transfection, cells were fixed in 2% paraformaldehyde and immunostained with anti-Flag antibodies. D) 293T cells were transfected with Flag-tagged Fbw7-α, Fbw7-αΔDC, or Fbw7-ΔN. 36 hours after transfection, cycloheximide (final concentration, 30μg/ml) was added to stop protein synthesis (time point 0). Cells were collected at the indicated time points and Fbw7 protein abundance was analyzed by Western blot using anti-Flag antibodies. Anti-GAPDH antibodies were used as a loading control.

Figure2.4. The homo-oligomeric interaction of Fbw7 isoforms is important for cyclin E proteolysis.

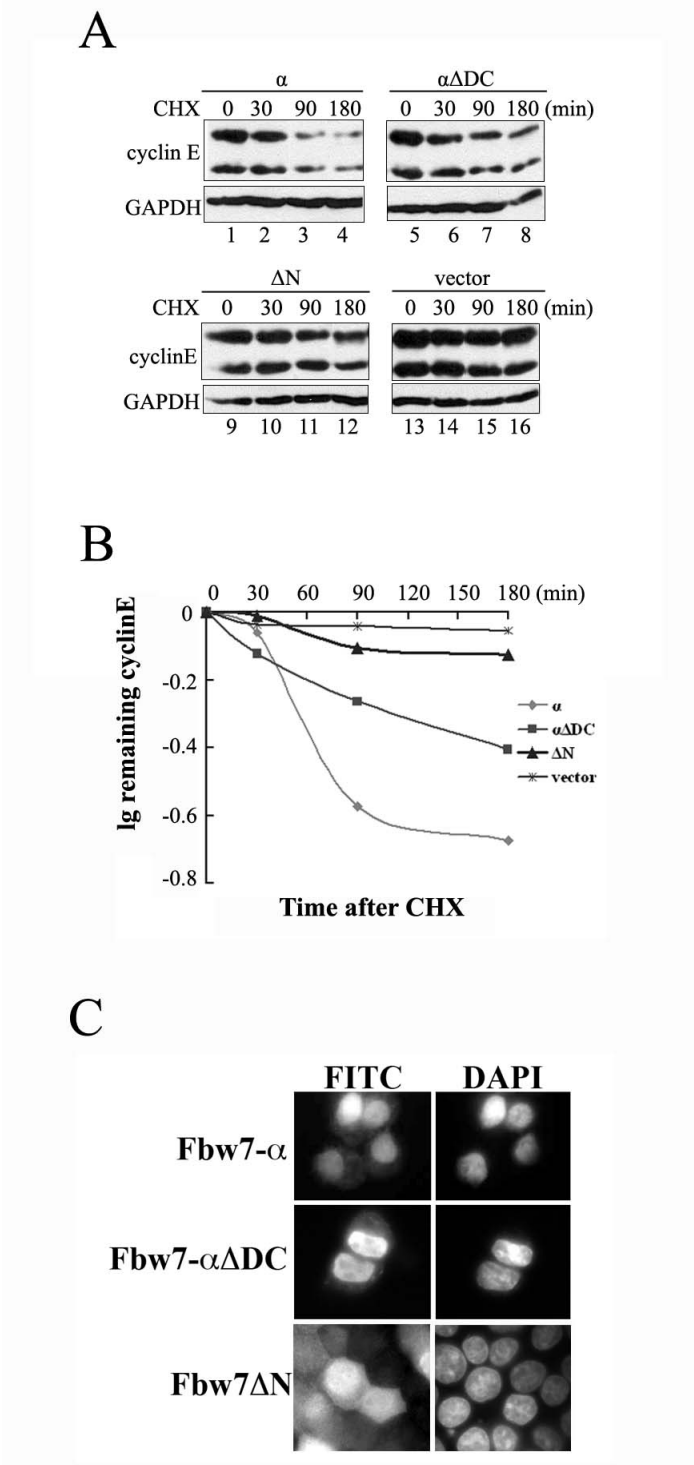

Fig 2.5 Supplemental Figure

Fbw7 mutants lacking the D domain co-immunoprecipitate with other Fbw7 isoforms.

Myc-tagged Fbw7-α or Fbw7-ΔD was co-transfected with the indicated Flag-tagged isoforms in 293T cells. Equal amounts of total protein extracted from cell lysates were incubated with 20 μl of anti-Flag M2 agarose for 2 hours followed by Western blot analysis with anti-Myc antibodies. The upper panels show expression levels whereas the lower panel shows the immunoprecipitation results. Lanes 7 and 8 are controls for non-specific binding to the Flag agarose.

Fig 2.5 Supplemental Figure

Fbw7 mutants lacking the D domain co-immunoprecipitate with other Fbw7 isoforms.

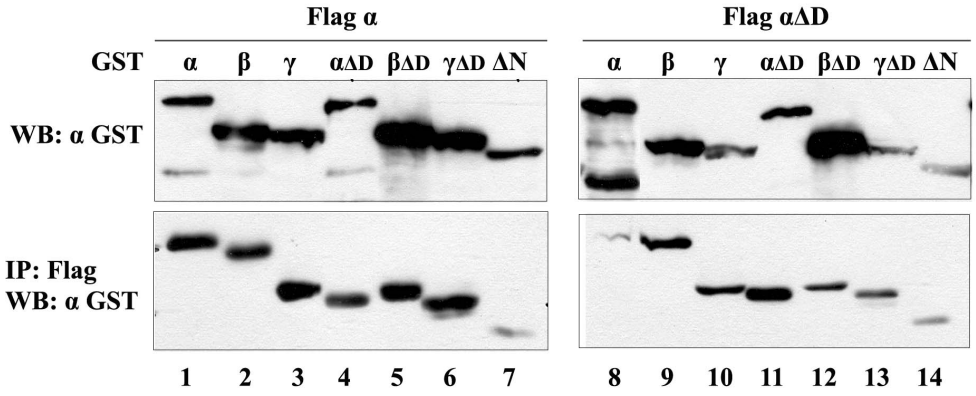

Chapter III:

Fbw7γ Isoform Proteolysis Is Regulated by SLP1 and Cdk2

Wei Zhang, Elithebeth Macdonald, and Deanna Koepp
Department of Genetics, Cell Biology and Development,
University of Minnesota -Twin Cities, Minneapolis, Minnesota

University of Minnesota
6-160 Jackson Hall
321 Church St. SE
Minneapolis, MN 55455

Running Title:

Key Words: ubiquitin, proteolysis, cyclin-dependent kinase, Fbw7, SLP1

Summary

Control of cellular proliferation is critical to cell viability and prevention of tumorigenesis. The F-box protein Fbw7 (hAgo/hCdc4/FBXW7) is a tumor suppressor that functions as a specificity factor for the modular Skp1-Cul1-F-box protein (SCF) ubiquitin ligase complex and targets several proteins required for cellular proliferation for ubiquitin-mediated destruction. In mammals, Fbw7 exists as three splice variants but the precise mechanistic role of each is not clear. To better understand the function of the Fbw7-γisoform, we examined the regulation of this protein. We show here that Fbw7-γ is an unstable protein and that its turnover is proteasome-dependent and regulated by cell cycle stage. Using a two-hybrid screen, we identify a novel isoform-specific interaction partner, SLP1, which binds the unique N-terminal domain of Fbw7-γ and blocks its degradation. Moreover, SLP1 is also an unstable protein and is degraded at the same cell cycle stages as Fbw7-γ. We demonstrate that Cdk2 also binds the unique N-terminal domain of Fbw7-γ and Cdk2 activity promotes the turnover of both Fbw7-γ and SLP1. We propose that Fbw7-γ and SLP1 are coordinately targeted for ubiquitin-mediated degradation by the activity of Cdk2.

Introduction

Ubiquitin-mediated proteolysis is critical for cellular proliferation and proteins that function in this pathway often contribute to tumorigenesis. The F-box protein Fbw7 (hAgo/hCdc4/FBXW7) functions as a specificity factor for the modular Skp1-Cul1-F-box protein (SCF) ubiquitin ligase complex and is a tumor suppressor. The Fbw7 locus is mutated in many human cancer cell lines and primary tumors (reviewed in [238]). In mice, the FBXW7 locus is required for viability [144, 145] but $Fbxw7^{+/-}$ heterozygotes exhibit increased incidence of tumor formation relative to wildtype animals [188].

The SCF^{Fbw7} complex targets a number of proteins required for cellular proliferation for ubiquitination and subsequent degradation by the proteasome, including cyclin E, c-Jun, c-Myc, mTOR, Notch, PGC1a, and SREBP [59, 127, 128, 132, 133, 138, 140, 143, 156, 158, 221, 222, 239]. The interaction of Fbw7 with its substrates is mediated through a phophodegron motif first identified in cyclin E [200]. Structural studies show that conserved arginine residues in the WD40 repeat region of both Fbw7 as well as Cdc4, the yeast ortholog of Fbw7, are important for binding to the phosphodegron motif [57, 58].

Fbw7 is conserved from yeast to humans, but only mammals exhibit splice variants. In humans, there are three splice variants of Fbw7, a, b, and g, which arise from the use of independent first exons [174]. The a isoform is widely expressed at high levels in many tissues, whereas the b and g isoforms are expressed at high levels in brain and skeletal muscle and in low levels in many other tissues [174]. Most mutations identified in humans are found in the WD40 substrate-interaction domain

[238], which is common to all three isoforms, but a few mutations have been identified in the unique N-termini of the α and β variants [174], suggesting that multiple variants may contribute to tumor suppression.

The precise role and significance of each Fbw7 splice variant is not well understood. Since Fbw7-α is the most highly expressed Fbw7 variant in most tissues [174], it is widely thought that this isoform is largely responsible for the ubiquitination of most Fbw7 targets, although there is conflicting evidence indicating that Fbw7-γ may be just as important in certain instances. A recent study in which isoform-specific knockout cell lines were generated is consistent with the Fbw7-α is primary model [210]. By contrast, other work suggests that Fbw7-γ is specific for the ubiquitination of c-Myc [133], whereas Fbw7-α is prevented from targeting c-Myc for degradation because of the action of a de-ubiquitinating enzyme [240]. In addition, there is evidence that Fbw7-α is key to a proline isomerization step that is required for the recognition of cyclin E by Fbw7-γ. In this model, the binding of cyclin E to Fbw7-α is simply a precursor to ubiquitination via Fbw7-γ [212]. Finally, expression levels of cyclin E may also play a role in determining which Fbw7 variant is utilized [241].

To better understand the function of Fbw7-γ, we examined the regulation of this protein. We found that Fbw7-γ is an unstable protein, consistent with a recent report [210]. We show here that Fbw7-γ turnover is proteasome-dependent and regulated by cell cycle stage. We have identified a novel isoform-specific interaction partner called SLP1 that binds the unique N-terminal domain of Fbw7-γ and blocks its degradation. Moreover, we show that SLP1 is also an unstable protein and is degraded at the same cell cycle stages as Fbw7-γ. We find that Cdk2 activity influences the turnover of both

Fbw7-γ and SLP1. Our studies support a model in which Fbw7-γ and SLP1 are coordinately targeted for ubiquitin-mediated degradation by Cdk2 kinase activity.

Results

Fbw7- γ proteolysis is regulated by a unique N-terminal domain and cell cycle stage

The Fbw7 isoforms (Figure 3.1A, p99) exhibit differences in protein stability. Previous work indicated that the β and γ isoforms were unstable proteins, whereas the α isoform is stable [210]. We observe similar results in a protein stability assay using epitope-tagged Fbw7 constructs expressed in human HEK293T cells (Figure 3.1B, lanes 1-4, p103). Briefly, cells expressing the indicated Fbw7 isoform were treated with the protein synthesis inhibitor cycloheximide and their turnover was monitored over time by immunoblotting. The turnover of the b and g isoforms is inhibited when cells are also treated with a proteasome inhibitor, LLnL (Figure 3.1B, lanes 5-8, p103), suggesting that they are targeted for proteasome-mediated degradation.

The Fbw7 isoforms arise from the use of a unique first exon, but are otherwise identical [174]. We chose to focus our studies on the degradation of Fbw7-γ, as this protein has proposed roles in targeting cyclin E and c-Myc for degradation in cancer cells [133, 212]. We reasoned that the unique N-terminal domain of Fbw7-γ might be responsible for its protein stability characteristics. As predicted, the unique N-terminal fragment of Fbw7-γ mimics the turnover of its full-length counterpart, with a nearly identical half-life (Figure 3.1C, p105). These results indicate that turnover of Fbw7-γ is not controlled by an autoubiquitination mechanism that has been shown for other F-box proteins [65]. However, when the lysines in γ isoform N-terminal fragments are

mutated, the protein is significantly stabilized (Figure 3.1D, p105), consistent with a model in which Fbw7-γ is targeted for degradation by the ubiquitin proteasome pathway.

As Fbw7 targets include cell cycle regulatory proteins (reviewed in [238]), we examined whether Fbw7-γ turnover might be controlled in cell cycle-dependent manner. Interestingly, turnover of Fbw7-γ is likely to fluctuate during the cell cycle as we observe distinct half-lives for the protein when cells are either arrested in S phase by treatment with hydroxyurea (HU) or in G2 by treatment with nocodazole (Figure 3.1E, see 105). Fbw7-γ is still unstable in HU-treated cells, although it is not turned over as quickly as in an asynchronous culture, which is likely to have a significant G1 population. By contrast, the Fbw7-γ protein is largely stabilized in nocodazole-treated cells. These results suggest that there is likely to be a requirement for $SCF^{Fbw7-\gamma}$ activity during G2 or M phase of the cell cycle.

Identification of SLP1 as an Fbw7-γ specific interaction partner that inhibits Fbw7-γ turnover

We hypothesized that regulation of Fbw7-γ protein stability would be controlled via isoform-specific binding partners that were able to recognize its unique N-terminus. To find isoform-specific interaction partners for Fbw7-γ, we used a two-hybrid screen using the Fbw7-γ unique N-terminal domain as bait. We identified a novel interactor, SLP1 (stomatin-like protein 1) using a HeLa cDNA library (Figure 3.2A, see p107). SLP1 is a stomatin-like protein and is not well characterized [242]. Stomatins and stomatin-like proteins have been proposed to function in neuronal

signaling in other systems [243, 244], but a function for SLP1 has not been identified. The specific interaction between Fbw7-γ and SLP1 was confirmed by reciprocal co-immunoprecipitation experiments (Figure 3.2B, see p107). Moreover, the co-immunoprecipitation occurred even when only the N-terminal fragment of Fbw7-γ was expressed.

We next examined whether Fbw7-γ and SLP1 were co-localized. Cells expressing both proteins were fractionated into cytoplasmic and nuclear extracts and then probed for the presence of Fbw7-γ or SLP1. The localization of Fbw7-γ has been reported as either nuclear or nucleolar, depending on cell type [133, 210], whereas stomatin-like proteins are predicted to be cytoplasmic [245]. We observed that Fbw7-γ is found predominantly in the nuclear fraction but that there is a substantial cytoplasmic population as well (Figure 3.2C, lanes 3 and 4, p107). Likewise, SLP1 was enriched in the cytoplasmic fraction, but retained a sizable population in the nucleus (Figure 3.2C, lanes 1 and 2, p107). Strikingly, SLP1 exhibited a ladder of higher molecular weight forms, which were most obvious in the cytoplasmic fraction. The nature of these modified forms remains to be determined. A cytoplasmic protein, alpha-tubulin, was used as a control to verify the quality of the fractionation. To determine whether Fbw7-γ and SLP1 interact in either the nucleus or cytoplasm, we performed co-immunoprecipitations using the nuclear and cytoplasmic extracts. As shown in Figure 3.2D, SLP1 and Fbw7-γ co-precipitate in both fractions, suggesting that they are able to interact in both the nucleus and cytoplasm.

To determine whether SLP1 had an effect on Fbw7-γ protein turnover, we performed protein stability assays in 293T cells overexpressing these proteins. When

SLP1 and Fbw7-γ are co-overexpressed, Fbw7-γ turnover is inhibited, increasing its 60-minute half-life at least three-fold (Figure 3.2E, p107). Thus, we conclude that SLP1 is a specific interaction partner for Fbw7-γ that binds Fbw7-γ's unique N-terminal domain and can interfere with Fbw7-γ proteolysis when overexpressed.

SLP1 is controlled by proteolysis

During our studies on the turnover of Fbw7-γ, we noticed that SLP1 itself is an unstable protein and that its degradation largely correlates with Fbw7-γ proteolysis. As shown in Figure 3.3A, in cycloheximide-treated cells, SLP1 is unstable and has a half-life of 2.5 hours. The turnover of SLP1 can be blocked by addition of the proteasome inhibitor LLnL. We examined the turnover of SLP1 in relation to Fbw7-γ and we find that SLP1 is also unstable in HU-treated cells but stabilized in nocodazole-treated cells similar to Fbw7-γ (Figure 3.3B, p109). These results suggest that proteolysis of Fbw7-γ and SLP1 may be coordinately regulated.

Cdk2 regulates both Fbw7-γ and SLP1 proteolysis

Our limited cell cycle analysis of Fbw7-γ and SLP1 proteolysis suggested that both of these proteins are likely unstable during G1 and S phases of the cell cycle. Since Cdk2 activity is highest during G1 and S, we examined whether Cdk2 might be involved in the regulation of Fbw7-γ and SLP1 degradation. In cells treated with Cdk2-specific siRNA, we find that the abundance (Figure 3.4A, p111) and stability (Figure 3.4B, p111) of SLP1 protein is increased compared to those cells treated with control siRNAs. Likewise, the turnover of Fbw7-γ is also decreased when Cdk2 is

inhibited by siRNA (Figure 3.4C, p113). By contrast, overexpression of Cdk2 accelerated the turnover of the Fbw7-γ protein, decreasing the 60-minute half-life to 180 minutes (Figure 3.4D, p113). The effect of Cdk2 was dependent on its kinase activity, as a kinase-dead mutant failed to produce the same result when overexpressed (Figure 3.4D, p113). Together, these results indicate that Cdk2 activity promotes the turnover of both Fbw7-γ and SLP1 and that Cdk2 and SLP1 have opposing effects on Fbw7-γ protein turnover.

Cdk2 interacts with both Fbw7-γ and SLP1

If Cdk2 directly regulates Fbw7-γ and SLP1 proteolysis, we would expect Cdk2 to form a complex with these proteins. To test this idea, we performed immunoprecipitations using protein extracts from HEK293T cells expressing epitope-tagged versions of Cdk2, Fbw7-γ and SLP1. As shown in Figure 3.5A (p115), Cdk2 and SLP1 co-immunoprecipitate and we find that the interaction is observed in reciprocal immunoprecipitations. In addition, we find that Cdk2 and Fbw7-γ also interact using reciprocal immunoprecipitations. Because cyclin E is proposed to be a target of Fbw7-γ, it is possible that Cdk2 may interact indirectly with Fbw7-γ as part of a complex with cyclin E as cyclin E is being targeted for ubiquitination. Fbw7 substrates bind the WD40 domain found in the C-terminal portion of the protein, a region common to all Fbw7 isoforms. If Cdk2 controls Fbw7-γ proteolysis distinct from its role in cyclin E ubiquitination, we reasoned that Cdk2 might bind the unique N-terminal domain of Fbw7-γ. To test this, we co-expressed Cdk2 and the Fbw7-γ unique N-terminal fragment and then performed co-immunoprecipitation experiments.

Under these conditions, we also observe co-immunoprecipitation of Cdk2 and the Fbw7-γ unique N-terminal domain (Figure 3.5B, p115), consistent with a separate role for Cdk2 in Fbw7-γ turnover. Together, our results indicate that Cdk2 can interact with both SLP1 and Fbw7-γ, although we cannot determine whether all three proteins are in a complex simultaneously from these data. Moreover, both Cdk2 and SLP1 interact with the unique N-terminal domain of Fbw7-γ, indicating that these interactions are part of an isoform-specific regulatory pathway.

We next asked whether SLP1 binds Cdk2 and Fbw7-γ using the same domain or distinct motifs. As shown in Figure 3.5C (p117), SLP1 contains a hydrophobic region in the N-terminal half of the protein, which in other stomatin family members is thought to be a membrane association domain (MAD) [245]. SLP1 also contains two consensus CDK phosphorylation sites, at S34 and S285. We generated three mutants that disrupted these regions: 1) S34A, a serine to alanine mutation at residue 34, 2) ΔSPK, an in-frame deletion of residues 285-287, and 3) ΔMAD, an in-frame deletion of the MAD motif (residues 48-79) to test whether any of these domains contributed to Cdk2 or Fbw7-γ binding. All three mutants exhibited equivalent protein expression levels (Figure 3.5D, top panel, S34A mutant not shown, p117), suggesting that the mutations do not dramatically disrupt the overall folding of the SLP1 protein. We next performed co-immunoprecipitation assays with epitope-tagged Cdk2 and Fbw7-γ. Using this approach, we find that the SLP1ΔMAD mutant co-precipitates less efficiently with Cdk2 whereas neither of the other two mutants exhibits any distinguishable changes in binding (Figure 3.5D, left panel, p117). Binding of Cdk2 and to the SLP1 S34A mutant is indistinguishable from binding to wildtype SLP1

(data not shown). By contrast, all three SLP1 mutants bind Fbw7-γ as efficiently as wildtype SLP1. (Figure 3.5D, right panel, p117). From these data, we conclude that distinct domains participate in SLP1 association with Cdk2 and Fbw7-γ. The MAD motif contributes to the interaction with Cdk2, whereas an as yet unidentified domain is required to bind Fbw7-γ.

Cdk2 promotes SLP1 turnover, releasing Fbw7-γ for targeted destruction

Our results are consistent with a model in which Cdk2 promotes the degradation of both SLP1 and Fbw7-γ, whereas SLP1 protects Fbw7-γ from being degraded. We tested this model by co-overexpressing Cdk2 and SLP1 and examined the effect on Fbw7-γ stability (Figure 3.6A, p119). When both Cdk2 and SLP1 are overexpressed Fbw7-γ is turned over as efficiently as when Fbw7-γ is expressed alone. This result indicates that Cdk2's positive role overcomes SLP1's inhibitory role in the degradation of Fbw7-γ. In addition, the effect of Cdk2 is dependent on its kinase activity as Fbw7-γ turnover when SLP1 and the Cdk2 kinase-dead mutant are co-overexpressed mimics the degradation rate observed when just SLP1 is overexpressed.

It is not clear if Cdk2 acts only on SLP1 to promote its degradation, which then releases Fbw7-γ to be targeted for destruction or whether Cdk2 acts independently on both SLP1 and Fbw7-γ. To distinguish between these two possibilities, we used the SLP1 ΔMAD mutant, which exhibits decreased Cdk2 binding but it still competent for association with Fbw7-γ. We anticipated that the SLP1 DMAD mutant protein would be stabilized because it no longer interacts efficiently with Cdk2. As shown in Figure 3.6B (p119), when a cycloheximide-based stability assay is performed, this is

precisely what we observe. We then examined the stability of Fbw7-γ when both Cdk2 and the SLP1ΔMAD mutant are co-overexpressed. In this situation, we find that Fbw7-γ is partially stabilized, suggesting that the SLP1ΔMAD mutant mitigates the Cdk2-dependent acceleration of Fbw7-γ turnover. This result is most consistent with a model in which Cdk2 first acts on SLP1 to promote its turnover, thus releasing Fbw7-γ to be targeted for destruction (Figure 3.6C, p121).

Discussion

We have identified a novel regulatory pathway that controls Fbw7-γ degradation in transformed cells. We show that SLP1 is an isoform-specific interaction partner for Fbw7-γ that can protect Fbw7-γ from proteolysis. Moreover, SLP1 is also targeted for destruction in a pathway that is coordinately regulated with Fbw7-γ degradation by the activity of Cdk2.

The full contributions of the individual isoforms of Fbw7 to cell cycle control are not understood. Recent work from the Clurman group suggests that Fbw7-α is primarily responsible for targeting the cell cycle targets of Fbw7 such as cyclin E and c-Myc, at least in HCT116 cells [246] even though this contradicts earlier work suggesting Fbw7-γ specifically targets c-Myc in nucleoli [133]. By contrast, results from the Reed group indicate that Fbw7-γ has an important role in cyclin E turnover, particularly in cell lines that have low cyclin E levels, whereas Fbw7-α is primarily responsible for cyclin E ubiquitination in cell lines with high cyclin E levels [241]. Our work does not directly address this issue, but the observations that Fbw7-γ turnover is dependent on Cdk2, that Fbw7-γ half-life changes in cells arrested at

distinct cell cycle stages, and that Cdk2 binds Fbw7-γ in its unique N-terminal domain are consistent with a cell cycle-dependent role for Fbw7-γ, at least in some transformed cell lines. If this is indeed the case, then we expect an $SCF^{Fbw7-\gamma}$ complex to have a G2 or M phase-specific substrate, as this is when Fbw7-γ appears to be most stable.

It is not known which E2/E3 complex targets Fbw7-γ or SLP1 for ubiquitination. The ubiquitin-mediated degradation of Fbw7-γ is not the result of an autocatalytic mechanism, as has been observed with some F-box proteins [65], because the unique N-terminal domain is required for turnover and this N-terminal fragment exhibits the same half-life as the full-length protein. In addition, deletion of the F-box domain from Fbw7-γ does not stabilize the protein, as would be expected for an autocatalytic means of destruction. We think it is unlikely that SLP1 is a target of an $SCF^{Fbw7-\gamma}$ complex because SLP1 does not bind the WD40 region as other substrates do and overexpression of Fbw7-γ has no effect on SLP1 stability (W. Zhang and D.M. Koepp, unpublished observations). We look forward to future studies that might identify the pathways responsible for both SLP1 and Fbw7-γ turnover.

Turnover of both Fbw7-γ and SLP1 is dependent on Cdk2 kinase activity, but is not clear whether either of these proteins is phosphorylated by Cdk2. Mutation of the two consensus CDK sites in SLP1 has little effect on the protein's function with respect to Fbw7-γ turnover and Fbw7-γ does not contain any CDK consensus sites in the unique N-terminal domain. One possibility is that additional proteins associate with the Fbw7-γ unique N-terminus that may be part of this regulatory pathway. Our two-hybrid screen did identify other Fbw7-γ-specific interaction partners, but their

effect on Fbw7-γ turnover has not been determined (E.M. MacDonald, W. Zhang, and D.M.Koepp, unpublished observations).

The identification of SLP1 as an interaction partner for Fbw7-γ was unexpected, as there was previously no evidence of stomatin family members interacting with SCF ubiquitin ligases in human cells or other systems. SLP1 is conserved from invertebrates to humans [242, 247] and the *C. elegans* homolog, *unc-24*, is proposed to have a role in neural function [243, 244]. Interestingly, human SLP1 mRNA expression is highest in neuronal tissue as is Fbw7-γ mRNA expression [174, 242], indicating that the proteins are likely expressed in the same type of cells.

How SLP1 inhibits Fbw7-γ turnover is an open question, but it seems likely that it could be via physically blocking access to the N-terminal domain of Fbw7-γ, which we show to be required for turnover. One possibility is that SLP1 inhibits Fbw7-γ turnover because it is a co-factor for the SCF ubiquitin ligase complex with a particular substrate protein. Such co-factors have been identified with other SCF-type complexes, such as Cks1 is required for the SCF^{Skp2}- mediated ubiquitination of p27 [206, 207].

It is not clear whether the Fbw7-γ-SLP1 interaction is most physiologically relevant in the nucleus or cytoplasm nor is it known whether Fbw7-γ and SLP1 proteolysis is localization-dependent. Previous work suggested that Fbw7-γ was a nuclear/nucleolar protein, although this conclusion was the result of steady-state immunofluorescence and GFP studies [133]. Our co-fractionation studies suggest that a fraction of the Fbw7-γ protein population is located in the cytoplasm and it is tempting to speculate that the protein may shuttle between the nucleus and cytoplasm.

In addition, it has been demonstrated that Cdk2 localizes to both the nucleus and cytoplasm [248], so in principle the interaction between Cdk2 and these proteins might occur in either compartment.

Together, our studies indicate that Fbw7-γ turnover is proteasome- and cell cycle-dependent. SLP1 is a novel Fbw7-γ specific interaction partner that binds the unique N-terminal domain of Fbw7-γ and blocks its degradation. SLP1 is also targeted for proteolysis and the timing of its degradation mimics that of Fbw7-γ. Cdk2 activity promotes the turnover of both Fbw7-γ and SLP1 and we propose a model in which Fbw7-γ and SLP1 are coordinately targeted for ubiquitin-mediated degradation by Cdk2 kinase activity.

Materials and Methods

Cell culture and reagents

HEK293T and Hela cells were maintained in Dulbecco's Modified Eagle's Medium (HyClone) with 10% Newborn Bovine Serum (Atlanta Biologicals), with 5% CO2.

Cell transfection and infection

HEK293T cells were transfected with Lipofectamine2000 (Invitrogen) according to manufacturer's instructions. 40 hours after transfection, cells were washed with PBS (137mM NaCl, 2.7mM KCl, 10mM Na_2HPO_4, 2mM KH_2PO_4) and collected. Transfections of siRNA (Dharmacon) used Lipofectamine RNAiMAX (Invitrogen) according to manufacturer's instructions.

Generation of expression constructs

Fbw7 isoform constructs have been described [249]. SLP1 and SLP1$^{\Delta MAD}$, SLP1 $^{\Delta SPK}$, SLP1 ^{S34A} mutants were cloned using EcoRI and SalI sites in p3xFlag-CMV 7.1 vector (Sigma). Myc-tagged SLP1 and Fbw7 were cloned into pCS2+Myc vector or pcDNA3.1Myc/His vector. The deletion mutants of Fbw7γ were cloned into p3X FLAG-CMV 7.1 expression vector (Sigma) by two-step PCR. A complete list of the constructs and primers used in this study are shown Table 1 and Table 2, respectively.

Western Blot Analysis and reagents

Cell lysates were prepared in NETN buffer (20mM Tris pH 8.0, 100mM NaCl, 1mM EDTA, 0.5% NP-40) containing 1mM NaF, 2.5mM β-glycerophosphate and protease inhibitor cocktail (Roche Applied Science). Protein concentrations were determined by the Bio-Rad protein assay (Bio-Rad Laboratories, Inc). Cell lysates were resolved by SDS-PAGE and electrophoretically transferred to nitrocellulose membrane. Membranes were blocked in PBST (137mM NaCl, 2.7mM KCl, 10mM Na_2HPO_4, 2mM KH_2PO_4, 0.5% Tween-20) containing 5% milk for at least 40 minutes at room temperature. Blots were probed with primary antibodies followed by labeling with horseradish peroxidase conjugated anti-mouse or anti-rabbit secondary antibody (Jackson Immunoresearch). Following antibody incubation, blots were developed on film using an Enhanced Chemiluminescence kit (PIERCE) according to the manufacturer's instructions. Densitometry of immunoblot bands was measured using NIH ImageJ. The primary antibodies used included: anti-Cdk2 antibody (M2, Santa Cruz), anti-Flag M2 antibody (Sigma), anti-HA (HA.11, Covance Research), anti-Myc (9E10, Covance Research), anti-cyclin E (HE-12, Santa Cruz), anti-GAPDH (Abcam), anti-tubulin (a generous gift from Dr. Sean Conner).

Two-hybrid screen

The screen used the pretransformed HeLa cDNA library with the Matchmaker kit (Clontech) and was performed according to manufacturer's instructions. Beta-galactosidase assays were performed as described [250].

Co-immunoprecipitation assays

Cells were lysed with NETN lysis buffer, and 200-500μl of cell lysate was incubated with antibody at 4°C for 4 hours, then 20μl of protein A/G agarose slurry (Santa Cruz Biotechnology) was added for another 2 hours or overnight. The beads were washed three times with at least 10 volumes of NETN lysis buffer before resolving by SDS-PAGE.

Protein stability assays

HEK293T cells were transfected with the construct(s) of interest. 36 to 40 hours after transfection, cycloheximide (Sigma) was added to a final concentration of 20μg/ml to stop protein synthesis. Cell extracts from each time point were analyzed by Western blotting. For proteasome inhibition, LLnL was added to the cells at 50μg/ml (Sigma) 5 hours before the stability assay.

Protein fractionation assay

$2x10^6$ transfected cells were harvested and washed twice with ice-cold PBS followed by resuspension in buffer A (10mM HEPES-K^+ pH7.5, 10mM KCl, 1.5mM $MgCl_2$, 0.5mM DTT) in the presence of protease inhibitor cocktail (PIC). Cells were pelleted by spinning at 1000×rpm 5 min and lysed in ice-cold buffer A containing 0.5% NP-40 with PIC on ice for 10 min. The nuclei were pelleted at 3,000 rpm 2 min at 4°C.

The supernatant was collected as the cytoplasmic fraction. Nuclear pellets were washed with buffer A and then resuspended in buffer C (20mM HEPES-K^+ pH7.9, 420mM NaCl, 0.2mM EDTA, 1.5mM $MgCl_2$, 0.5mM DTT, 25% Glycerol) with PIC. Nuclei were incubated on ice for another 30 min with occasional vortex. Supernatant containing nuclear protein was collected by spinning at 14,500rpm for 10 min at 4°C.

Cell synchronization

Cells were transfected with constructs of interest using Lipofectamine 2000 (Invitrogen). 40 hours after transfection, cells were split to 25% confluence and incubated for 12 hours prior to addition of hydroxyurea (2mM, US Biological) or nocodazole (100ng/ml, Sigma) for 24 hours.

Conflict of Interest Statement

The authors declare that there are no conflicts of interest.

Acknowledgments

This work was funded by the NIH grant GM076663 and awards from the V Foundation for Cancer Research, the Leukemia Research Fund, and the American Cancer Society Institutional research grant (University of Minnesota) to DMK.

Table 1, Plasmids used in this study

Name	Description	Reference
pFlag-Fbw7γ	CMV promoter, Flag-Fbw7α	[130]
pFlag-Fbw7γ	CMV promoter, Flag-Fbw7γ	[130]
p3xFlag-Fbw7γ unique	CMV promoter, Flag-Fbw7γ residues 1-49	This study
p3xFlag-Fbw7γ $^{K\ to\ A}$	CMV promoter, Flag-Fbw7γ K3A K6A K19A K22A K32A	This study
p3xFlag-Fbw7γ ΔF box	CMV promoter, Flag-Fbw7γ D166-206	This study
p3xFlag-Fbw7 common	CMV promoter, Flag-Fbw7 residues 50-589	This study
pCS2+MT Fbw7γ	CMV promoter, 6MYC-Fbw7γ	This study
pCS2+MT Fbw7 unique	CMV promoter, 6MYC-Fbw7γ residues 1-49	This study
p3xFlag-SLP1	CMV promoter, Flag-SLP1	This study
p3xFlag-SLP1$^{\Delta MAD}$	CMV promoter, Flag-SLP1 D48-79	This study
p3xFlag-SLP1$^{\Delta SPK}$	CMV promoter, Flag-SLP1 D285-287	This study
p3xFlag-SLP1^{S34A}	CMV promoter, Flag-SLP1 S34A	This study
pCS2+MT-SLP1	CMV promoter, 6MYC-SLP1	This study
HA-Cdk2	CMV promoter, HA-Cdk2	[251]
HA-Cdk2-DN	CMV promoter, HA-Cdk2 D146N	[251]
pAS2-Fbw7γ unique	*ADH1* promoter, *GAL4*(1-147) HA- Fbw7γ residues 1-49 *TRP1*	This study

Figure3.1. **Fbw7-γ is an unstable protein and its proteolysis is dependent on the proteasome**

A) Diagram of Fbw7 isoforms. The F-box motif and WD40 repeats are marked as shown.

B) Fbw7-γ and β are unstable proteins, and their degradation is proteasome-dependent. The Fbw7 isoforms were expressed in HEK293T cells and protein stability assays were performed as described in Materials and Methods. Quantitation of a representative experiment is shown in the graph.

Figure3.1. Fbw7-γ is an unstable protein and its proteolysis is dependent on the proteasome

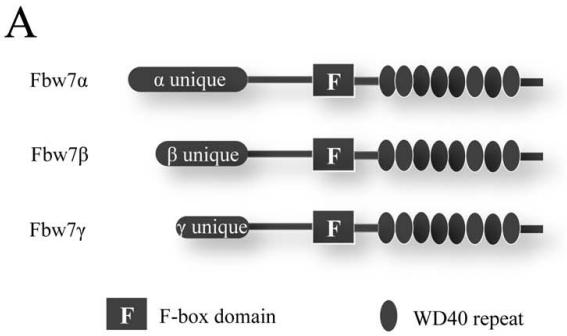

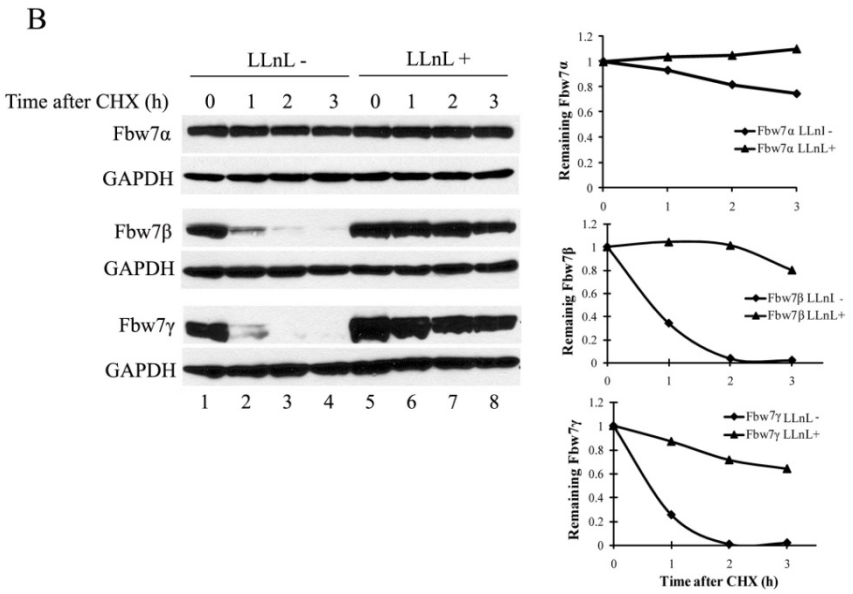

C) The N-terminal unique region is critical for Fbw7-γ degradation. Protein stability assays were performed as described in (B) with cells expressing the indicated proteins. Quantitation of a representative experiment is shown in the graph.

D) The lysine residues within the unique region of Fbw7-γ are critical for degradation. Protein stability assays were performed as described in (B) with cells expressing the indicated proteins. Quantitation of a representative experiment is shown in the graph.

E) Fbw7-γ turnover is regulated in a cell cycle-dependent manner. Protein stability assays were performed as described in (B) with cells expressing the indicated proteins except that cells were arrested in hydroxyurea (lanes 5-8) or nocodazole (lanes 9-12) for 24 hours to synchronize cells. Quantitation of a representative experiment is shown in the graph.

C

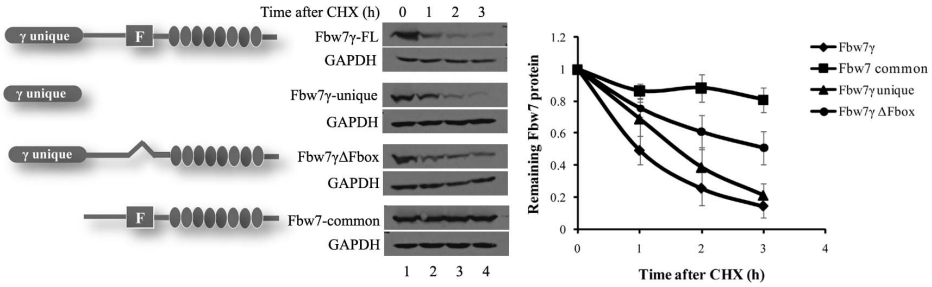
Time after CHX (h) 0 1 2 3
γ unique
F
Fbw7γ-FL
GAPDH
γ unique
Fbw7γ-unique
GAPDH
γ unique
Fbw7γΔFbox
GAPDH
F
Fbw7-common
GAPDH
1 2 3 4
Remaining Fbw7 protein
Time after CHX (h)
Fbw7γ
Fbw7 common
Fbw7γ unique
Fbw7γ ΔFbox

D

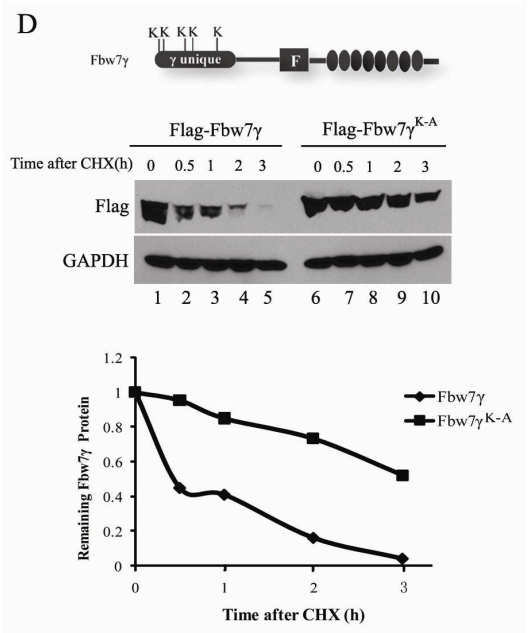
Fbw7γ
KK KK K
γ unique
F
Flag-Fbw7γ
Flag-Fbw7γ K-A
Time after CHX(h) 0 0.5 1 2 3 0 0.5 1 2 3
Flag
GAPDH
1 2 3 4 5 6 7 8 9 10
Remaining Fbw7γ Protein
Time after CHX (h)
Fbw7γ
Fbw7γ K-A

E

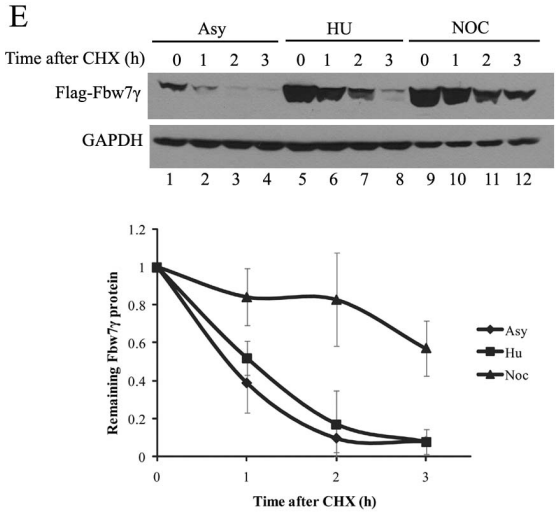
Asy
HU
NOC
Time after CHX (h) 0 1 2 3 0 1 2 3 0 1 2 3
Flag-Fbw7γ
GAPDH
1 2 3 4 5 6 7 8 9 10 11 12
Remaining Fbw7γ protein
Time after CHX (h)
Asy
Hu
Noc

Figure3.2. SLP1 is an Fbw7-γ-specific interacting protein.

A) SLP1 was identified using a yeast two-hybrid screen. Representative beta-galactosidase assay with SLP1 positive colony (line 1) and vector control (line 2).

B) Fbw7-γ co-immunoprecipitates (co-IP) with SLP1. Flag tagged SLP1 was co-expressed with Myc-tagged Fbw7-γ (lane1) or vector (lane2) in HEK293T cells. Immunoprecipitation was performed as described in Materials and Methods. Reciprocal co-IP is shown in the right panel (lanes 3, 4).

C) SLP1 and Fbw7-γ co-fractionate. Standard fractionation assays were performed as described in Materials and Methods. Tubulin, a cytosolic protein, was used as a control.

D) SLP1 and Fbw7-γ co-immunoprecipitate in both nuclear and cytosolic fractions. Co-IPs were performed as in (B), except that cellular fractions from (C) were used.

E) SLP1 inhibits Fbw7-γ turnover. Fbw7 γ was co transfected with SLPL1 (lane 1-4) or empty vector (lane 5-8) into HEK293T cells and protein stability assays were performed as described in Materials and Methods. Quantitation of three independent experiments is shown on the graph. Error bars indicate standard deviations.

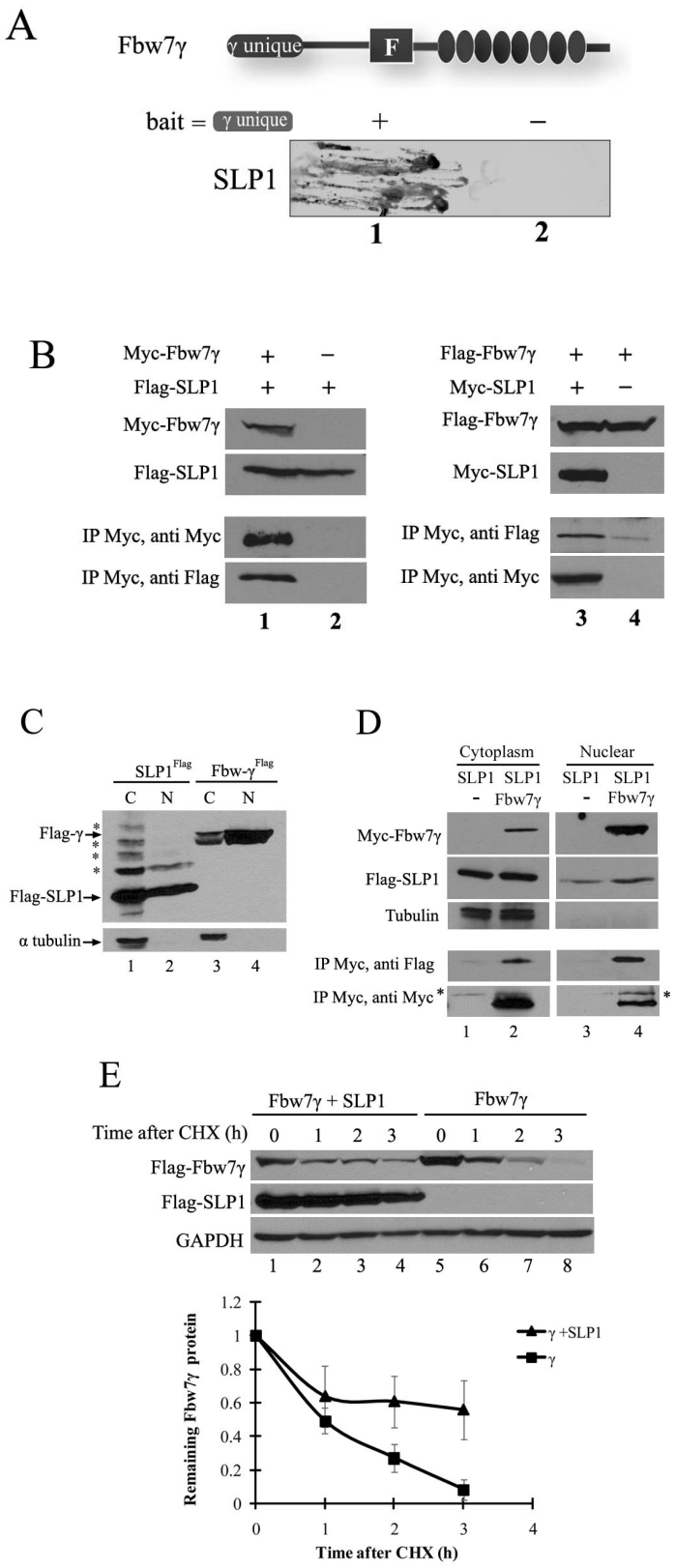
A
Fbw7γ
γ unique
F
bait = γ unique
+
–
SLP1
1
2
B
Myc-Fbw7γ + –
Flag-SLP1 + +
Myc-Fbw7γ
Flag-SLP1
IP Myc, anti Myc
IP Myc, anti Flag
1 2
Flag-Fbw7γ + +
Myc-SLP1 + –
Flag-Fbw7γ
Myc-SLP1
IP Myc, anti Flag
IP Myc, anti Myc
3 4
C
SLP1Flag
Fbw-γFlag
C N C N
Flag-γ
Flag-SLP1
α tubulin
1 2 3 4
D
Cytoplasm
Nuclear
SLP1 SLP1 SLP1 SLP1
- Fbw7γ - Fbw7γ
Myc-Fbw7γ
Flag-SLP1
Tubulin
IP Myc, anti Flag
IP Myc, anti Myc
1 2 3 4
E
Fbw7γ + SLP1
Fbw7γ
Time after CHX (h) 0 1 2 3 0 1 2 3
Flag-Fbw7γ
Flag-SLP1
GAPDH
1 2 3 4 5 6 7 8
Remaining Fbw7γ protein
1.2
1
0.8
0.6
0.4
0.2
0
0 1 2 3 4
Time after CHX (h)
γ +SLP1
γ

Figure3.3. SLP1 is an unstable protein.

A) SLP is an unstable protein, and its proteolysis is proteasome-dependent. Protein stability assays in cells expressing SLP1 were performed as described in Materials and Methods. Quantitation of a representative experiment is shown in the graph.

B) SLP1 turnover is regulated in a cell cycle-dependent manner. Protein stability assays were performed as in (A), except that hydroxyurea (lanes 5-8) or nocodazole (lanes 9-12) was added to synchronize cells for 24 hours. Quantitation of three independent experiments is shown on the graph. Error bars indicate standard deviations.

Figure3.3. SLP1 is an unstable protein.

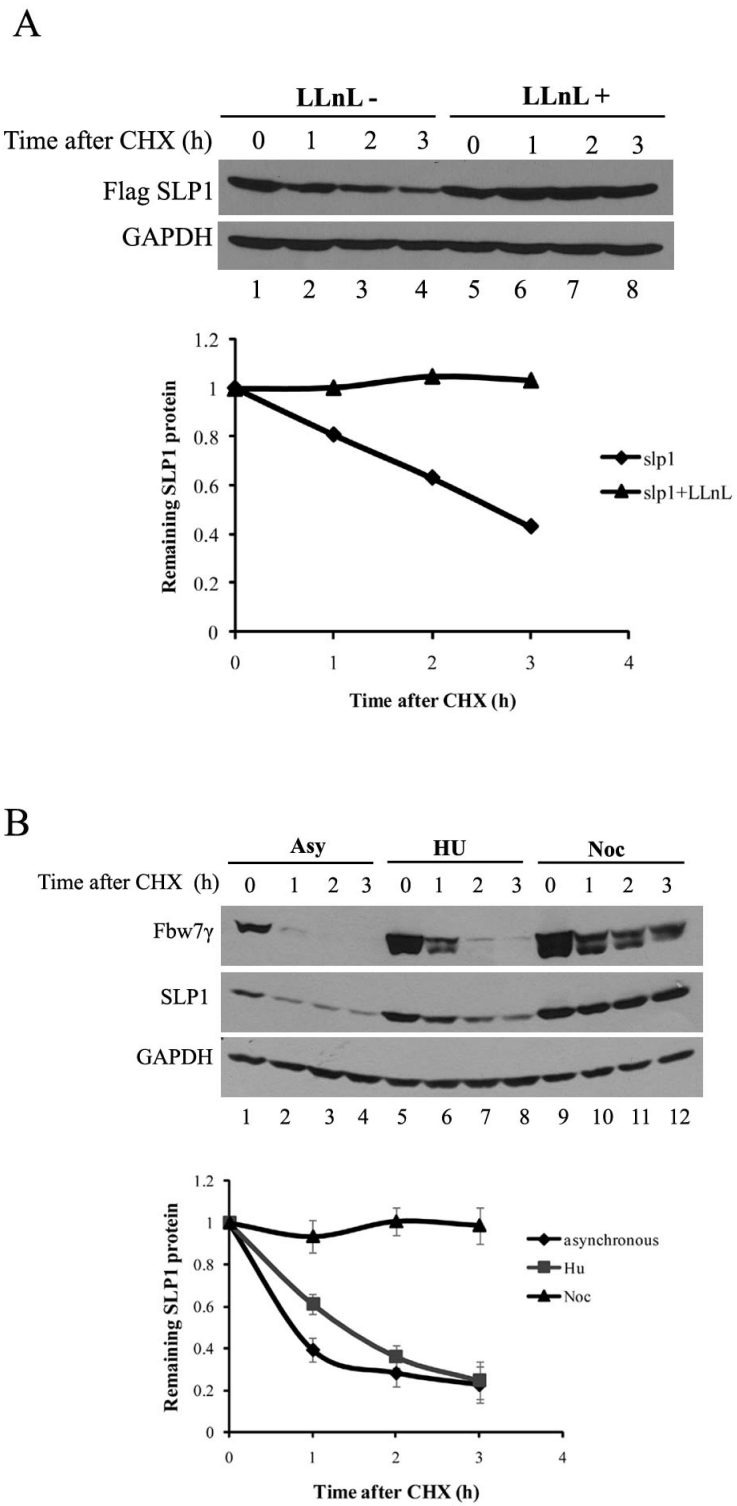

Figure3.4. Cdk2 promotes SLP1 and Fbw7-γ turnover.

A) Abundance of SLP1 is increased protein abundance when Cdk2 is inhibited by siRNA. Cells expressing Flag-tagged SLP1 were transfected with either Cdk2 siRNA (lane 1) or control siRNA (lane 2). Quantitation of three independent experiments is shown on the graph. Error bars indicate standard deviations.

B) SLP1 shows increased protein stability when Cdk2 was knocked down by siRNA. Cells were transfected as in (A) and standard stability assay was performed as described in Materials and Methods. Quantitation of a representative experiment is shown in the graph.

A

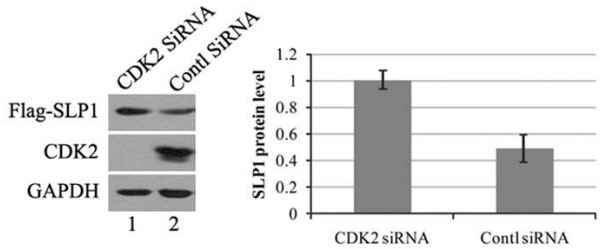
CDK2 SiRNA
Contl SiRNA
Flag-SLP1
CDK2
GAPDH
1 2
SLP1 protein level
1.2
1
0.8
0.6
0.4
0.2
0
CDK2 siRNA
Contl siRNA

B

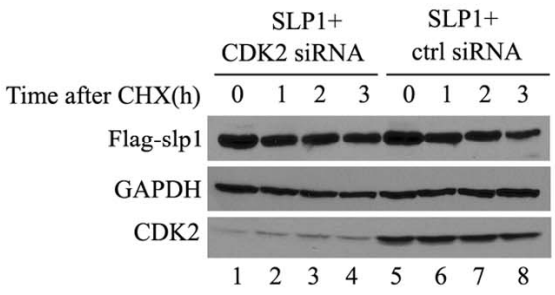
SLP1+
CDK2 siRNA
SLP1+
ctrl siRNA
Time after CHX(h) 0 1 2 3 0 1 2 3
Flag-slp1
GAPDH
CDK2
1 2 3 4 5 6 7 8

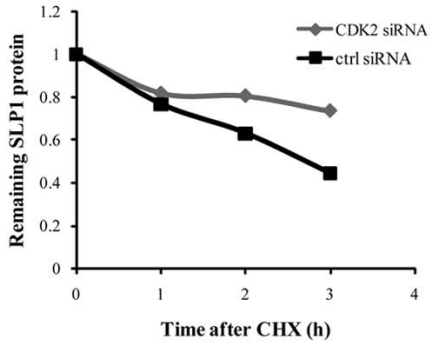
CDK2 siRNA
ctrl siRNA
Remaining SLP1 protein
1.2
1
0.8
0.6
0.4
0.2
0
0 1 2 3 4
Time after CHX (h)

Figure 3.4 (continue)

C) Fbw7-γ turnover is inhibited when Cdk2 is inhibited by siRNA. Cells were transfected as in (A) and standard stability assay was performed as described in Materials and Methods. Quantitation of a representative experiment is shown in the graph.

D) Fbw7-γ shows decreased protein stability when Cdk2 is co-expressed. Protein stability assays were performed as in (B) on cells expressing the indicated constructs. Quantitation of three independent experiments is shown on the graph. Error bars indicate standard deviations.

Figure3.4. Cdk2 promotes SLP1 and Fbw7-γ turnover.

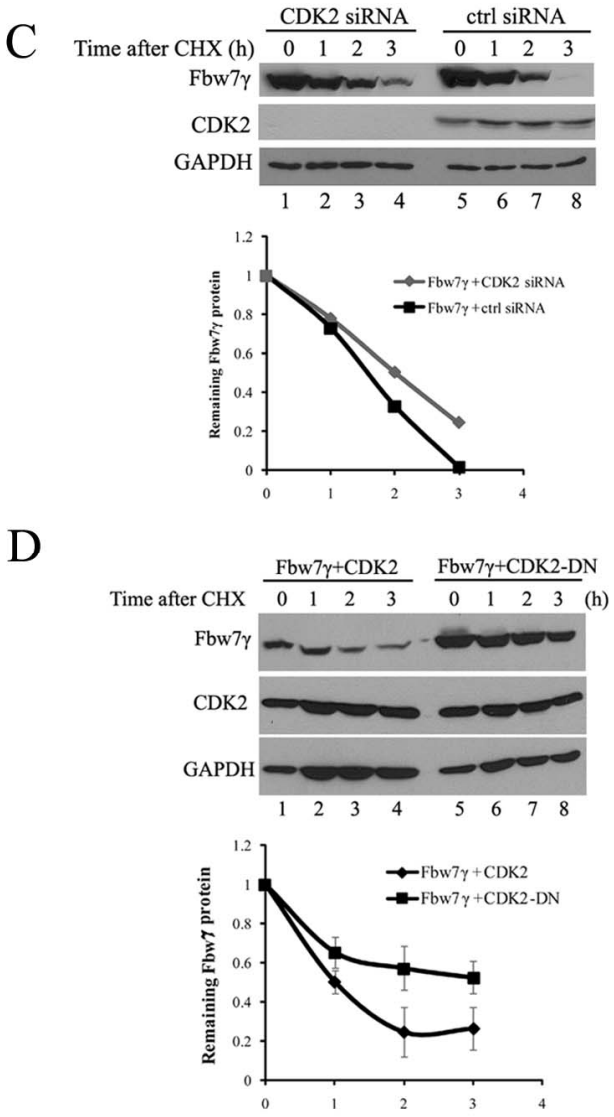

Figure3.5. SLP1 and Fbw7-γ interact with Cdk2.

A) SLP1 interacts with Cdk2. HA-tagged Cdk2 was transfected with Flag-tagged SLP1 or empty vector into HEK293T cells. Co-immunoprecipitations were performed as described in Materials and Methods.

B) Cdk2 interacts with Fbw7-γ. Co-IPs were performed as in (A) in cells expressing the indicated proteins.

A

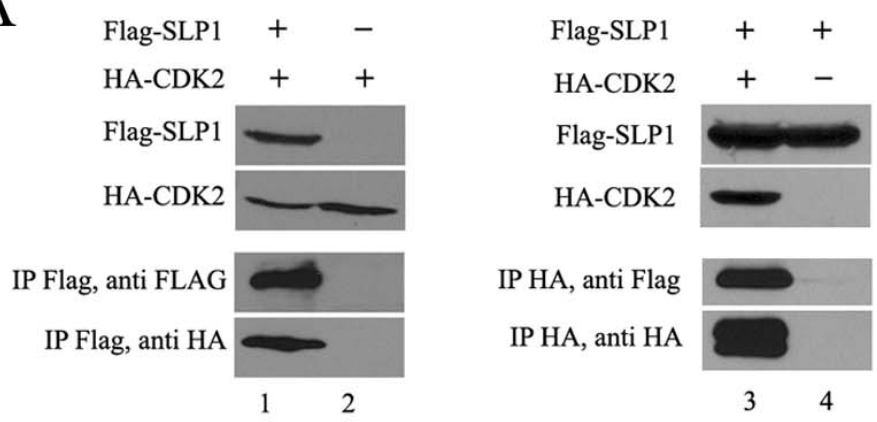
Flag-SLP1 + −
HA-CDK2 + +
Flag-SLP1
HA-CDK2
IP Flag, anti FLAG
IP Flag, anti HA
1 2
Flag-SLP1 + +
HA-CDK2 + −
Flag-SLP1
HA-CDK2
IP HA, anti Flag
IP HA, anti HA
3 4

B

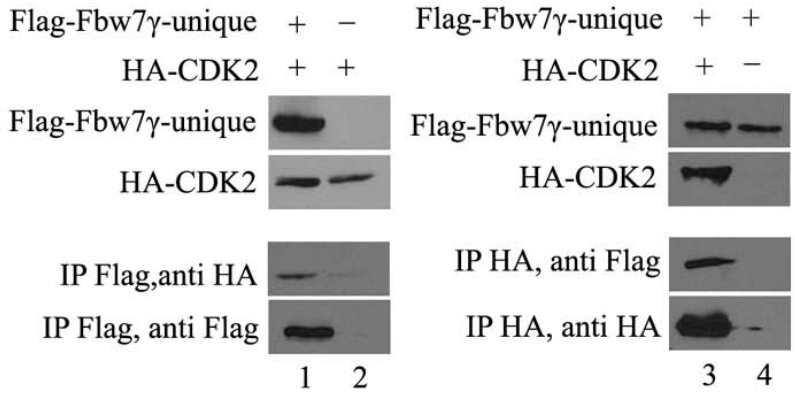
Flag-Fbw7γ-unique + −
HA-CDK2 + +
Flag-Fbw7γ-unique
HA-CDK2
IP Flag,anti HA
IP Flag, anti Flag
1 2
Flag-Fbw7γ-unique + +
HA-CDK2 + −
Flag-Fbw7γ-unique
HA-CDK2
IP HA, anti Flag
IP HA, anti HA
3 4

Fig 3.5 (continue)

C) Domain diagram of SLP1. Mutants generated for this study are indicated.

D) SLP1 interacts with Cdk2 and Fbw7-γ using different domains. $SLP1^{\Delta MAD}$ or $SLP1^{\Delta SPK}$ was co expressed with HA-tagged Cdk2 or empty vector (lanes 1-6). $SLP1^{\Delta MAD}$ or $SLP1^{\Delta SPK}$ was co expressed with Myc-tagged Fbw7-γ or empty vector (lanes 7-12). Co-IPs were performed as in (A).

Figure3.5. SLP1 and Fbw7-γ interact with Cdk2.

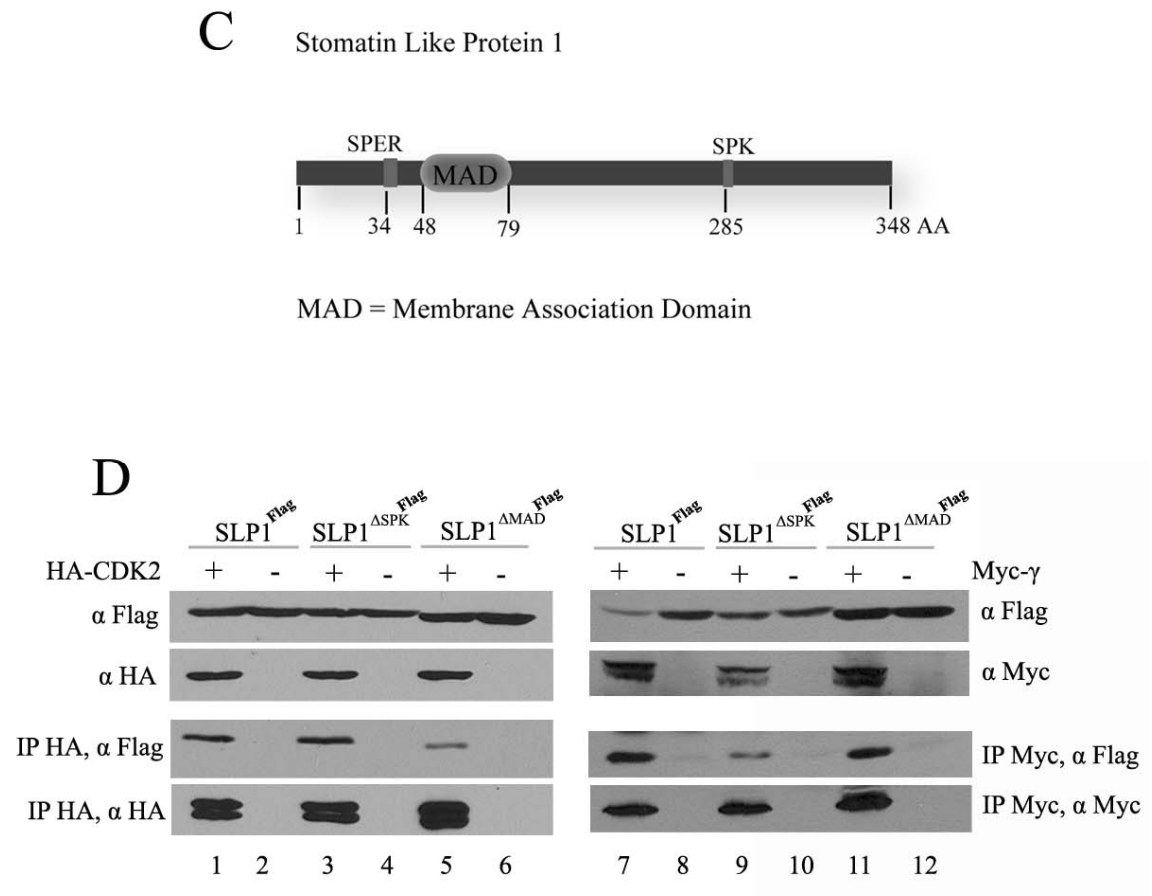

Figure3.6. Cdk2 regulates Fbw7-γ turnover through SLP1.

A) Cdk2 promotes Fbw7-γ turnover, regardless of SLP1 overexpression. Protein stability assays were performed as described in Materials and Methods in cells expressing the indicated proteins. Quantitation of a representative experiment is shown in the graph.

B) Cdk2-dependent acceleration of Fbw7-γ turnover is inhibited by the SLP1$^{\Delta MAD}$ mutant. Protein stability assays were performed as described in Materials and Methods in cells expressing the indicated proteins. Quantitation of a representative experiment is shown in the graph.

Figure3.6. Cdk2 regulates Fbw7-γ turnover through SLP1.

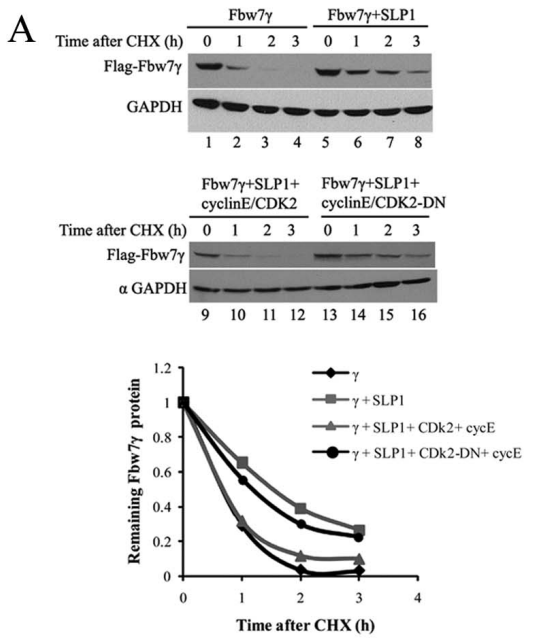

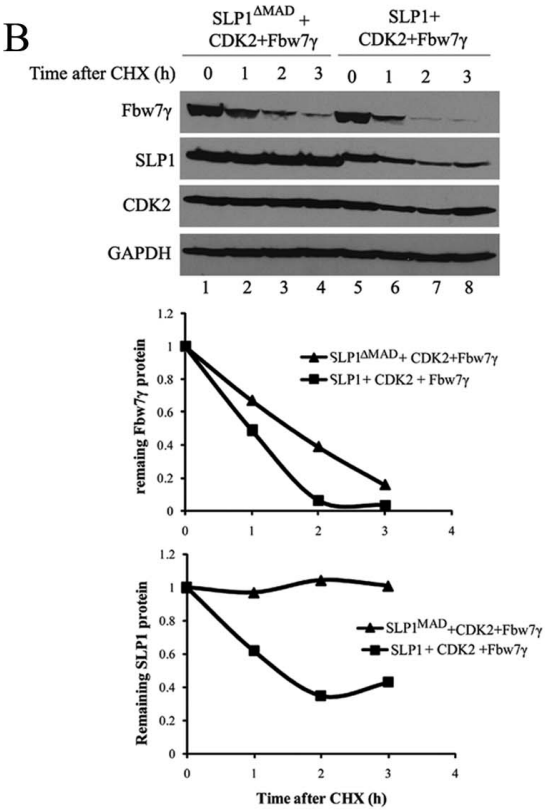

C) Model for regulation of Fbw7-γ turnover. SLP1 binds to the unique region of Fbw7-γ and stabilizes the protein. Cdk2/cyclin E complex interacts with SLP1 and facilitates both SLP1 and Fbw7-γ turnover.

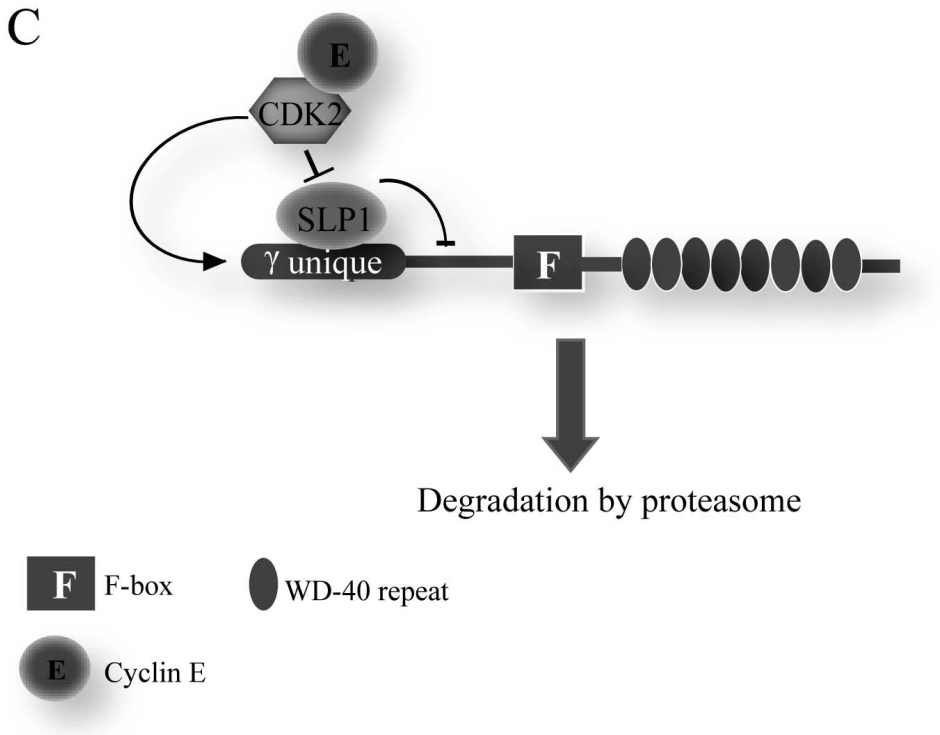
C
E
CDK2
SLP1
γ unique
F
Degradation by proteasome
F F-box
WD-40 repeat
E Cyclin E

Chapter IV.

Discussion and Future Perspectives

1. Fbw7

1.1 Fbw7 isoforms dimerization

Fbw7, an F-box component in the SCF^{Fbw7} E3 ligase, is one of the most important F-box proteins in humans, and it targets many protein substrates for ubiquitin dependent degradation. Since these substrates play critical roles in cell cycle regulation, transcription, and signal transduction, Fbw7 functions as a tumor suppressor. Thus, studies on how Fbw7 recognizes its substrates may provide significant insights on many aspects of biology.

It has been known that human Fbw7 has three isoforms, α, β, and γ, resulting from alternative splicing. They have distinct N-terminal regions, whereas the rest of the protein sequence is identical. It is well known that the F-box and WD40 motifs reside in the C-terminal common sequence, suggesting that the isoforms should have the same substrates. While expression of individual isoform mRNA shows some tissue specificity, they do exist in the same cell lines [174]. I am interested to figure out the biological relevance of the co-existence of more than one isoform especially when they seem to have no difference in substrate selectivity based on primary sequence.

We demonstrate that the three isoforms of Fbw7 can form dimers, either homo or hetero dimers through a region immediately upstream of the F-box motif, named D (dimerization) domain. This dimerization does not affect either Fbw7 binding to Skp1 (and presumably the rest of the SCF complex) or its substrate, cyclin E or its subcellular localization. However, the abolishment of D domain will largely inhibit cyclin E turnover, underlying the role of Fbw7 as a tumor suppressor. More

importantly, its research contributes to the identification of a presumably general mechanism that cullin-RING E3 ubiquitin ligases binds to their phosphorylated substrates by F-box protein dimerization.

Although the conclusive mechanism of how Fbw7 dimerization affects cyclin E turnover remains to be determined, there are several hypotheses.

First, by forming dimers, the processivity of the cyclin E ubiquitination may be enhanced. It is possible that an Fbw7-Fbw7 dimer, bound through the D domain upstream of the F-box motif, could potentially dock with the SCF complex with two cyclin E molecules loaded. Therefore, one SCF complex can ubiquitinate two cyclin E molecules at a time. The enhanced cyclin E ubiquitination by Fbw7 isoform dimerization may be more important when cyclin E level is abnormally high, which can be seen in many primary cancer and cancer cell lines. Perhaps, in an environment with elevated cyclin E level, Fbw7 dimerization is induced to efficiently degrade cyclin E and prevent subsequent deleteriousness.

Alternatively, dimerization or oligomerization of F-box proteins might influence the neddylation-deneddylation cycle proposed for Cul1 [229]. In this cycle, Neddylation of Cul1 leads to its release from its inhibitor, CAND1, and subsequent binding by a new F-box protein [230, 231]. There is evidence that cyclin E turnover is regulated by the Cop9 signalosome in both *Drosophila* and mice [232, 233]. Intriguingly, recent work on the SCF^{Skp2} complex indicates that increasing the amount of the Skp1-Skp2 subcomplex enhances Cul1 dissociation from CAND1 and that increased Skp2-substrate subcomplex inhibits Cul1 deneddylation [234]. Likewise, perhaps Fbw7 dimers are more efficient than monomers at dissociation of Cul1 from

CAND1 or an Fbw7-Fbw7 dimer bound to cyclin E might prevent Cul1 from being deneddylated by the CSN for a longer period of time. In either case, the result would be an increase in the active pool of Cul1 and a decrease in the inactive pool of Cul1.

The Clurman group published a paper three months after mine (in chapter 2) with the similar results [252]: they also found that the Fbw7 isoforms can form dimers, and they mapped the dimerization domain upstream of F-box motif, but they narrowed the domain to a region of 5 amino acids, whereas my dimerization domain is much larger. However, there are some discrepancies on how dimerization affects cyclin E turnover between our results. They did not observe a dramatic change of the wild type cyclin E abundance by abolishing dimerization. This can be explained by two points. First of all, my dimerization domain is bigger than theirs, which could potentially have some effects on the Fbw7 functions, including cyclin E turnover. Secondly, Clurman group focused on cyclin E protein abundance, and we looked more in detail on cyclin E stability. If only compared the cyclin E abundance, I did not see significant differences either between Fbw7 or Fbw7ΔDC mutant (figure 2.4). However, when I check the protein stability, I was able to see that the turnover rate of cyclin E was decreased in the presence of Fbw7ΔDC mutant. Indeed, stability is a better readout of the proteolysis of a protein, because transcription can also contribute to the abundance change of a protein. In the stability assay, protein synthesis is almost totally inhibited by cycloheximide, thus the difference we detect is in principle fully due to protein degradation.

In addition to what is discussed above, Welcker et al did identify some interesting results: when serine 384 (S384) of cyclin E is mutated to alanine, abolishment of

dimerization shows dramatic effects on this mutated form of cyclin E. It has been known that S384 is one of the two sites within the C-terminal phosphodegron of cyclin E. S384 phosphorylation together with T380 phosphorylation is required for cyclin E ubiquitination by SCF^{Fbw7}. The reason for cyclin E S384A mutant accumulation is that this mutated form of cyclin E shows a decreased binding affinity to Fbw7. They suggest that Fbw7 S384 site provides a +4 negative charge that is important for binding to Fbw7.

Structural evidence: around the same time as Clurman lab's paper, there was another paper published in Molecular Cell, providing the structural data of Skp1-Fbw7-cyclin E complex [58]. In this paper, Hao et al proposed a model that can potentially explain why Fbw7 dimerization affects cyclin E degradation.

Binding between Fbw7 and cyclin E: They crystallized the truncated Fbw7 (203-707, from 18aa upstream of F-box motif to the end of the protein) together with Skp1, and bind the complex with the C terminal cyclin E phospho degron (360-390, triple phosphorylated at S372, T380 and S384) or N terminal phospho degron (55-68, single phosphorylated at T62). What they found can be summarized as following:

The C terminal central fragment (374-385) of cyclin E binds tightly to the narrow face of WD40 repeats of Fbw7, and T380 and S384 are right within this region. However, the N terminal degron of cyclin E has a much weaker contact with Fbw7. Therefore both T380 and S384 of cyclin E are required for high affinity binding to Fbw7, whereas the role of N terminal degron is minor [58].

S462, T463, and R465 within the WD40 repeat motif of Fbw7 are required for optimal cyclin E binding. Among these three amino acids, R465 is the one contacting

with both T380 and S384 of cyclin E [58].

Binding between Cdc4 and Sic1: Cdc4 is the yeast homologue of Fbw7, which targets Sic1 for degradation. Previous studies suggest that the N terminal of Sic1 is responsible for its binding to Cdc4 [122]. There are 9 conserved phosphorylation sites within the N terminus of Sic1, which cluster in three groups (T2/T5/T9, T33/T45/T48, S69/S76/S80) [122]. In each potential phospho degron, T5, T45 and S76 have been shown to be important for Cdc4 binding, so they are primary sites [122, 168]. Hao et al used three sets of Sic1 peptides corresponding to the three degrons and measured their affinity to Skp1-Cdc4 complex. The result is quite interesting: for the degrons singly phosphorylated at the primary sites, the binding affinity is weak; however, when the +4 position of each primary site is phosphorylated, the binding affinity is up to 19 fold increased, suggesting the second +4 position phosphate group interacts with Cdc4. Therefore, Sic1 contains three phospho degrons; each of them binds to Cdc4 at their primary phosphorylation site (T5, T45, S76, just like T380 of cyclin E) and a second +4 position phosphorylation site analogous to S384 of cyclin E [58].

Hao et al did not provide direct structural data of isoform dimerization, because the truncated Fbw7 they used for crystallization did not include the D domain. But they did confirm the Fbw7 dimerization by immunoprecipitation assay. Moreover, they also observed Cdc4 (Fbw7 yeast homologue) dimerization by gel filtration and sedimentation equilibrium assays. Wild type cyclin E turnover is partially decreased in the dimerization deletion mutant of Fbw7 [58]. More importantly, they found that cyclin E S384A mutant was significantly stabilized by the abolishment of dimerization [58], which was consistent with the finding from Clurman lab [252]. It

was also true for Sic1 binding to Cdc4. When Sic1 is not optimally phosphorylated at all its three degrons, dimerization of Cdc4 will largely enhance its degradation. It seems like the Fbw7 isoform dimerization is required for the ubiquitination of those weakly associated substrates, such as cyclin E S384A mutant, which lacks the +4 position phosphorylation.

In the following *in vitro* ubiquitination assay, they find that the dimerization of Cdc4 increases the initiation rate of Sic1 ubiquitination and the formation of higher molecular weight polyubiquitin conjugates, an indicator of the processivity of ubiquitination.

Based on their structural and biochemical data, they proposed a model: F-box protein dimerization leads to the formation of a dimeric SCF complex, two entire SCF complexes bind together through the D domain of F-box protein. Each F-box protein binds one phosphodegron of the same substrate or each F-box protein binds distinct substrate [58] (figure 4.1, see p136). Irrespective of whether one or two substrates bind to the dimeric SCF, presumably the lysine(s) in the vicinity of a phosphodegron will be presented more optimally to the E2 active site of the adjacent SCF, thus enhancing the rate of ubiquitination initiation and elongation [58].

1.2 Fbw7 dimerization and its role in cancer development

Because most FBW7 mutations have identified in tumors are heterozygous FBW7 mutations or deletions, with a functional FBW7 allele left, FBW7 is considered as a haploinsufficient tumor suppressor (heterozygotes exhibit a phenotype). However,

studies of FBW7 mice shows that FBW7 heterozygotes are normal in terms of tumor development. Besides, conditional knockout of one allele of FBW7 in T cells do not result in lymphomagenesis [144, 145, 173]. The reasons underlying these findings may be partially explained by Fbw7 dimerization.

Point mutations of FBW7 can be found along the whole sequence, some of which are nonsense mutations, resulting in a premature stop. How do these nonsense mutations affect Fbw7 function is depending on where the stops occur. If the stop codons occur downstream of the dimerization domain, a truncated Fbw7 will still be able to bind the wildtype Fbw7 through the dimerization domain, but not the protein substrates, thus dominantly interfering with the normal function of wildtype Fbw7. On the other hand, if the stop codons occur upstream of the dimerization domain, it will simply produce non-functional Fbw7 proteins [253].

Nearly three quarters of FBW7 point mutations have been identified so far are missense mutations in the WD40 repeat motif, which cause amino acid substitution in key residues that form the substrate binding surface, especially the three arginines directly contacting to cyclin E phosphodegron (R465, R479), leading to impaired substrate binding ability of Fbw7 [253]. It is most evident in the T-ALL, where only missense mutations are found. Fbw7 carrying mutations in its WD40 repeat motif can still dimerize to the wildtype allele, and it is possible this mutated allele could dominantly interfere with the function of the wildtype allele, leading to halpoinsufficiency [253](Figure 4.2, see 138). Indeed, Fbw7 and Cdc4 arginine mutants are shown to dominantly interfere with the ability of the wild-type protein to degrade their substrates, such as cyclin E, Sic1 and MYC [146, 181, 254].

Apparently, not all F-box proteins can dimerize. A big proportion of the F-box proteins do not contain the dimerization domain at all. Indeed, the dimerization seems only happen to the Fbws, a subset of F-box proteins contain WD40 repeats as the substrate binding motif. The other two subgroups of F-box proteins Fbls and Fbxs have not showed any dimeric properties. The leucine rich repeats, required for Fbls binding to substrates, are structurally different from the WD40 repeats. Perhaps Fbws dimerization could provide more than one WD40 repeats to make better contacts to substrates containing multiple low affinity phosphodegrons. If that is true, the substrates of Fbls and Fbxs should contain only high affinity phosphodegrons, which are sufficient to tightly associate with these F-box proteins.

The studies on Fbw7 dimerization can be summarized as following points

- The three isoforms of Fbw7 can form both homo- and hetero- dimers through "dimerization" domain immediately upstream of F-box motif.
- Abolishment of dimerization partially inhibits wild-type cyclin E turnover, but dramatically inhibits cyclin E S384A mutant turnover, suggesting dimerization is more critical when cyclin E lacks the primary phosphodegron, resulting in a weaker binding affinity.
- Dimerization has been identified as a general mechanism for almost all Fbws (WD40 motif containing F-box proteins); it either enhances the binding affinity between substrates and WD40 motif of F-box proteins or it optimizes the conformation of the substrate, making them spatially closer to the E2

active site. By either or both of above mechanisms, dimerization facilitates substrate ubiquitination.

2. SLP1

As mentioned above, both our lab and Clurman lab [210] observed that the three isoforms of Fbw7 have different stability pattern: the α isoform is very stable whereas the β and γ isoforms are not. The study of how F-box proteins are regulated is still in the early stages. It has been suggested that the F-box protein components in SCF E3s are unstable; however, it probably not true for all F-box proteins, considering the Fbw7α isoform is stable. Since the only difference of their sequences resides in the unique N termini, it is likely that the unique region is responsible for the stability of three isoforms. Previous studies indicate that F-box proteins are degraded by an autoubiquitination mechanism through the binding to the SCF catalytic core [65]. However, results from my experiments indicate that the unique region also contributes to the stability of at least β and γ isoforms of Fbw7, because deleting F-box domain, which abolishes the interaction between Fbw7 and the catalytic core, only partially stabilizes the two isoforms. The autoubiquitination might be a simplified model, and at same time other regulatory mechanisms may also count.

It is plausible that other proteins are involved in regulating β and γ isoforms turnover by physical interaction. In the effort to identify these regulators, SLP1 (Stomatin like protein 1) was pulled out as an Fbw7γ unique region interacting partner by a yeast-2-hybrid screen. In the process of studying this under-characterized protein, SLP1 itself was found to be also unstable. Given the fact that γ is part of an E3 ligase, the obvious hypothesis could be that SLP1 is a substrate of SCF^{Fbw7}. However, the abundance of SLP1 is not regulated by Fbw7γ. It is not surprising, because SLP1 binds to the N- terminus of Fbw7γ, far away from the WD40 repeat motif, which is

known for substrate binding. SLP1 on the contrary, regulates Fbw7γ by protecting it from proteolysis.

Interestingly, Cdk2 was also found as an Fbw7γ unique region interacting protein, although it was not identified by the same yeast-2-hybrid screen. Functionally, Cdk2 promotes the proteolysis of both Fbw7γ and SLP1 by unknown mechanisms. This function of Cdk2 relies on its kinase activity, since the kinase-dead form of Cdk2 can no longer promote Fbw7γ and SLP1 turnover. Moreover, Cdk2 also interacts with SLP1, and its interaction is largely mediated by the membrane association domain (MAD) of SLP1. When SLP1 and Cdk2 are transfected together with Fbw7γ, it seems Cdk2 acts upstream of SLP1, considering SLP1 can no longer stabilize Fbw7γ. It is likely that Cdk2 promotes SLP1 turnover and releases Fbw7γ from proteolysis.

2.1 SLP1 belongs to SPFH super family

The identification of SLP1 was unexpected, since SLP1 has yet not shown obvious ubiquitination related functions. SLP1 belongs to SPFH super family, which includes Stomatins, Prohibitins, Flotillins and HflK/C, since they all share a SPFH domain, also known as prohibitin domain (PHB). Stomatin family (also termed band 7 integral membrane protein, protein 7.2b, or band 7.2) includes stomatin, stomatin like protein (SLP1, 2, 3) and prodocin. Stomatin is the first identified member of stomatin family. It named after the rare human haemolytic anaemia hereditary stomatocytosis. In some cases of this anaemia, in which the red cells leak sodium and potassium ions, stomatin is absent from the membrane, suggesting its role in the regulation of ion

transport. However, there are no mutations have been identified in the stomatin gene *EPB72* of the patients [255]. Stomatin has been suggested to play a role in regulating ion channel, or to function as a phospholipid scrambler [255]. Stomatin is widely expressed in human tissues except brain [256]. SLP1, however, is highly expressed in brain, presumably compensating for the lack of stomatin in the central nerve system, but the function of SLP1 is unknown [242]. SLP2 (hSLP2) is a widely expressed oligomeric peripheral membrane protein that has been shown to be overexpressed in many human tumors, with unknown functions [257]. SLP3 is an olfactory neuronal protein sharing 84% similarity with stomatin, and it functions as skin mechanoreceptors [258, 259]. Podocin, a raft associated protein, is 73% homologous to stomatin and exclusively expressed in kidney. Mutations in the podocin gene result in nephritic syndrome, eventually leading to renal failure [260, 261]. Although stomatin homologues have been studied in mouse, zebrafish and other vertebrates [262], the *C.elegans* homologues such as UNC-1, UNC-24 and MEC-2 are better characterized. UNC-1 is broadly expressed in the *C. elegans* nervous system and controls the sensitivity to volatile anesthetics, whereas UNC-24 and MEC-2 are required for mechanosensory in specific motor neurons [263-265]. Sequence analysis suggests that SLP1 is the human homologue of UNC-24 [242, 263], and stomatin is the human homologue of UNC-1.

In addition to sharing the SPFH domain, all members of this superfamily show some common features, such as detergent insolubility, association with membranes and a propensity to form high order oligomers.[266, 267] The functions of almost all human stomatin family members are not well understood. However, the widespread

distribution of Stomatins and their associated disease strongly suggests that their biological functions are of great importance [247].

2.2 Stomatin family proteins in protein proteolysis:

SLP2, SLP2 has been reported to stabilize prohibitin and other respiratory chain complex subunits [268]. SLP2 attaches to the inner membrane of mitochondria and interact with prohibitin [268]. Prohibitin is another SPFH family member, which is important for proliferation, aging and respiratory complex assembly [269]. Prohibitin regulates membrane protein degradation through AAA proteases in mitochondria [270]. Depletion of SLP2 increases the proteolysis of prohibitin presumably by AAA proteases [268]. Mitochondria stresses induced by chloramphenicol (CAP) will up regulate SLP2 and prohibitin, and the stabilization of prohibitin is SLP2 dependent. Thus, SLP2 is required to stabilize at least prohibitin at mitochondria, and these two proteins could be part of a complex regulating protein turnover by AAA proteases at the mitochondria membrane [268].

UNC-24: *C.elegans* homologue of SLP1 has been reported to regulate the localization and possible protein stability of UNC-1 (stomatin homologue). In *C. elegans*, UNC-1 is normally localized at the plasma membrane of axons whereas in *unc-24* mutants, UNC-1 is close to nuclei [271]. More importantly, in *unc-24* mutants, UNC-1 protein can hardly be detected by immunostaining without a marked change on UNC-1 transcription. Interestingly, these two proteins physically interact with each other [271]. Given the fact that stomatin is able to form oligomers [272], it is possible

that UNC-24 is required to initiate or maintain the UNC-1 oligomer [271].

Erlin1 and Erlin2: erlins are two new members of prohibitin family [273]. They also share the SPFH domain like the other members in SPFH superfamily. Recently, erlin-2 together with erlin-1 have been shown to target the inositol 1,4,5-trisphosphate receptor (IP3R) for degradation through the ER-associated degradation (ERAD) pathway [274]. ERAD pathway is a process in which misfolded protein substrates are polyubiquitinatd and translocated into the cytosol for proteasomal degradation [275]. IP3R is localized at ER membrane, and upon activation, it can be transformed from a stable protein to an ERAD substrate, and its ubiquitinaiton is dependent on E2 Ubc7 and an unknown E3 [276]. Erlin 1 and Erlin-2 form a Ring-like 2-MD huge complex including 50 erlin proteins [277]. This complex will rapidly associate with IP3R after its activation and other established components of the ERAD pathway [274]. RNAi knockdown of erlin proteins inhibits the ubiquitination and degradation of IP3R [274]. Since the erlin complex is able to associate with non-ubiquitinated IP3R and this association occurs much more rapidly compared to its association with other ERAD components, the erlin complex may function in the early substrate recognition step [274]. The composition of erlin complex is important, since deletion either one of the two proteins will largely affect IP3R ubiquitination [277]. Moreover, the ring-shape structure is reminiscent of the chaperonin family of molecular chaperones, which interact with exposed hydrophobic regions on nascent proteins and use intrinsic ATPase activity to regulate protein folding [278]. Although the SPFH1/2 complex has no obvious ATPase activity, the ring-shaped structure may allow for analogous binding to hydrophobic surfaces exposed on IP3R protein upon activation [277].

These findings also suggest that certain part of ER membrane (microdomains), where erlin1 and erlin2 proteins are enriched, can exist as specialized centers for processing ERAD substrates [277].

2.3 Speculation on SLP1's function in regulating Fbw7γ

2.3.1 SLP1 may change the subcellular localization of Fbw7γ

The subcellular localization of SLP1 has not been elucidated because of the lack of antibody. In my immunostaining experiment, SLP1 was mainly localized to the cytoplasm, and co-localized with the ER marker calnexin. In the fractionation experiments, SLP1 appears in both nuclear and cytoplasmic fractions with the majority in cytoplasm. However, recent results from Prohaska group suggested late endosome localization [245]. Moreover, SLP1 is able to interact with stomatin and relocalize stomatin from the plasma membrane to the late endosome. The interaction among SPFH family proteins seems very common. In *C.elegans,* SLP1 homologue UNC-24 interacts with another stomatin family protein UNC-1 and relocalizes UNC-1 from cell membrane to cytoplasm [271]. In humans, SLP2 interacts with SPHF family protein prohibitin at the ER [268]. So far, there are few reports about stomatin family members interacting with non-SPFH proteins except for erlin2, which associates with many components of the ERAD pathway [274].

It is plausible to speculate SLP1 relocalizes a fraction of Fbw7γ from the nucleus to cytoplasm. I do observe in some of the HeLa cell co-expressing SLP1, the localization of Fbw7γ is more diffuse, suggesting part of the Fbw7γ protein

population may relocalize to the cytoplasm. However, I have not further analyzed the data in detail. In order to understand whether SLP1 regulates Fbw7γ localization, one could examine the exact localization of SLP1 and Fbw7γ by more accurate co-immunostaining and fractionation assays. Moreover, SLP1's regulation may be cell type sensitive, in addition to over-expressing these two proteins in Hela cells, cells derived from the nervous system would be ideal, considering both proteins are highly abundant in the nervous system.

2.3.2 SLP1 may be required for Fbw7γ substrate binding at certain cellular compartments

Given the fact that SLP1 interacts with stomatin [245], and the SPFH family proteins tend to form high order oligomers, it is possible that SLP1 forms a complex at the ER with stomatin or just by itself. Similar to the erlin complex, the formation of SLP1/stomatin complex may be required for substrates binding of Fbw7γ. In my experiments, the interaction between cyclin E and Fbw7γ is not very affected by SLP1. However, I have not ruled out the possibility that SLP1 is required for Fbw7γ binding to other substrates, especially those that may have transient ER localization, such as SREBP1. If SLP1's Fbw7γ regulatory function mainly occurs at the ER, then using cyclin E as a functional readout may not be appropriate. Alternatively, Fbw7γ may have other unidentified substrates at the ER membrane. In either case, Fbw7γ may be recruited to the adjacent area of the ER, once the ERAD substrate is translocated into the cytosol, Fbw7γ can get involved. SLP1 itself or SLP1/stomatin complex may function in the membrane of the ER, binds to the ERAD substrate and facilitates the

translocation of the substrate from the ER to the cytosol. At the same time, SLP1 also binds and stabilizes Fbw7γ to enhance the substrate ubiquitination in the cytosol.

How can SLP1 stabilize Fbw7γ? Five F-box proteins have been identified to specifically recognize glycoproteins and target them for polyubiquitination and proteolysis (FBXO2, 6, 17, 27, 44) [279]. Instead of WD40 repeats, FBA (F-box associated) domain is the substrate binding motif [280]. Of these F-box proteins, FBXO2 is found to bind CHIP, co chaperone/ubiquitin ligase, through the N terminal PEST domain of FBXO2 [281]. PEST domain are sequences enrich with proline (P), glutamic acid (E), serine (S) and threonine (T), which is commonly found in short lived proteins [282]. SCF^{FBXO2} binds the protein substrate and present it to CHIP E3 [281]. Within the 50 amino acid unique region of Fbw7γ, there are 10 PEST amino acids. Perhaps $FBW7^{Fbw7\gamma}$ shares a similar mechanism as CHIP: by interacting directly with SLP1 through its N- terminal region, SLP1 recruits ERAD substrates and present it to the proximity to $SCF^{Fbw7\gamma}$ to facilitate its ubiquitinated degradation. Because SLP1 interacts with the N terminal unique region of Fbw7γ, which is important for its turnover, presumably SLP1 blocks off other regulatory proteins.

The study of mechanisms of SLP1 regulating Fbw7γ stability is largely restrained by the very limited knowledge about SLP1 functions. Thus, it will be important to initiate a screen for SLP1 interacting proteins. On one hand, the information of interacting proteins will help us to understand this novel protein. On the other hand, it will also bring some insights into better understanding of the biological functions Fbw7γ and the SCF E3s.

2.4 Cdk2 promotes SLP1 and Fbw7γ degradation

Most substrates of SCF E3 ligases need to be phosphorylated at specific sites in order to bind the WD40 motif of F-box proteins. When Cdk2 was observed to promote Fbw7γ turnover, we first speculated Cdk2 may phosphorylate Fbw7γ in order to trigger Fbw7γ autoubiquitination by the SCF^{Fbw7} complex, as a mechanism to prevent the over degradation of cyclin E by $SCF^{Fbw7\gamma}$. Given the fact that the α isoform is quite stable, and Cdk2 binds to the unique sequence of Fbw7γ, a likely explanation might have been that Cdk2 can recognize an Fbw7/Cdc4 phosphodegron within the unique region. Unfortunately, no such phosphodegrons (S/TXXXA, where A is a negative charged amino acid) reside in the Fbw7γ unique region. Thus, the interaction between Cdk2 and Fbw7γ is unlikely meant to facilitate Fbw7γ's autoubiquitination.

There are multiple serines and threonines in this region, though, but we have not mutated them yet. However, knowing whether Fbw7γ is directly phosphorylated by Cdk2 is informative, it is possible that Fbw7γ is ubiquitinated by other E3 ligases, and the phosphorylation by Cdk2 is required for the recognition of Fbw7γ by other E3s. Thus, currently, whether Cdk2 affects Fbw7γ stability by direct phosphorylating Fbw7γ has not been elucidated.

It is not clear whether SLP1 is directly phosphorylated by Cdk2. The destruction of two potential Cdk2 phosphorylation sites (ΔSPK and S34A) in SLP1 did not affect SLP1's function in terms of stabilizing Fbw7γ. There are two potential CDC4/Fbw7 phosphodegrons in SLP1, one is in the membrane association domain (TFPIS), and

the other is in the C terminus (SGTQS). As it binds to the unique region of Fbw7γ, SLP1 is not expected as a substrate of Fbw7γ. Thus, it is unlikely that two phosphodegrons are really implicated in SLP1 degradation.

Interestingly, when the putative membrane association domain (MAD) of SLP1 is deleted, the interaction between SLP1 and Cdk2 is largely abolished. Moreover, SLP1ΔMAD can only partially co-localize with ER marker, suggesting a localization shift. However, it is not clear whether the localization change is due to loss the membrane association or the result of loss the interaction with Cdk2.

Figure 4.1 Models of substrate cross-ubiquitination by a dimeric SCF.

Irrespective of whether one or two multi-degron substrates bind to the dimeric SCF, it is possible that the lysine(s) in the vicinity of a phosphodegron bound to one SCF is presented more optimally to the E2 active site of the adjacent SCF, thus enhancing the rate of ubiquitination. Ubiquitin chain elongation may similarly be enhanced by cross-dimer ubiquitination.

Hao, et al. *Mol. Cell*, 2007, 26, 131-143

Figure 4.1 Models of substrate cross-ubiquitination by a dimeric SCF.

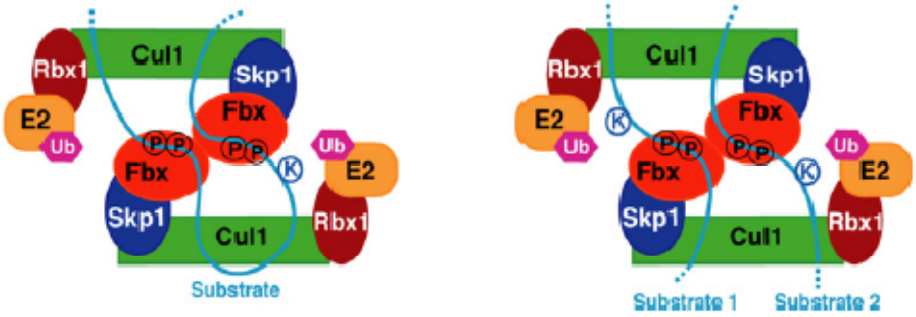

Hao, et al. *Mol. Cell*, 2007, 26, 131-143

Figure 4.2 Consequences of heterozygous mutations in *FBW7*

Most mutations in *FBW7* (F-box and WD repeat domain-containing 7) are heterozygous and, because FBW7 dimerizes, the various kinds of mutations can have different effects on FBW7 function. Any single allelic mutation will lead to haploinsufficiency for the remaining wild-type allele with regards to monomeric Fbw7 functions because it reduces the amount of wild-type FBW7 by 50%. Gene deletions and stop codons before the dimerization domain are also haploinsufficient for FBW7 dimers. However, mutants that retain an intact dimerization domain (stop codons after the dimerization domain and hot-spot mutants) can dominantly interfere with wild-type Fbw7 through dimerization, and this will eliminate most of the active Fbw7 dimers. So, mutants that retain the ability to dimerize might affect FBW7 function more profoundly than simple loss-of-function mutations.

Ref, Markus Welcker and Bruce E. Clurman, *Nat. Rev. Cancer*, 2007 Vol. 8: 83-93

Figure 4.2 Consequences of heterozygous mutations in *FBW7*

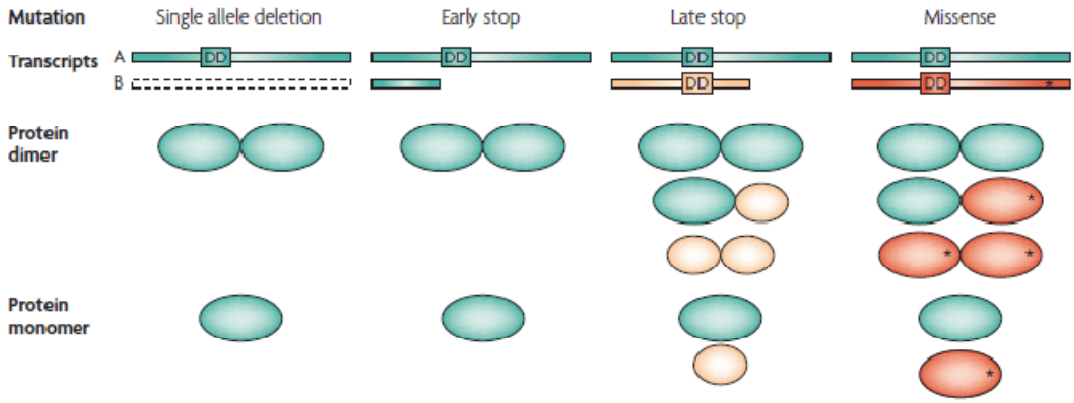

Ref, Markus Welcker and Bruce E. Clurman, *Nat. Rev. Cancer*, 2007 Vol. 8: 83-93

References

1. Zacksenhaus, E. and R. Sheinin, *Molecular cloning, primary structure and expression of the human X linked A1S9 gene cDNA which complements the ts A1S9 mouse L cell defect in DNA replication.* EMBO J, 1990. **9**(9): p. 2923-9.
2. McGrath, J.P., S. Jentsch, and A. Varshavsky, *UBA 1: an essential yeast gene encoding ubiquitin-activating enzyme.* EMBO J, 1991. **10**(1): p. 227-36.
3. Jin, J., et al., *Dual E1 activation systems for ubiquitin differentially regulate E2 enzyme charging.* Nature, 2007. **447**(7148): p. 1135-8.
4. Hershko, A., et al., *Components of ubiquitin-protein ligase system. Resolution, affinity purification, and role in protein breakdown.* J Biol Chem, 1983. **258**(13): p. 8206-14.
5. Miura, T., et al., *Characterization of the binding interface between ubiquitin and class I human ubiquitin-conjugating enzyme 2b by multidimensional heteronuclear NMR spectroscopy in solution.* J Mol Biol, 1999. **290**(1): p. 213-28.
6. Lee, I. and H. Schindelin, *Structural insights into E1-catalyzed ubiquitin activation and transfer to conjugating enzymes.* Cell, 2008. **134**(2): p. 268-78.
7. Ye, Y. and M. Rape, *Building ubiquitin chains: E2 enzymes at work.* Nat Rev Mol Cell Biol, 2009. **10**(11): p. 755-64.
8. Cook, W.J., L.J. Walter, and M.R. Walter, *Drug binding by calmodulin: crystal structure of a calmodulin-trifluoperazine complex.* Biochemistry, 1994. **33**(51): p. 15259-65.
9. Worthylake, D.K., et al., *Crystal structure of the Saccharomyces cerevisiae ubiquitin-conjugating enzyme Rad6 at 2.6 A resolution.* J Biol Chem, 1998. **273**(11): p. 6271-6.
10. Jiang, F. and R. Basavappa, *Crystal structure of the cyclin-specific ubiquitin-conjugating enzyme from clam, E2-C, at 2.0 A resolution.* Biochemistry, 1999. **38**(20): p. 6471-8.
11. Chau, V., et al., *A multiubiquitin chain is confined to specific lysine in a targeted short-lived protein.* Science, 1989. **243**(4898): p. 1576-83.
12. Hofmann, R.M. and C.M. Pickart, *Noncanonical MMS2-encoded ubiquitin-conjugating enzyme functions in assembly of novel polyubiquitin chains for DNA repair.* Cell, 1999. **96**(5): p. 645-53.
13. Mastrandrea, L.D., et al., *E2/E3-mediated assembly of lysine 29-linked polyubiquitin chains.* J Biol Chem, 1999. **274**(38): p. 27299-306.
14. Chen, P., et al., *Multiple ubiquitin-conjugating enzymes participate in the in vivo degradation of the yeast MAT alpha 2 repressor.* Cell, 1993. **74**(2): p. 357-69.
15. Treier, M., L.M. Staszewski, and D. Bohmann, *Ubiquitin-dependent c-Jun degradation in vivo is mediated by the delta domain.* Cell, 1994. **78**(5): p. 787-98.
16. Hou, D., et al., *Activation-dependent ubiquitination of a T cell antigen receptor subunit on multiple intracellular lysines.* J Biol Chem, 1994. **269**(19): p. 14244-7.
17. Lawson, T.G., et al., *Identification and characterization of a protein destruction signal in the encephalomyocarditis virus 3C protease.* J Biol Chem, 1999. **274**(14): p. 9871-80.
18. Glotzer, M., A.W. Murray, and M.W. Kirschner, *Cyclin is degraded by the ubiquitin pathway.* Nature, 1991. **349**(6305): p. 132-8.
19. Yamano, H., et al., *The role of the destruction box and its neighbouring lysine residues in cyclin B for anaphase ubiquitin-dependent proteolysis in fission yeast: defining the D-box receptor.* EMBO J, 1998. **17**(19): p. 5670-8.
20. Laney, J.D. and M. Hochstrasser, *Substrate targeting in the ubiquitin system.* Cell, 1999. **97**(4): p. 427-30.
21. Haglund, K. and I. Dikic, *Ubiquitylation and cell signaling.* EMBO J, 2005. **24**(19): p. 3353-9.
22. Hayden, M.S. and S. Ghosh, *Shared principles in NF-kappaB signaling.* Cell, 2008. **132**(3): p. 344-62.
23. Hicke, L. and R. Dunn, *Regulation of membrane protein transport by ubiquitin and ubiquitin-binding proteins.* Annu Rev Cell Dev Biol, 2003. **19**: p. 141-72.

24. Pickart, C.M., *Mechanisms underlying ubiquitination.* Annu Rev Biochem, 2001. **70**: p. 503-33.
25. Li, W., et al., *Genome-wide and functional annotation of human E3 ubiquitin ligases identifies MULAN, a mitochondrial E3 that regulates the organelle's dynamics and signaling.* PLoS One, 2008. **3**(1): p. e1487.
26. Scheffner, M., et al., *The HPV-16 E6 and E6-AP complex functions as a ubiquitin-protein ligase in the ubiquitination of p53.* Cell, 1993. **75**(3): p. 495-505.
27. Huibregtse, J.M., J.C. Yang, and S.L. Beaudenon, *The large subunit of RNA polymerase II is a substrate of the Rsp5 ubiquitin-protein ligase.* Proc Natl Acad Sci U S A, 1997. **94**(8): p. 3656-61.
28. Huang, L., et al., *Structure of an E6AP-UbcH7 complex: insights into ubiquitination by the E2-E3 enzyme cascade.* Science, 1999. **286**(5443): p. 1321-6.
29. Nuber, U., et al., *Cloning of human ubiquitin-conjugating enzymes UbcH6 and UbcH7 (E2-F1) and characterization of their interaction with E6-AP and RSP5.* J Biol Chem, 1996. **271**(5): p. 2795-800.
30. Kumar, S., W.H. Kao, and P.M. Howley, *Physical interaction between specific E2 and Hect E3 enzymes determines functional cooperativity.* J Biol Chem, 1997. **272**(21): p. 13548-54.
31. Rotin, D. and S. Kumar, *Physiological functions of the HECT family of ubiquitin ligases.* Nat Rev Mol Cell Biol, 2009. **10**(6): p. 398-409.
32. Gao, M., et al., *Jun turnover is controlled through JNK-dependent phosphorylation of the E3 ligase Itch.* Science, 2004. **306**(5694): p. 271-5.
33. Massague, J. and R.R. Gomis, *The logic of TGFbeta signaling.* FEBS Lett, 2006. **580**(12): p. 2811-20.
34. Kamynina, E., et al., *A novel mouse Nedd4 protein suppresses the activity of the epithelial Na+ channel.* FASEB J, 2001. **15**(1): p. 204-214.
35. Harvey, K.F., et al., *The Nedd4-like protein KIAA0439 is a potential regulator of the epithelial sodium channel.* J Biol Chem, 2001. **276**(11): p. 8597-601.
36. Lu, C., et al., *The PY motif of ENaC, mutated in Liddle syndrome, regulates channel internalization, sorting and mobilization from subapical pool.* Traffic, 2007. **8**(9): p. 1246-64.
37. Pak, Y., et al., *Transport of LAPTM5 to lysosomes requires association with the ubiquitin ligase Nedd4, but not LAPTM5 ubiquitination.* J Cell Biol, 2006. **175**(4): p. 631-45.
38. Saksena, S., et al., *ESCRTing proteins in the endocytic pathway.* Trends Biochem Sci, 2007. **32**(12): p. 561-73.
39. Morita, E. and W.I. Sundquist, *Retrovirus budding.* Annu Rev Cell Dev Biol, 2004. **20**: p. 395-425.
40. Garcia-Gonzalo, F.R., et al., *Requirement of phosphatidylinositol-4,5-bisphosphate for HERC1-mediated guanine nucleotide release from ARF proteins.* FEBS Lett, 2005. **579**(2): p. 343-8.
41. Zhao, X., et al., *The HECT-domain ubiquitin ligase Huwe1 controls neural differentiation and proliferation by destabilizing the N-Myc oncoprotein.* Nat Cell Biol, 2008. **10**(6): p. 643-53.
42. Froyen, G., et al., *Submicroscopic duplications of the hydroxysteroid dehydrogenase HSD17B10 and the E3 ubiquitin ligase HUWE1 are associated with mental retardation.* Am J Hum Genet, 2008. **82**(2): p. 432-43.
43. Borden, K.L., *RING domains: master builders of molecular scaffolds?* J Mol Biol, 2000. **295**(5): p. 1103-12.
44. Deshaies, R.J., *SCF and Cullin/Ring H2-based ubiquitin ligases.* Annu Rev Cell Dev Biol, 1999. **15**: p. 435-67.
45. Tyers, M. and P. Jorgensen, *Proteolysis and the cell cycle: with this RING I do thee destroy.* Curr Opin Genet Dev, 2000. **10**(1): p. 54-64.
46. Page, A.M. and P. Hieter, *The anaphase-promoting complex: new subunits and regulators.* Annu Rev Biochem, 1999. **68**: p. 583-609.
47. Joazeiro, C.A. and A.M. Weissman, *RING finger proteins: mediators of ubiquitin ligase activity.* Cell, 2000. **102**(5): p. 549-52.
48. Kamura, T., et al., *Rbx1, a component of the VHL tumor suppressor complex and SCF*

ubiquitin ligase. Science, 1999. **284**(5414): p. 657-61.
49. Zheng, N., et al., *Structure of a c-Cbl-UbcH7 complex: RING domain function in ubiquitin-protein ligases.* Cell, 2000. **102**(4): p. 533-9.
50. Lorick, K.L., et al., *RING fingers mediate ubiquitin-conjugating enzyme (E2)-dependent ubiquitination.* Proc Natl Acad Sci U S A, 1999. **96**(20): p. 11364-9.
51. Christensen, D.E., P.S. Brzovic, and R.E. Klevit, *E2-BRCA1 RING interactions dictate synthesis of mono- or specific polyubiquitin chain linkages.* Nat Struct Mol Biol, 2007. **14**(10): p. 941-8.
52. Seol, J.H., et al., *Cdc53/cullin and the essential Hrt1 RING-H2 subunit of SCF define a ubiquitin ligase module that activates the E2 enzyme Cdc34.* Genes Dev, 1999. **13**(12): p. 1614-26.
53. Scherer, D.C., et al., *Signal-induced degradation of I kappa B alpha requires site-specific ubiquitination.* Proc Natl Acad Sci U S A, 1995. **92**(24): p. 11259-63.
54. Petroski, M.D. and R.J. Deshaies, *Context of multiubiquitin chain attachment influences the rate of Sic1 degradation.* Mol Cell, 2003. **11**(6): p. 1435-44.
55. Feldman, R.M., et al., *A complex of Cdc4p, Skp1p, and Cdc53p/cullin catalyzes ubiquitination of the phosphorylated CDK inhibitor Sic1p.* Cell, 1997. **91**(2): p. 221-30.
56. Skowyra, D., et al., *F-box proteins are receptors that recruit phosphorylated substrates to the SCF ubiquitin-ligase complex.* Cell, 1997. **91**(2): p. 209-19.
57. Orlicky, S., et al., *Structural basis for phosphodependent substrate selection and orientation by the SCFCdc4 ubiquitin ligase.* Cell, 2003. **112**(2): p. 243-56.
58. Hao, B., et al., *Structure of a Fbw7-Skp1-cyclin E complex: multisite-phosphorylated substrate recognition by SCF ubiquitin ligases.* Mol Cell, 2007. **26**(1): p. 131-43.
59. Koepp, D.M., et al., *Phosphorylation-dependent ubiquitination of cyclin E by the SCFFbw7 ubiquitin ligase.* Science, 2001. **294**(5540): p. 173-7.
60. Lahav-Baratz, S., et al., *Reversible phosphorylation controls the activity of cyclosome-associated cyclin-ubiquitin ligase.* Proc Natl Acad Sci U S A, 1995. **92**(20): p. 9303-7.
61. Rudner, A.D. and A.W. Murray, *Phosphorylation by Cdc28 activates the Cdc20-dependent activity of the anaphase-promoting complex.* J Cell Biol, 2000. **149**(7): p. 1377-90.
62. Zachariae, W., et al., *Control of cyclin ubiquitination by CDK-regulated binding of Hct1 to the anaphase promoting complex.* Science, 1998. **282**(5394): p. 1721-4.
63. Harper, J.W., J.L. Burton, and M.J. Solomon, *The anaphase-promoting complex: it's not just for mitosis any more.* Genes Dev, 2002. **16**(17): p. 2179-206.
64. Peters, J.M., *The anaphase promoting complex/cyclosome: a machine designed to destroy.* Nat Rev Mol Cell Biol, 2006. **7**(9): p. 644-56.
65. Zhou, P. and P.M. Howley, *Ubiquitination and degradation of the substrate recognition subunits of SCF ubiquitin-protein ligases.* Mol Cell, 1998. **2**(5): p. 571-80.
66. Galan, J.M. and M. Peter, *Ubiquitin-dependent degradation of multiple F-box proteins by an autocatalytic mechanism.* Proc Natl Acad Sci U S A, 1999. **96**(16): p. 9124-9.
67. Ryoo, H.D., et al., *Regulation of Drosophila IAP1 degradation and apoptosis by reaper and ubcD1.* Nat Cell Biol, 2002. **4**(6): p. 432-8.
68. Mallery, D.L., C.J. Vandenberg, and K. Hiom, *Activation of the E3 ligase function of the BRCA1/BARD1 complex by polyubiquitin chains.* EMBO J, 2002. **21**(24): p. 6755-62.
69. Duda, D.M., et al., *Structural insights into NEDD8 activation of cullin-RING ligases: conformational control of conjugation.* Cell, 2008. **134**(6): p. 995-1006.
70. Rape, M., S.K. Reddy, and M.W. Kirschner, *The processivity of multiubiquitination by the APC determines the order of substrate degradation.* Cell, 2006. **124**(1): p. 89-103.
71. Tan, X., et al., *Mechanism of auxin perception by the TIR1 ubiquitin ligase.* Nature, 2007. **446**(7136): p. 640-5.
72. Hao, B., et al., *Structural basis of the Cks1-dependent recognition of p27(Kip1) by the SCF(Skp2) ubiquitin ligase.* Mol Cell, 2005. **20**(1): p. 9-19.
73. Grziwa, A., et al., *Localization of subunits in proteasomes from Thermoplasma acidophilum by immunoelectron microscopy.* FEBS Lett, 1991. **290**(1-2): p. 186-90.
74. Groll, M., et al., *Structure of 20S proteasome from yeast at 2.4 A resolution.* Nature, 1997.

386(6624): p. 463-71.
75. Kopp, F., et al., *Size and shape of the multicatalytic proteinase from rat skeletal muscle.* Biochim Biophys Acta, 1986. **872**(3): p. 253-60.
76. Lowe, J., et al., *Crystal structure of the 20S proteasome from the archaeon T. acidophilum at 3.4 A resolution.* Science, 1995. **268**(5210): p. 533-9.
77. Kopp, F., B. Dahlmann, and K.B. Hendil, *Evidence indicating that the human proteasome is a complex dimer.* J Mol Biol, 1993. **229**(1): p. 14-9.
78. Kopp, F., et al., *The human proteasome subunit HsN3 is located in the inner rings of the complex dimer.* J Mol Biol, 1995. **248**(2): p. 264-72.
79. Zwickl, P., J. Kleinz, and W. Baumeister, *Critical elements in proteasome assembly.* Nat Struct Biol, 1994. **1**(11): p. 765-70.
80. Peters, J.M., et al., *Structural features of the 26 S proteasome complex.* J Mol Biol, 1993. **234**(4): p. 932-7.
81. Gray, C.W., C.A. Slaughter, and G.N. DeMartino, *PA28 activator protein forms regulatory caps on proteasome stacked rings.* J Mol Biol, 1994. **236**(1): p. 7-15.
82. Borissenko, L. and M. Groll, *20S proteasome and its inhibitors: crystallographic knowledge for drug development.* Chem Rev, 2007. **107**(3): p. 687-717.
83. Ganoth, D., et al., *A multicomponent system that degrades proteins conjugated to ubiquitin. Resolution of factors and evidence for ATP-dependent complex formation.* J Biol Chem, 1988. **263**(25): p. 12412-9.
84. Goldberg, A.L., et al., *The importance of the proteasome and subsequent proteolytic steps in the generation of antigenic peptides.* Mol Immunol, 2002. **39**(3-4): p. 147-64.
85. Kisselev, A.F., et al., *The sizes of peptides generated from protein by mammalian 26 and 20 S proteasomes. Implications for understanding the degradative mechanism and antigen presentation.* J Biol Chem, 1999. **274**(6): p. 3363-71.
86. Glickman, M.H., et al., *A subcomplex of the proteasome regulatory particle required for ubiquitin-conjugate degradation and related to the COP9-signalosome and eIF3.* Cell, 1998. **94**(5): p. 615-23.
87. Forster, A., et al., *The 1.9 A structure of a proteasome-11S activator complex and implications for proteasome-PAN/PA700 interactions.* Mol Cell, 2005. **18**(5): p. 589-99.
88. Smith, D.M., et al., *Docking of the proteasomal ATPases' carboxyl termini in the 20S proteasome's alpha ring opens the gate for substrate entry.* Mol Cell, 2007. **27**(5): p. 731-44.
89. Rabl, J., et al., *Mechanism of gate opening in the 20S proteasome by the proteasomal ATPases.* Mol Cell, 2008. **30**(3): p. 360-8.
90. Groll, M., et al., *A gated channel into the proteasome core particle.* Nat Struct Biol, 2000. **7**(11): p. 1062-7.
91. Kohler, A., et al., *The axial channel of the proteasome core particle is gated by the Rpt2 ATPase and controls both substrate entry and product release.* Mol Cell, 2001. **7**(6): p. 1143-52.
92. Whitby, F.G., et al., *Structural basis for the activation of 20S proteasomes by 11S regulators.* Nature, 2000. **408**(6808): p. 115-20.
93. Gillette, T.G., et al., *Differential roles of the COOH termini of AAA subunits of PA700 (19 S regulator) in asymmetric assembly and activation of the 26 S proteasome.* J Biol Chem, 2008. **283**(46): p. 31813-22.
94. Walz, J., et al., *26S proteasome structure revealed by three-dimensional electron microscopy.* J Struct Biol, 1998. **121**(1): p. 19-29.
95. Lee, C., S. Prakash, and A. Matouschek, *Concurrent translocation of multiple polypeptide chains through the proteasomal degradation channel.* J Biol Chem, 2002. **277**(38): p. 34760-5.
96. Weber-Ban, E.U., et al., *Global unfolding of a substrate protein by the Hsp100 chaperone ClpA.* Nature, 1999. **401**(6748): p. 90-3.
97. Braun, B.C., et al., *The base of the proteasome regulatory particle exhibits chaperone-like activity.* Nat Cell Biol, 1999. **1**(4): p. 221-6.
98. Liu, C.W., et al., *Conformational remodeling of proteasomal substrates by PA700, the 19 S regulatory complex of the 26 S proteasome.* J Biol Chem, 2002. **277**(30): p. 26815-20.

99. Navon, A. and A.L. Goldberg, *Proteins are unfolded on the surface of the ATPase ring before transport into the proteasome.* Mol Cell, 2001. **8**(6): p. 1339-49.
100. Benaroudj, N., et al., *ATP hydrolysis by the proteasome regulatory complex PAN serves multiple functions in protein degradation.* Mol Cell, 2003. **11**(1): p. 69-78.
101. Lee, C., et al., *ATP-dependent proteases degrade their substrates by processively unraveling them from the degradation signal.* Mol Cell, 2001. **7**(3): p. 627-37.
102. Verma, R., et al., *Role of Rpn11 metalloprotease in deubiquitination and degradation by the 26S proteasome.* Science, 2002. **298**(5593): p. 611-5.
103. Yao, T. and R.E. Cohen, *A cryptic protease couples deubiquitination and degradation by the proteasome.* Nature, 2002. **419**(6905): p. 403-7.
104. Maytal-Kivity, V., et al., *MPN+, a putative catalytic motif found in a subset of MPN domain proteins from eukaryotes and prokaryotes, is critical for Rpn11 function.* BMC Biochem, 2002. **3**: p. 28.
105. Gallery, M., et al., *The JAMM motif of human deubiquitinase Poh1 is essential for cell viability.* Mol Cancer Ther, 2007. **6**(1): p. 262-8.
106. Zheng, N., et al., *Structure of the Cul1-Rbx1-Skp1-F boxSkp2 SCF ubiquitin ligase complex.* Nature, 2002. **416**(6882): p. 703-9.
107. Michel, J.J. and Y. Xiong, *Human CUL-1, but not other cullin family members, selectively interacts with SKP1 to form a complex with SKP2 and cyclin A.* Cell Growth Differ, 1998. **9**(6): p. 435-49.
108. Dias, D.C., et al., *CUL7: A DOC domain-containing cullin selectively binds Skp1.Fbx29 to form an SCF-like complex.* Proc Natl Acad Sci U S A, 2002. **99**(26): p. 16601-6.
109. Stebbins, C.E., W.G. Kaelin, Jr., and N.P. Pavletich, *Structure of the VHL-ElonginC-ElonginB complex: implications for VHL tumor suppressor function.* Science, 1999. **284**(5413): p. 455-61.
110. Geyer, R., et al., *BTB/POZ domain proteins are putative substrate adaptors for cullin 3 ubiquitin ligases.* Mol Cell, 2003. **12**(3): p. 783-90.
111. Xu, L., et al., *BTB proteins are substrate-specific adaptors in an SCF-like modular ubiquitin ligase containing CUL-3.* Nature, 2003. **425**(6955): p. 316-21.
112. Furukawa, M., et al., *Targeting of protein ubiquitination by BTB-Cullin 3-Roc1 ubiquitin ligases.* Nat Cell Biol, 2003. **5**(11): p. 1001-7.
113. Pintard, L., et al., *The BTB protein MEL-26 is a substrate-specific adaptor of the CUL-3 ubiquitin-ligase.* Nature, 2003. **425**(6955): p. 311-6.
114. Shiyanov, P., A. Nag, and P. Raychaudhuri, *Cullin 4A associates with the UV-damaged DNA-binding protein DDB.* J Biol Chem, 1999. **274**(50): p. 35309-12.
115. Ulane, C.M. and C.M. Horvath, *Paramyxoviruses SV5 and HPIV2 assemble STAT protein ubiquitin ligase complexes from cellular components.* Virology, 2002. **304**(2): p. 160-6.
116. Wertz, I.E., et al., *Human De-etiolated-1 regulates c-Jun by assembling a CUL4A ubiquitin ligase.* Science, 2004. **303**(5662): p. 1371-4.
117. Bai, C., et al., *SKP1 connects cell cycle regulators to the ubiquitin proteolysis machinery through a novel motif, the F-box.* Cell, 1996. **86**(2): p. 263-74.
118. Kamura, T., et al., *The Elongin BC complex interacts with the conserved SOCS-box motif present in members of the SOCS, ras, WD-40 repeat, and ankyrin repeat families.* Genes Dev, 1998. **12**(24): p. 3872-81.
119. Hori, T., et al., *Covalent modification of all members of human cullin family proteins by NEDD8.* Oncogene, 1999. **18**(48): p. 6829-34.
120. Kawakami, T., et al., *NEDD8 recruits E2-ubiquitin to SCF E3 ligase.* EMBO J, 2001. **20**(15): p. 4003-12.
121. Lyapina, S., et al., *Promotion of NEDD-CUL1 conjugate cleavage by COP9 signalosome.* Science, 2001. **292**(5520): p. 1382-5.
122. Verma, R., R.M. Feldman, and R.J. Deshaies, *SIC1 is ubiquitinated in vitro by a pathway that requires CDC4, CDC34, and cyclin/CDK activities.* Mol Biol Cell, 1997. **8**(8): p. 1427-37.
123. Schwob, E., et al., *The B-type cyclin kinase inhibitor p40SIC1 controls the G1 to S transition in S. cerevisiae.* Cell, 1994. **79**(2): p. 233-44.

124. Hwang, H.C. and B.E. Clurman, *Cyclin E in normal and neoplastic cell cycles.* Oncogene, 2005. **24**(17): p. 2776-86.
125. Tsai, L.H., E. Harlow, and M. Meyerson, *Isolation of the human cdk2 gene that encodes the cyclin A- and adenovirus E1A-associated p33 kinase.* Nature, 1991. **353**(6340): p. 174-7.
126. Koff, A., et al., *Formation and activation of a cyclin E-cdk2 complex during the G1 phase of the human cell cycle.* Science, 1992. **257**(5077): p. 1689-94.
127. Moberg, K.H., et al., *Archipelago regulates Cyclin E levels in Drosophila and is mutated in human cancer cell lines.* Nature, 2001. **413**(6853): p. 311-6.
128. Strohmaier, H., et al., *Human F-box protein hCdc4 targets cyclin E for proteolysis and is mutated in a breast cancer cell line.* Nature, 2001. **413**(6853): p. 316-22.
129. Welcker, M., et al., *Multisite phosphorylation by Cdk2 and GSK3 controls cyclin E degradation.* Mol Cell, 2003. **12**(2): p. 381-92.
130. Ye, X., et al., *Recognition of phosphodegron motifs in human cyclin E by the SCF(Fbw7) ubiquitin ligase.* J Biol Chem, 2004. **279**(48): p. 50110-9.
131. Grandori, C., et al., *The Myc/Max/Mad network and the transcriptional control of cell behavior.* Annu Rev Cell Dev Biol, 2000. **16**: p. 653-99.
132. Yada, M., et al., *Phosphorylation-dependent degradation of c-Myc is mediated by the F-box protein Fbw7.* EMBO J, 2004. **23**(10): p. 2116-25.
133. Welcker, M., et al., *The Fbw7 tumor suppressor regulates glycogen synthase kinase 3 phosphorylation-dependent c-Myc protein degradation.* Proc Natl Acad Sci U S A, 2004. **101**(24): p. 9085-90.
134. Yeh, E., et al., *A signalling pathway controlling c-Myc degradation that impacts oncogenic transformation of human cells.* Nat Cell Biol, 2004. **6**(4): p. 308-18.
135. Shaulian, E. and M. Karin, *AP-1 as a regulator of cell life and death.* Nat Cell Biol, 2002. **4**(5): p. E131-6.
136. Musti, A.M., M. Treier, and D. Bohmann, *Reduced ubiquitin-dependent degradation of c-Jun after phosphorylation by MAP kinases.* Science, 1997. **275**(5298): p. 400-2.
137. Fuchs, S.Y., et al., *c-Jun NH2-terminal kinases target the ubiquitination of their associated transcription factors.* J Biol Chem, 1997. **272**(51): p. 32163-8.
138. Nateri, A.S., et al., *The ubiquitin ligase SCFFbw7 antagonizes apoptotic JNK signaling.* Science, 2004. **303**(5662): p. 1374-8.
139. Sundqvist, A., et al., *Control of lipid metabolism by phosphorylation-dependent degradation of the SREBP family of transcription factors by SCF(Fbw7).* Cell Metab, 2005. **1**(6): p. 379-91.
140. Punga, T., M.T. Bengoechea-Alonso, and J. Ericsson, *Phosphorylation and ubiquitination of the transcription factor sterol regulatory element-binding protein-1 in response to DNA binding.* J Biol Chem, 2006. **281**(35): p. 25278-86.
141. Artavanis-Tsakonas, S., M.D. Rand, and R.J. Lake, *Notch signaling: cell fate control and signal integration in development.* Science, 1999. **284**(5415): p. 770-6.
142. Hubbard, E.J., et al., *sel-10, a negative regulator of lin-12 activity in Caenorhabditis elegans, encodes a member of the CDC4 family of proteins.* Genes Dev, 1997. **11**(23): p. 3182-93.
143. Oberg, C., et al., *The Notch intracellular domain is ubiquitinated and negatively regulated by the mammalian Sel-10 homolog.* J Biol Chem, 2001. **276**(38): p. 35847-53.
144. Tetzlaff, M.T., et al., *Defective cardiovascular development and elevated cyclin E and Notch proteins in mice lacking the Fbw7 F-box protein.* Proc Natl Acad Sci U S A, 2004. **101**(10): p. 3338-45.
145. Tsunematsu, R., et al., *Mouse Fbw7/Sel-10/Cdc4 is required for notch degradation during vascular development.* J Biol Chem, 2004. **279**(10): p. 9417-23.
146. O'Neil, J., et al., *FBW7 mutations in leukemic cells mediate NOTCH pathway activation and resistance to gamma-secretase inhibitors.* J Exp Med, 2007. **204**(8): p. 1813-24.
147. Thompson, B.J., et al., *The SCFFBW7 ubiquitin ligase complex as a tumor suppressor in T cell leukemia.* J Exp Med, 2007. **204**(8): p. 1825-35.
148. Palomero, T., et al., *NOTCH1 directly regulates c-MYC and activates a feed-forward-loop transcriptional network promoting leukemic cell growth.* Proc Natl Acad Sci U S A, 2006. **103**(48): p. 18261-6.

149. Weng, A.P., et al., *c-Myc is an important direct target of Notch1 in T-cell acute lymphoblastic leukemia/lymphoma.* Genes Dev, 2006. **20**(15): p. 2096-109.
150. Sharma, V.M., et al., *Notch1 contributes to mouse T-cell leukemia by directly inducing the expression of c-myc.* Mol Cell Biol, 2006. **26**(21): p. 8022-31.
151. Wu, G., et al., *Evidence for functional and physical association between Caenorhabditis elegans SEL-10, a Cdc4p-related protein, and SEL-12 presenilin.* Proc Natl Acad Sci U S A, 1998. **95**(26): p. 15787-91.
152. Li, J., et al., *SEL-10 interacts with presenilin 1, facilitates its ubiquitination, and alters A-beta peptide production.* J Neurochem, 2002. **82**(6): p. 1540-8.
153. Ramsay, R.G. and T.J. Gonda, *MYB function in normal and cancer cells.* Nat Rev Cancer, 2008. **8**(7): p. 523-34.
154. Kitagawa, K., et al., *Fbw7 promotes ubiquitin-dependent degradation of c-Myb: involvement of GSK3-mediated phosphorylation of Thr-572 in mouse c-Myb.* Oncogene, 2009. **28**(25): p. 2393-405.
155. Hay, N. and N. Sonenberg, *Upstream and downstream of mTOR.* Genes Dev, 2004. **18**(16): p. 1926-45.
156. Mao, J.H., et al., *FBXW7 targets mTOR for degradation and cooperates with PTEN in tumor suppression.* Science, 2008. **321**(5895): p. 1499-502.
157. Feige, J.N. and J. Auwerx, *Transcriptional coregulators in the control of energy homeostasis.* Trends Cell Biol, 2007. **17**(6): p. 292-301.
158. Olson, B.L., et al., *SCFCdc4 acts antagonistically to the PGC-1alpha transcriptional coactivator by targeting it for ubiquitin-mediated proteolysis.* Genes Dev, 2008. **22**(2): p. 252-64.
159. Kumar, A. and J.V. Paietta, *The sulfur controller-2 negative regulatory gene of Neurospora crassa encodes a protein with beta-transducin repeats.* Proc Natl Acad Sci U S A, 1995. **92**(8): p. 3343-7.
160. Durfee, T., et al., *The retinoblastoma protein associates with the protein phosphatase type 1 catalytic subunit.* Genes Dev, 1993. **7**(4): p. 555-69.
161. Harper, J.W., et al., *The p21 Cdk-interacting protein Cip1 is a potent inhibitor of G1 cyclin-dependent kinases.* Cell, 1993. **75**(4): p. 805-16.
162. Jin, J., et al., *Systematic analysis and nomenclature of mammalian F-box proteins.* Genes Dev, 2004. **18**(21): p. 2573-80.
163. Hartwell, L.H., et al., *Genetic Control of the Cell Division Cycle in Yeast: V. Genetic Analysis of cdc Mutants.* Genetics, 1973. **74**(2): p. 267-286.
164. Meimoun, A., et al., *Degradation of the transcription factor Gcn4 requires the kinase Pho85 and the SCF(CDC4) ubiquitin-ligase complex.* Mol Biol Cell, 2000. **11**(3): p. 915-27.
165. Henchoz, S., et al., *Phosphorylation- and ubiquitin-dependent degradation of the cyclin-dependent kinase inhibitor Far1p in budding yeast.* Genes Dev, 1997. **11**(22): p. 3046-60.
166. Perkins, G., L.S. Drury, and J.F. Diffley, *Separate SCF(CDC4) recognition elements target Cdc6 for proteolysis in S phase and mitosis.* EMBO J, 2001. **20**(17): p. 4836-45.
167. Drury, L.S., G. Perkins, and J.F. Diffley, *The Cdc4/34/53 pathway targets Cdc6p for proteolysis in budding yeast.* EMBO J, 1997. **16**(19): p. 5966-76.
168. Nash, P., et al., *Multisite phosphorylation of a CDK inhibitor sets a threshold for the onset of DNA replication.* Nature, 2001. **414**(6863): p. 514-21.
169. Maruyama, S., et al., *Characterization of a mouse gene (Fbxw6) that encodes a homologue of Caenorhabditis elegans SEL-10.* Genomics, 2001. **78**(3): p. 214-22.
170. Ding, M., et al., *Spatial regulation of an E3 ubiquitin ligase directs selective synapse elimination.* Science, 2007. **317**(5840): p. 947-51.
171. Mortimer, N.T. and K.H. Moberg, *The Drosophila F-box protein Archipelago controls levels of the Trachealess transcription factor in the embryonic tracheal system.* Dev Biol, 2007. **312**(2): p. 560-71.
172. Ho, M.S., et al., *Gcm protein degradation suppresses proliferation of glial progenitors.* Proc Natl Acad Sci U S A, 2009. **106**(16): p. 6778-83.
173. Onoyama, I., et al., *Conditional inactivation of Fbxw7 impairs cell-cycle exit during T cell*

differentiation and results in lymphomatogenesis. J Exp Med, 2007. **204**(12): p. 2875-88.
174. Spruck, C.H., et al., *hCDC4 gene mutations in endometrial cancer.* Cancer Res, 2002. **62**(16): p. 4535-9.
175. Lee, J.W., et al., *Mutational analysis of the hCDC4 gene in gastric carcinomas.* Eur J Cancer, 2006. **42**(14): p. 2369-73.
176. Maser, R.S., et al., *Chromosomally unstable mouse tumours have genomic alterations similar to diverse human cancers.* Nature, 2007. **447**(7147): p. 966-71.
177. Kemp, Z., et al., *CDC4 mutations occur in a subset of colorectal cancers but are not predicted to cause loss of function and are not associated with chromosomal instability.* Cancer Res, 2005. **65**(24): p. 11361-6.
178. Hubalek, M.M., et al., *Cyclin E dysregulation and chromosomal instability in endometrial cancer.* Oncogene, 2004. **23**(23): p. 4187-92.
179. Koh, M.S., et al., *CDC4 gene expression as potential biomarker for targeted therapy in prostate cancer.* Cancer Biol Ther, 2006. **5**(1): p. 78-83.
180. Calhoun, E.S., et al., *BRAF and FBXW7 (CDC4, FBW7, AGO, SEL10) mutations in distinct subsets of pancreatic cancer: potential therapeutic targets.* Am J Pathol, 2003. **163**(4): p. 1255-60.
181. Akhoondi, S., et al., *FBXW7/hCDC4 is a general tumor suppressor in human cancer.* Cancer Res, 2007. **67**(19): p. 9006-12.
182. Malyukova, A., et al., *The tumor suppressor gene hCDC4 is frequently mutated in human T-cell acute lymphoblastic leukemia with functional consequences for Notch signaling.* Cancer Res, 2007. **67**(12): p. 5611-6.
183. Kwak, E.L., et al., *Infrequent mutations of Archipelago (hAGO, hCDC4, Fbw7) in primary ovarian cancer.* Gynecol Oncol, 2005. **98**(1): p. 124-8.
184. Nowak, D., et al., *Mutation analysis of hCDC4 in AML cells identifies a new intronic polymorphism.* Int J Med Sci, 2006. **3**(4): p. 148-51.
185. Sgambato, A., et al., *Low frequency of hCDC4 mutations in human primary ovarian cancer.* Gynecol Oncol, 2007. **105**(2): p. 553-5.
186. Woo Lee, J., et al., *Somatic mutation of hCDC4 gene is rare in lung adenocarcinomas.* Acta Oncol, 2006. **45**(4): p. 487-8.
187. Yan, T., et al., *hCDC4 variation in osteosarcoma.* Cancer Genet Cytogenet, 2006. **169**(2): p. 138-42.
188. Mao, J.H., et al., *Fbxw7/Cdc4 is a p53-dependent, haploinsufficient tumour suppressor gene.* Nature, 2004. **432**(7018): p. 775-9.
189. Bortner, D.M. and M.P. Rosenberg, *Induction of mammary gland hyperplasia and carcinomas in transgenic mice expressing human cyclin E.* Mol Cell Biol, 1997. **17**(1): p. 453-9.
190. Spruck, C.H., K.A. Won, and S.I. Reed, *Deregulated cyclin E induces chromosome instability.* Nature, 1999. **401**(6750): p. 297-300.
191. Minella, A.C., et al., *p53 and p21 form an inducible barrier that protects cells against cyclin E-cdk2 deregulation.* Curr Biol, 2002. **12**(21): p. 1817-27.
192. Yoon, H.J., et al., *Proteomics analysis identifies new components of the fission and budding yeast anaphase-promoting complexes.* Curr Biol, 2002. **12**(23): p. 2048-54.
193. Schwab, M., A.S. Lutum, and W. Seufert, *Yeast Hct1 is a regulator of Clb2 cyclin proteolysis.* Cell, 1997. **90**(4): p. 683-93.
194. Burton, J.L. and M.J. Solomon, *D box and KEN box motifs in budding yeast Hsl1p are required for APC-mediated degradation and direct binding to Cdc20p and Cdh1p.* Genes Dev, 2001. **15**(18): p. 2381-95.
195. Shirayama, M., et al., *The Polo-like kinase Cdc5p and the WD-repeat protein Cdc20p/fizzy are regulators and substrates of the anaphase promoting complex in Saccharomyces cerevisiae.* EMBO J, 1998. **17**(5): p. 1336-49.
196. Lukas, C., et al., *Accumulation of cyclin B1 requires E2F and cyclin-A-dependent rearrangement of the anaphase-promoting complex.* Nature, 1999. **401**(6755): p. 815-8.
197. Jaspersen, S.L., J.F. Charles, and D.O. Morgan, *Inhibitory phosphorylation of the APC regulator Hct1 is controlled by the kinase Cdc28 and the phosphatase Cdc14.* Curr Biol, 1999.

9(5): p. 227-36.
198. Dulic, V., E. Lees, and S.I. Reed, *Association of human cyclin E with a periodic G1-S phase protein kinase.* Science, 1992. **257**(5078): p. 1958-61.
199. Lew, D.J., V. Dulic, and S.I. Reed, *Isolation of three novel human cyclins by rescue of G1 cyclin (Cln) function in yeast.* Cell, 1991. **66**(6): p. 1197-206.
200. Won, K.A. and S.I. Reed, *Activation of cyclin E/CDK2 is coupled to site-specific autophosphorylation and ubiquitin-dependent degradation of cyclin E.* Embo J, 1996. **15**(16): p. 4182-93.
201. Clurman, B.E., et al., *Turnover of cyclin E by the ubiquitin-proteasome pathway is regulated by cdk2 binding and cyclin phosphorylation.* Genes Dev, 1996. **10**(16): p. 1979-90.
202. Sherr, C.J. and J.M. Roberts, *CDK inhibitors: positive and negative regulators of G1-phase progression.* Genes Dev, 1999. **13**(12): p. 1501-12.
203. Coats, S., et al., *Requirement of p27Kip1 for restriction point control of the fibroblast cell cycle.* Science, 1996. **272**(5263): p. 877-80.
204. Chu, I.M., L. Hengst, and J.M. Slingerland, *The Cdk inhibitor p27 in human cancer: prognostic potential and relevance to anticancer therapy.* Nat Rev Cancer, 2008. **8**(4): p. 253-67.
205. Carrano, A.C., et al., *SKP2 is required for ubiquitin-mediated degradation of the CDK inhibitor p27.* Nat Cell Biol, 1999. **1**(4): p. 193-9.
206. Ganoth, D., et al., *The cell-cycle regulatory protein Cks1 is required for SCF(Skp2)-mediated ubiquitinylation of p27.* Nat Cell Biol, 2001. **3**(3): p. 321-4.
207. Spruck, C., et al., *A CDK-independent function of mammalian Cks1: targeting of SCF(Skp2) to the CDK inhibitor p27Kip1.* Mol Cell, 2001. **7**(3): p. 639-50.
208. Ekholm-Reed, S., et al., *Mutation of hCDC4 leads to cell cycle deregulation of cyclin E in cancer.* Cancer Res, 2004. **64**(3): p. 795-800.
209. Welcker, M., et al., *A nucleolar isoform of the Fbw7 ubiquitin ligase regulates c-Myc and cell size.* Curr Biol, 2004. **14**(20): p. 1852-7.
210. Grim, J.E., et al., *Isoform- and cell cycle-dependent substrate degradation by the Fbw7 ubiquitin ligase.* J Cell Biol, 2008. **181**(6): p. 913-20.
211. Reed, S.I., *Cooperation between different Cdc4/Fbw7 isoforms may be associated with 2-step inactivation of SCF(Cdc4) targets.* Cell Cycle, 2006. **5**(17): p. 1923-4.
212. van Drogen, F., et al., *Ubiquitylation of cyclin E requires the sequential function of SCF complexes containing distinct hCdc4 isoforms.* Mol Cell, 2006. **23**(1): p. 37-48.
213. Sangfelt, O., et al., *Both SCF(Cdc4alpha) and SCF(Cdc4gamma) are required for cyclin E turnover in cell lines that do not overexpress cyclin E.* Cell Cycle, 2008. **7**(8): p. 1075-82.
214. Kimura, T., et al., *hCDC4b, a regulator of cyclin E, as a direct transcriptional target of p53.* Cancer Sci, 2003. **94**(5): p. 431-6.
215. Bonetti, P., et al., *Nucleophosmin and its AML-associated mutant regulate c-Myc turnover through Fbw7 gamma.* J Cell Biol, 2008. **182**(1): p. 19-26.
216. Borer, R.A., et al., *Major nucleolar proteins shuttle between nucleus and cytoplasm.* Cell, 1989. **56**(3): p. 379-90.
217. Falini, B., et al., *Cytoplasmic nucleophosmin in acute myelogenous leukemia with a normal karyotype.* N Engl J Med, 2005. **352**(3): p. 254-66.
218. Cassia, R., et al., *Cyclin E gene (CCNE) amplification and hCDC4 mutations in endometrial carcinoma.* J Pathol, 2003. **201**(4): p. 589-95.
219. Willmarth, N.E., D.G. Albertson, and S.P. Ethier, *Chromosomal instability and lack of cyclin E regulation in hCdc4 mutant human breast cancer cells.* Breast Cancer Res, 2004. **6**(5): p. R531-9.
220. Moberg, K.H., et al., *The Drosophila F box protein archipelago regulates dMyc protein levels in vivo.* Curr Biol, 2004. **14**(11): p. 965-74.
221. Gupta-Rossi, N., et al., *Functional interaction between SEL-10, an F-box protein, and the nuclear form of activated Notch1 receptor.* J Biol Chem, 2001. **276**(37): p. 34371-8.
222. Wu, G., et al., *SEL-10 is an inhibitor of notch signaling that targets notch for ubiquitin-mediated protein degradation.* Mol Cell Biol, 2001. **21**(21): p. 7403-15.

223. Yeh, E.S., B.O. Lew, and A.R. Means, *The loss of PIN1 deregulates cyclin E and sensitizes mouse embryo fibroblasts to genomic instability.* J Biol Chem, 2006. **281**(1): p. 241-51.
224. Kominami, K., I. Ochotorena, and T. Toda, *Two F-box/WD-repeat proteins Pop1 and Pop2 form hetero- and homo-complexes together with cullin-1 in the fission yeast SCF (Skp1-Cullin-1-F-box) ubiquitin ligase.* Genes Cells, 1998. **3**(11): p. 721-35.
225. Kominami, K. and T. Toda, *Fission yeast WD-repeat protein pop1 regulates genome ploidy through ubiquitin-proteasome-mediated degradation of the CDK inhibitor Rum1 and the S-phase initiator Cdc18.* Genes Dev, 1997. **11**(12): p. 1548-60.
226. Wolf, D.A., F. McKeon, and P.K. Jackson, *F-box/WD-repeat proteins pop1p and Sud1p/Pop2p form complexes that bind and direct the proteolysis of cdc18p.* Curr Biol, 1999. **9**(7): p. 373-6.
227. Yamano, H., et al., *Requirement of the SCFPop1/Pop2 Ubiquitin Ligase for Degradation of the Fission Yeast S Phase Cyclin Cig2.* J Biol Chem, 2004. **279**(18): p. 18974-80.
228. Suzuki, H., et al., *Homodimer of two F-box proteins betaTrCP1 or betaTrCP2 binds to IkappaBalpha for signal-dependent ubiquitination.* J Biol Chem, 2000. **275**(4): p. 2877-84.
229. Cope, G.A. and R.J. Deshaies, *COP9 signalosome: a multifunctional regulator of SCF and other cullin-based ubiquitin ligases.* Cell, 2003. **114**(6): p. 663-71.
230. Zheng, J., et al., *CAND1 binds to unneddylated CUL1 and regulates the formation of SCF ubiquitin E3 ligase complex.* Mol Cell, 2002. **10**(6): p. 1519-26.
231. Liu, J., et al., *NEDD8 modification of CUL1 dissociates p120(CAND1), an inhibitor of CUL1-SKP1 binding and SCF ligases.* Mol Cell, 2002. **10**(6): p. 1511-8.
232. Doronkin, S., I. Djagaeva, and S.K. Beckendorf, *The COP9 signalosome promotes degradation of Cyclin E during early Drosophila oogenesis.* Dev Cell, 2003. **4**(5): p. 699-710.
233. Lykke-Andersen, K., et al., *Disruption of the COP9 signalosome Csn2 subunit in mice causes deficient cell proliferation, accumulation of p53 and cyclin E, and early embryonic death.* Mol Cell Biol, 2003. **23**(19): p. 6790-7.
234. Bornstein, G., D. Ganoth, and A. Hershko, *Regulation of neddylation and deneddylation of cullin1 in SCFSkp2 ubiquitin ligase by F-box protein and substrate.* Proc Natl Acad Sci U S A, 2006. **103**(31): p. 11515-20.
235. Cope, G.A. and R.J. Deshaies, *Targeted silencing of Jab1/Csn5 in human cells downregulates SCF activity through reduction of F-box protein levels.* BMC Biochem, 2006. **7**: p. 1.
236. Schulman, B.A., et al., *Insights into SCF ubiquitin ligases from the structure of the Skp1-Skp2 complex.* Nature, 2000. **408**(6810): p. 381-6.
237. Liu, Q., et al., *The univector plasmid-fusion system, a method for rapid construction of recombinant DNA without restriction enzymes.* Curr Biol, 1998. **8**(24): p. 1300-9.
238. Welcker, M. and B.E. Clurman, *FBW7 ubiquitin ligase: a tumour suppressor at the crossroads of cell division, growth and differentiation.* Nature Reviews Cancer, 2008. **8**(2): p. 83-93.
239. Sundqvist, A., et al., *Control of lipid metabolism by phosphorylation-dependent degradation of the SREBP family of transcription factors by SCFFbw7.* Cell Metabolism, 2005. **1**(6): p. 379-391.
240. Popov, N., et al., *The ubiquitin-specific protease USP28 is required for MYC stability.* Nature Cell Biology, 2007. **9**(7): p. 765-U71.
241. Sangfelt, O., et al., *Both SCFCdc4 alpha and SCFCdc4 gamma are required for cyclin E turnover in cell lines that do not overexpress cyclin E.* Cell Cycle, 2008. **7**(8): p. 1075-1082.
242. Seidel, G. and R. Prohaska, *Molecular cloning of hSLP-1, a novel human brain-specific member of the band 7/MEC-2 family similar to Caenorhabditis elegans UNC-24.* Gene, 1998. **225**(1-2): p. 23-9.
243. Sedensky, M.M., et al., *A stomatin and a degenerin interact in lipid rafts of the nervous system of Caenorhabditis elegans.* Am J Physiol Cell Physiol, 2004. **287**(2): p. C468-74.
244. Zhang, S.F., et al., *MEC-2 is recruited to the putative mechanosensory complex in C-elegans touch receptor neurons through its stomatin-like domain.* Current Biology, 2004. **14**(21): p. 1888-1896.
245. Mairhofer, M., et al., *Stomatin-like protein-1 interacts with stomatin and is targeted to late endosomes.* J Biol Chem, 2009. **284**(42): p. 29218-29.
246. Grim, J.E., et al., *Isoform- and cell cycle-dependent substrate degradation by the Fbw7*

ubiquitin ligase. Journal of Cell Biology, 2008. **181**(6): p. 913-920.
247. Green, J.B. and J.P. Young, *Slipins: ancient origin, duplication and diversification of the stomatin protein family.* BMC Evol Biol, 2008. **8**: p. 44.
248. Jackman, M., et al., *Cyclin A- and cyclin E-Cdk complexes shuttle between the nucleus and the cytoplasm.* Mol Biol Cell, 2002. **13**(3): p. 1030-45.
249. Zhang, W. and D.M. Koepp, *Fbw7 isoform interaction contributes to cyclin E proteolysis.* Mol Cancer Res, 2006. **4**(12): p. 935-43.
250. Bai, C. and S.J. Elledge, *Gene identification using the yeast two-hybrid system.* Methods Enzymol, 1996. **273**: p. 331-47.
251. van den Heuvel, S. and E. Harlow, *Distinct roles for cyclin-dependent kinases in cell cycle control.* Science, 1993. **262**(5142): p. 2050-4.
252. Welcker, M. and B.E. Clurman, *Fbw7/hCDC4 dimerization regulates its substrate interactions.* Cell Div, 2007. **2**: p. 7.
253. Welcker, M. and B.E. Clurman, *FBW7 ubiquitin ligase: a tumour suppressor at the crossroads of cell division, growth and differentiation.* Nat Rev Cancer, 2008. **8**(2): p. 83-93.
254. Tang, X., et al., *Suprafacial orientation of the SCFCdc4 dimer accommodates multiple geometries for substrate ubiquitination.* Cell, 2007. **129**(6): p. 1165-76.
255. Stewart, G.W., A.C. Argent, and B.C. Dash, *Stomatin: a putative cation transport regulator in the red cell membrane.* Biochim Biophys Acta, 1993. **1225**(1): p. 15-25.
256. Unfried, I., B. Entler, and R. Prohaska, *The organization of the gene (EPB72) encoding the human erythrocyte band 7 integral membrane protein (protein 7.2b).* Genomics, 1995. **30**(3): p. 521-8.
257. Zhang, L., et al., *Stomatin-like protein 2 is overexpressed in cancer and involved in regulating cell growth and cell adhesion in human esophageal squamous cell carcinoma.* Clin Cancer Res, 2006. **12**(5): p. 1639-46.
258. Goldstein, B.J., H.M. Kulaga, and R.R. Reed, *Cloning and characterization of SLP3: a novel member of the stomatin family expressed by olfactory receptor neurons.* J Assoc Res Otolaryngol, 2003. **4**(1): p. 74-82.
259. Wetzel, C., et al., *A stomatin-domain protein essential for touch sensation in the mouse.* Nature, 2007. **445**(7124): p. 206-9.
260. Roselli, S., et al., *Podocin localizes in the kidney to the slit diaphragm area.* Am J Pathol, 2002. **160**(1): p. 131-9.
261. Boute, N., et al., *NPHS2, encoding the glomerular protein podocin, is mutated in autosomal recessive steroid-resistant nephrotic syndrome.* Nat Genet, 2000. **24**(4): p. 349-54.
262. Schlegel, W., I. Unfried, and R. Prohaska, *Cloning and analysis of a cDNA encoding the BALB/c murine erythrocyte band 7 integral membrane protein.* Gene, 1996. **178**(1-2): p. 115-8.
263. Barnes, T.M., et al., *The Caenorhabditis elegans behavioral gene unc-24 encodes a novel bipartite protein similar to both erythrocyte band 7.2 (stomatin) and nonspecific lipid transfer protein.* J Neurochem, 1996. **67**(1): p. 46-57.
264. Huang, M., et al., *A stomatin-like protein necessary for mechanosensation in C. elegans.* Nature, 1995. **378**(6554): p. 292-5.
265. Rajaram, S., M.M. Sedensky, and P.G. Morgan, *Unc-1: a stomatin homologue controls sensitivity to volatile anesthetics in Caenorhabditis elegans.* Proc Natl Acad Sci U S A, 1998. **95**(15): p. 8761-6.
266. Mairhofer, M., et al., *Stomatin is a major lipid-raft component of platelet alpha granules.* Blood, 2002. **100**(3): p. 897-904.
267. Salzer, U. and R. Prohaska, *Stomatin, flotillin-1, and flotillin-2 are major integral proteins of erythrocyte lipid rafts.* Blood, 2001. **97**(4): p. 1141-3.
268. Da Cruz, S., et al., *SLP-2 interacts with prohibitins in the mitochondrial inner membrane and contributes to their stability.* Biochim Biophys Acta, 2008. **1783**(5): p. 904-11.
269. McClung, J.K., et al., *Prohibitin: potential role in senescence, development, and tumor suppression.* Exp Gerontol, 1995. **30**(2): p. 99-124.
270. Steglich, G., W. Neupert, and T. Langer, *Prohibitins regulate membrane protein degradation by the m-AAA protease in mitochondria.* Mol Cell Biol, 1999. **19**(5): p. 3435-42.

271. Sedensky, M.M., J.M. Siefker, and P.G. Morgan, *Model organisms: new insights into ion channel and transporter function. Stomatin homologues interact in Caenorhabditis elegans.* Am J Physiol Cell Physiol, 2001. **280**(5): p. C1340-8.
272. Snyers, L., E. Umlauf, and R. Prohaska, *Oligomeric nature of the integral membrane protein stomatin.* J Biol Chem, 1998. **273**(27): p. 17221-6.
273. Browman, D.T., et al., *Erlin-1 and erlin-2 are novel members of the prohibitin family of proteins that define lipid-raft-like domains of the ER.* J Cell Sci, 2006. **119**(Pt 15): p. 3149-60.
274. Pearce, M.M., et al., *SPFH2 mediates the endoplasmic reticulum-associated degradation of inositol 1,4,5-trisphosphate receptors and other substrates in mammalian cells.* J Biol Chem, 2007. **282**(28): p. 20104-15.
275. Meusser, B., et al., *ERAD: the long road to destruction.* Nat Cell Biol, 2005. **7**(8): p. 766-72.
276. Webster, J.M., et al., *Inositol 1,4,5-trisphosphate receptor ubiquitination is mediated by mammalian Ubc7, a component of the endoplasmic reticulum-associated degradation pathway, and is inhibited by chelation of intracellular Zn2+.* J Biol Chem, 2003. **278**(40): p. 38238-46.
277. Pearce, M.M., et al., *An endoplasmic reticulum (ER) membrane complex composed of SPFH1 and SPFH2 mediates the ER-associated degradation of inositol 1,4,5-trisphosphate receptors.* J Biol Chem, 2009. **284**(16): p. 10433-45.
278. Horwich, A.L., et al., *Two families of chaperonin: physiology and mechanism.* Annu Rev Cell Dev Biol, 2007. **23**: p. 115-45.
279. Winston, J.T., et al., *A family of mammalian F-box proteins.* Curr Biol, 1999. **9**(20): p. 1180-2.
280. Yoshida, Y., et al., *E3 ubiquitin ligase that recognizes sugar chains.* Nature, 2002. **418**(6896): p. 438-42.
281. Nelson, R.F., et al., *A novel route for F-box protein-mediated ubiquitination links CHIP to glycoprotein quality control.* J Biol Chem, 2006. **281**(29): p. 20242-51.
282. Rogers, S., R. Wells, and M. Rechsteiner, *Amino acid sequences common to rapidly degraded proteins: the PEST hypothesis.* Science, 1986. **234**(4774): p. 364-8.

APPENDICES

The C. elegans L1CAM homologue LAD-2 functions as a coreceptor in MAB-20/Sema2- mediated axon guidance

Xuelin Wang,[1] Wei Zhang,[1,2] Thomas Cheever,[1] Valentin Schwarz,[3] Karla Opperman,[1] Harald Hutter,[3,4] Deanna Koepp,[1,2] and Lihsia Chen[1]

1 Department of Genetics, Cell Biology, and Development, Developmental Biology Center, and 2 University of Minnesota Cancer Center,
University of Minnesota,
Minneapolis, MN 55455

3 Max Planck Institute for Medical Research, 69210 Heidelberg, Germany

4 Department of Biological Sciences, Simon Fraser University,
Burnaby V5A 1S6, Canada

(This material has appeared as "The *C. elegans* L1CAM homologue LAD-2 functions as a coreceptor in MAB-20/Sema2- mediated axon guidance" by Wang et al in *Journal of Cell Bioogy* 2008, Jan; Vol. 180(1)233-246. It is used here by permission)

The *C. elegans* L1CAM homologue LAD-2 functions as a coreceptor in MAB-20/Sema2–mediated axon guidance

Xuelin Wang,[1] Wei Zhang,[1,2] Thomas Cheever,[1] Valentin Schwarz,[3] Karla Opperman,[1] Harald Hutter,[3,4] Deanna Koepp,[1,2] and Lihsia Chen[1]

[1]Department of Genetics, Cell Biology, and Development, Developmental Biology Center, and [2]University of Minnesota Cancer Center, University of Minnesota, Minneapolis, MN 55455
[3]Max Planck Institute for Medical Research, 69210 Heidelberg, Germany
[4]Department of Biological Sciences, Simon Fraser University, Burnaby V5A 1S6, Canada

The L1 cell adhesion molecule (L1CAM) participates in neuronal development. Mutations in the human L1 gene can cause the neurological disorder CRASH (corpus callosum hypoplasia, retardation, adducted thumbs, spastic paraplegia, and hydrocephalus). This study presents genetic data that shows that L1-like adhesion gene 2 (LAD-2), a *Caenorhabditis elegans* L1CAM, functions in axon pathfinding. In the SDQL neuron, LAD-2 mediates dorsal axon guidance via the secreted MAB-20/Sema2 and PLX-2 plexin receptor, the functions of which have largely been characterized in epidermal morphogenesis. We use targeted misexpression experiments to provide in vivo evidence that MAB-20/Sema2 acts as a repellent to SDQL. Coimmunoprecipitation assays reveal that MAB-20 weakly interacts with PLX-2; this interaction is increased in the presence of LAD-2, which can interact independently with MAB-20 and PLX-2. These results suggest that LAD-2 functions as a MAB-20 coreceptor to secure MAB-20 coupling to PLX-2. In vertebrates, L1 binds neuropilin1, the obligate receptor to the secreted Sema3A. However, invertebrates lack neuropilins. LAD-2 may thus function in the semaphorin complex by combining the roles of neuropilins and L1CAMs.

Introduction

During nervous system development, complex neural networks and connections are formed to ensure proper connections at appropriate times. An important aspect in the construction of these neural networks is directed migration of axons, a process that depends on the ability of the axons to sense and respond to environmental cues that include semaphorins, netrins, and slits (for review see Chilton, 2006). Axonal response to these cues is dependent on how the different receptors for these molecules integrate the variety of signals the axons encounter.

Semaphorins are a large family of secreted or membrane-associated glycoproteins that can act as both repellents and attractants to direct axon migration (for review see Kruger et al., 2005). The transmembrane semaphorins bind directly to plexins, the predominant family of semaphorin receptors that transduces semaphorin signaling, which results in actin cytoskeleton rearrangement via proteins that include collapsin response mediator protein and Rac GTPases. In contrast to the membrane-bound semaphorins, the Sema3 class of secreted semaphorins generally does not bind plexins. Instead, they bind directly to neuropilins, transmembrane proteins that are required to link Sema3 to plexin receptors, which transduce Sema3 signaling (for review see Kruger et al., 2005).

The L1 family of cell adhesion molecules (L1CAMs), which is composed of L1, NrCAM, neurofascin, and CHL1, has been implicated in mediating axon guidance via the semaphorin pathway. In vertebrates, mutations in the X-linked L1 gene can result in the neurological CRASH disorder (corpus callosum hypoplasia, retardation, adducted thumbs, spastic paraplegia, and hydrocephalus; for review see Kenwrick et al., 2000). Analysis of L1 knockout mice revealed axon guidance defects in the corticospinal tract (Cohen et al., 1998). Cortical neurons cultured from L1 knockout mice are unresponsive to Sema3A (Castellani et al., 2000), which suggests a role for L1 in Sema3 signaling. L1 was subsequently shown to physically interact with neuropilin1.

Correspondence to L. Chen: chenx260@umn.edu

Abbreviations used in this paper: Co-IP, coimmunoprecipitation; dsRNA, double-stranded RNA; LAD, L1-like adhesion gene; LICAM, L1 cell adhesion molecule; VNC, ventral nerve cord.

The online version of this paper contains supplemental material.

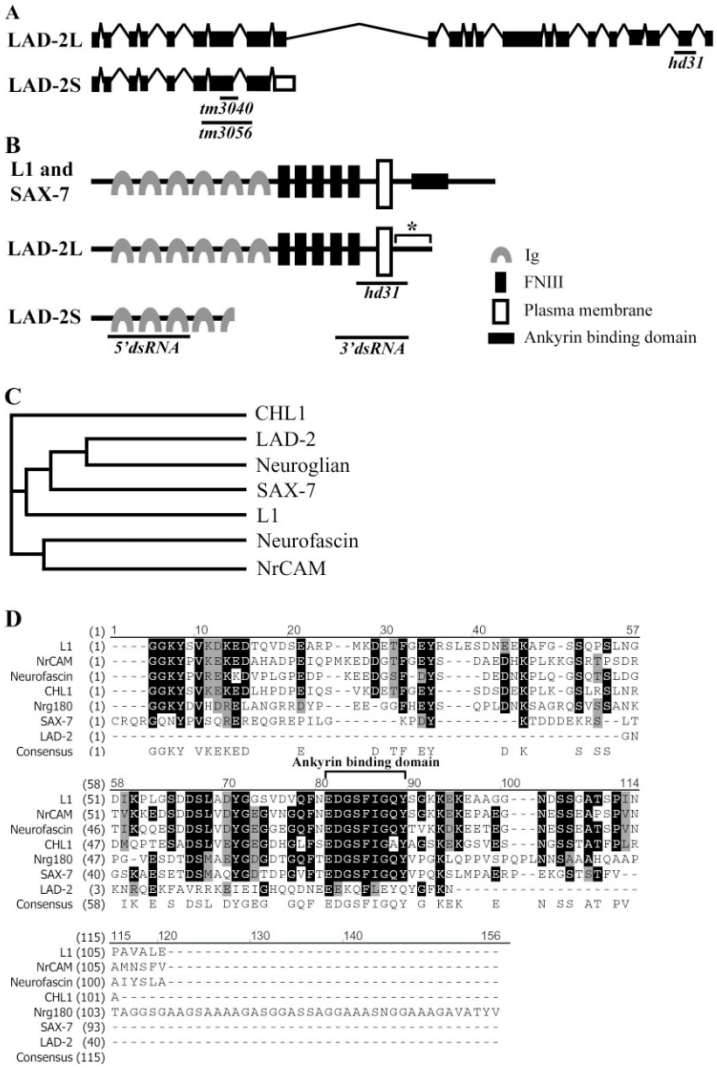

Figure 1. **The *lad-2* gene encodes a non-canonical L1CAM homologue in *C. elegans*.** (A) Genomic organization of the alternatively spliced isoforms (not drawn to scale). The black boxes represent exons; the inverted Vs represent introns; and the open boxes represent an alternatively spliced exon. Black bars mark the end points of the *hd31*, *tm3040*, and *tm3056* deletions. (B) A schematic of the protein structure of L1, SAX-7, and the LAD-2 isoforms LAD-2L and LAD-2S. Anti–LAD-2 antibodies were generated against the LAD-2 cytoplasmic tail (asterisk). Black bars mark the LAD-2 regions that are removed by the *hd31* deletion or targeted by the dsRNAs in RNAi experiments. 5′ dsRNA targets the 5′ sequence that is shared by both LAD-2L and LAD-2S, whereas 3′ dsRNA targets the 3′ sequence that is unique to LAD-2L. (C) A phylogenetic tree of the L1CAM extracellular domains shows that LAD-2 is most closely related to the *D. melanogaster* neuroglian. (D) An amino acid sequence alignment of the L1CAM cytoplasmic tails reveals that LAD-2 has a divergent cytoplasmic tail.

Although it is not clear in vivo how L1 functions in Sema3A signaling, cell culture assays reveal that the L1–neuropilin1 interaction may result in Sema3A-induced endocytosis of neuropilin1, which raises the possibility that L1 may regulate axon sensitivity to Sema3A (Castellani et al., 2000, 2004). Recently, NrCAM was similarly shown to bind Nrp2 to mediate Sema3B signaling (Falk et al., 2005).

L1CAMs, semaphorins, and plexins are conserved in both *Caenorhabitis elegans* and *Drosophila melanogaster* but they lack a neuropilin, raising the possibility that neuropilins may have evolved more recently in vertebrates. The *C. elegans* semaphorins are comprised of the transmembrane Sema1 proteins encoded by the *smp-1* and *smp-2* genes and the secreted Sema2 protein encoded by *mab-20* (Roy et al., 2000; Ginzburg et al., 2002). These semaphorins function in epidermal morphogenesis via the plexins encoded by *plx-1* and *plx-2* (Fujii et al., 2002; Ikegami et al., 2004) but their roles in axon guidance are not known. The *C. elegans* L1CAMs are encoded by *L1-like adhesion gene 1* (*lad-1*)/*sax-7* and *lad-2*. The LAD-1/SAX-7 protein was previously characterized as having roles in maintaining neuronal positioning (Sasakura et al., 2005; Wang et al., 2005).

This study demonstrates that the *C. elegans* L1CAM homologue LAD-2 functions in axon pathfinding. LAD-2 mediates the functions of the secreted MAB-20/Sema2 and its plexin receptor PLX-2 to control axon navigation of the SDQL neuron, which responds to MAB-20 as a repulsive cue. Biochemical data

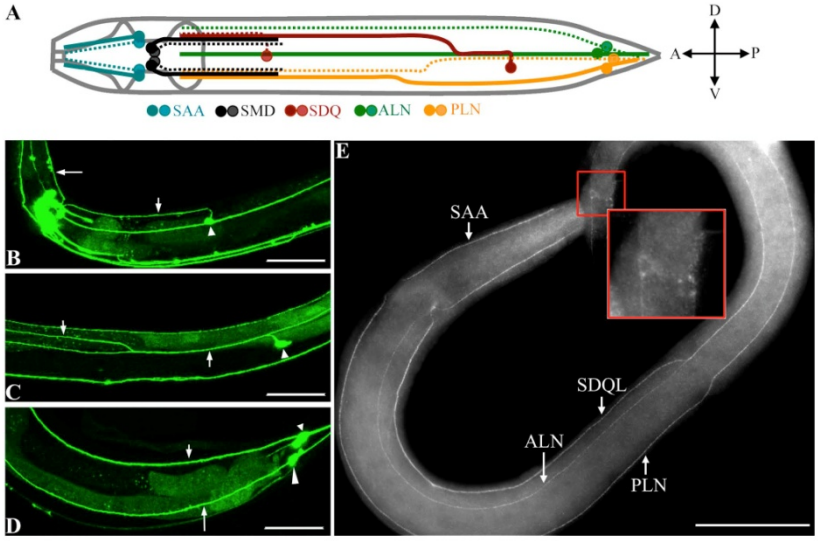

Figure 2. ***lad-2* is expressed in 14 neurons and associated axons.** (A) A schematic depiction of *lad-2*–expressing neurons. Dark colored circles and solid lines represent cell bodies and axons on the left side of the animal. Light colored circles and dotted lines represent cell bodies and axons on the right side of the animal. (B–D) Confocal micrographs of adult wild-type animals expressing $P_{lad\text{-}2}$*::gfp*; left lateral view. (B) The SAA axon (long arrow), SDQR axon (short arrow), and SDQR cell body (arrowhead) are shown. (C) The arrows follow the anterior axon migration of the SDQL neuron (arrowhead). (D) The ALN neuron (small arrowhead) and axon (small arrow) and the PLN neuron (large arrowhead) and axon (long arrow) are shown. (E) A whole-mount immunostaining of a wild-type third-stage larva using the 1622 anti–LAD-2 antibody. Insets show LAD-2 localization on the surface of ALN and PLN cell bodies. Bars, 50 μm.

show that LAD-2 (a) forms protein complexes independently with MAB-20 and PLX-2 and (b) acts to reinforce coupling of MAB-20 to PLX-2, which can interact by themselves, albeit weakly. These results suggest that LAD-2 may function similarly to neuropilin by acting as a MAB-20 coreceptor to secure MAB-20 with PLX-2 in a protein complex required for semaphorin signaling, revealing an ancient role of L1CAM in the conserved process of semaphorin signaling in axon pathfinding.

Results

LAD-2 is a neuronal-specific noncanonical L1CAM

The Y54G2A.25 gene that is located on linkage group IV was previously reported to show homology to L1CAMs (Aurelio et al., 2002); we have named the gene *lad-2*. We performed both 5′ and 3′ rapid amplification of cDNA ends and isolated two alternatively spliced *lad-2* isoforms (Fig. 1 A). One isoform is predicted to encode a 56.3-kD protein containing four immunoglobulin repeats that is likely to be secreted extracellularly (LAD-2S, available from GenBank/EMBL/DDBJ under accession no. EF584657), whereas the larger isoform is predicted to encode a 135.9-kD single-pass transmembrane protein (LAD-2L, available from GenBank/EMBL/DDBJ under accession no. EF584655; Fig. 1 B). The LAD-2L extracellular domain contains six immunoglobulin domains and five fibronectin type III repeats, structural motifs that are also present in vertebrate L1CAMs as well as the *C. elegans* L1CAM LAD-1/SAX-7 (hereafter referred to as SAX-7; for review see Kenwrick et al., 2000; Chen et al., 2001). A phylogenetic analysis of the L1CAM extracellular domain suggests that LAD-2 is most closely related to the *D. melanogaster* L1CAM neuroglian (Fig. 1 C). In contrast to the extracellular domain, the LAD-2L cytoplasmic tail is completely divergent from SAX-7, neuroglian, and the vertebrate L1CAMs. The LAD-2L cytoplasmic tail contains only 40 amino acids and no known motifs such as the ankyrin-binding motif that is conserved in SAX-7 and vertebrate L1CAM cytoplasmic tails (Fig. 1, B and D). Hence, unlike SAX-7, we consider LAD-2 a noncanonical L1CAM.

To determine LAD-2 expression and localization, we performed whole-mount immunostaining using two different affinity-purified polyclonal antibodies generated against the LAD-2 cytoplasmic tail (Fig. 1 B). Both antibodies, which recognize LAD-2L but not LAD-2S, revealed LAD-2 localization at the plasma membrane of 14 neurons and their associated axons (Fig. 2 E). These 14 neurons include the SAA, SMD, SDQ, PLN, and ALN neurons (Fig. 2 A), which is in agreement with the LAD-2 expression pattern inferred from a transcriptional GFP reporter (Fig. 2, B–D; Aurelio et al., 2002). LAD-2 staining is not detected in *lad-2* mutant animals (Fig. S1, available at http://www.jcb.org/cgi/content/full/jcb.200704178/DC1), which indicates antibody specificity. *lad-2* expression, which can be detected when these neurons are born, persists throughout and after axon extension. Indeed, embryonically born ALN and SMD neurons (Sulston et al., 1983) as well as SDQL, SDQR, and PLN neurons, which are born in the L1 larval stage (Sulston and Horvitz, 1977), show

lad-2 expression when they are born. This expression continues during axon migration, which is completed postembryonically, and persists in these neurons and their axons throughout adulthood.

lad-2 is required for proper axon pathfinding

We performed a PCR-based ethyl methanesulfonate–induced mutagenesis screen and isolated a single mutation, *hd31*, in the *lad-2* gene. We detected abnormal axon trajectories in the *lad-2*–expressing neurons SMD, PLN, SDQR, and SDQL; no defects were observed in non–*lad-2*–expressing neurons (unpublished data). These abnormalities can be categorized into guidance defects affecting (a) longitudinal migration of the SMD and PLN axons and (b) dorsal migration of the SDQR and SDQL axons.

In wild-type animals, SMD neurons, which are located near the nerve ring, extend axons posteriorly along the sublateral axon tracts (Figs. 2 A and 3 A). In *lad-2* animals, we observed aberrant SMD axons that suggest general wanderings as well as ectopic dorsal or ventral turns (Fig. 3, B and J). PLN neurons, which are located in the tail of the animal, extend axons anteriorly into the nerve ring in wild-type animals (Figs. 2 A and 3 C). In *lad-2* animals, PLN axons migrate posteriorly after an initial anterior extension (Fig. 3, D and J). In wild-type animals, SDQR and SDQL axons exhibit dorsal projections at specific points during their anterior migration along the lateral and sublateral axon tracts. The SDQR cell body sends out a single axon dorsally into the dorsal sublateral cord where it migrates anteriorly toward the nerve ring (Figs. 2 A and 3 E). In *lad-2* animals, after a short migration along the sublateral cord, SDQR axons project ventrally to the ventral nerve cord (VNC), where they migrate along the VNC before terminating prematurely (Fig. 3, F and J). In wild-type animals, SDQL sends out a single axon dorsally into the lateral axon tract where it briefly extends anteriorly before turning dorsally again to join the dorsal sublateral cord, where it then migrates anteriorly toward the nerve ring (Figs. 2 A and 3 G). The SDQL axon in *lad-2* animals exhibits abnormal ventral projections to the VNC, where it migrates along the VNC before terminating prematurely (Fig. 3 H). Approximately half of these neurons also exhibit bipolar axon outgrowths where a single process extends dorsally and prematurely terminates, whereas a second process extends ventrally and migrates anteriorly along the VNC before terminating prematurely (Fig. 3 I).

Loss of *sax-7* function was previously shown to result in abnormal axon trajectories and displaced neuronal cell bodies because of the inability of neurons to maintain their positions (Sasakura et al., 2005; Wang et al., 2005). To determine whether *lad-2* also has a maintenance role, we chose to examine SMD neurons in *lad-2* animals for an age-dependent increase in the number of animals showing axon abnormalities. In wild-type animals, extension and migration of the SMD axons occur at the L1 larval stage and continue through all the larval stages until adulthood. In *lad-2* animals, we detected abnormal SMD axon trajectories as early as the L1 stage. In addition, the penetrance of this phenotype did not increase with the age of the animals (unpublished data). Moreover, unlike in *sax-7* mutant animals, we did not detect displacement of the cell bodies of neurons exhibiting abnormal axons in *lad-2* animals. Collectively, these results suggest the abnormal axon trajectories exhibited in *lad-2* animals are a result of defective axon pathfinding rather than defective positional maintenance.

Axon guidance defects in *lad-2* animals are caused by a loss of *lad-2* function

The *hd31* lesion is a 702-bp deletion that is predicted to result in an in-frame deletion of amino acids 1,080–1,162 removing part of the fifth FNIII repeat, the transmembrane domain, and half of the cytoplasmic tail of LAD-2L (Fig. 1, A and B). Because the *hd31* mutation is located downstream of the LAD-2S coding region, it is not expected to affect LAD-2S (Fig. 1 A). Whole-mount antibody staining did not reveal LAD-2 staining in *hd31* animals (Fig. S1). As *hd31* deletes part of the cytoplasmic tail, it is conceivable that *hd31* animals could produce a mutant form of LAD-2L that lacks the epitopes recognized by the LAD-2 antibodies. Semiquantitative RT-PCR analysis of LAD-2L transcripts revealed equivalent levels of *lad-2L* transcripts between *hd31* and wild-type animals (Fig. S2 B, available at http://www.jcb.org/cgi/content/full/jcb.200704178/DC1), which is suggestive of a stable pool of mutant *lad-2L* transcripts and possible mutant LAD-2L protein in *lad-2* animals.

If a mutant form of LAD-2L were produced in *hd31* animals, the protein would be predicted to be secreted because of the loss of the transmembrane domain and thus may act in a dominant fashion to cause the observed axon abnormalities. Several pieces of evidence argue against this possibility and instead support the hypothesis that *hd31* acts as a loss-of-function allele. First, *hd31* is a recessive mutation; *hd31*/+ animals do not exhibit an axon phenotype and are indistinguishable from wild-type animals (unpublished data). Second, the axon pathfinding defect in *lad-2* animals can be rescued by transgenic expression of wild-type genomic *lad-2* (Fig. 3 J). Third, we performed *lad-2*(*RNAi*) in the *eri-1*(*mg366*);*lin-15*(*n744*) animals, which are hypersensitive to RNAi in the nervous system (Sieburth et al., 2005). We used double-stranded RNAs (dsRNAs) that target either the 5′ or 3′ end of the *lad-2* gene, the former of which would reduce both *lad-2S* and *lad-2L* transcripts (Fig. 1 B). Examination of these RNAi-treated animals revealed that *lad-2*(*RNAi*) phenocopies *hd31* animals with similar penetrance, which is consistent with *hd31* as a loss-of-function allele (Fig. S2 A). To further demonstrate that *hd31* animals do not produce a mutant form of LAD-2L harboring some function, we similarly performed *lad-2*(*RNAi*) in *lad-2*(*hd31*) animals that are hypersensitive to RNAi (*lad-2 eri-1*;*lin-15*). *lad-2*(*RNAi*) in these animals phenocopied *hd31* animals with similar penetrance and did not suppress or enhance *lad-2*(*hd31*) defects (Fig. S2 A). *lad-2*(*RNAi*) was successful in dramatically reducing the level of *lad-2* transcripts as analyzed by semiquantitative RT-PCR of *lad-2* transcripts in RNAi-treated animals (Fig. S2 B). Collectively, these results suggest that the axon defects exhibited by *lad-2*(*hd31*) animals are a result of the loss of *lad-2* function and not a mutant protein with a dominant or novel function. The *lad-2*(*RNAi*) results also indicate that reduction of LAD-2S along with mutant LAD-2L does not result in either enhanced axon defects or additional phenotypes relative to those seen with reduction of only LAD-2L.

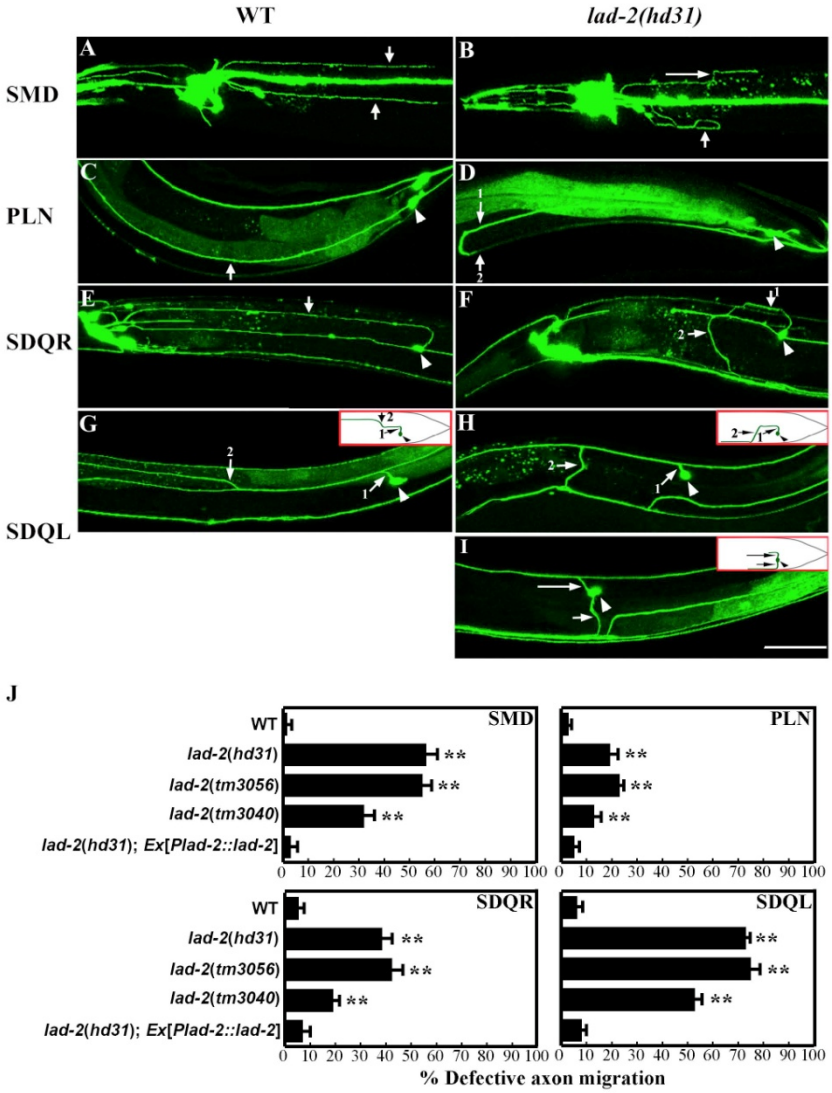

Figure 3. ***lad-2* animals exhibit defective axon trajectories.** (A–I) Confocal micrographs of wild-type and *lad-2(hd31)* axon trajectories of the SMD (A and B), PLN (C and D), SDQR (E and F), and SDQL (G, H, and I) neurons are shown. Arrows point to axons. Numbered arrows follow the sequential progression of axon extension from the cell body (arrowheads). Insets in G–I show schematics of wild-type (G) and *lad-2(hd31)* (H and I) SDQL migration. *lad-2* animals (B) display aberrant ventral or dorsal (long arrow) turns and general wandering (short arrow) in SMD axons, abnormal ventral migration to the VNC of the SDQR (D) and SDQL axons (H), and a bipolar phenotype in the SDQL neuron (I) where one axon extends dorsally (long arrow) but terminates prematurely and a second axon extends ventrally (short arrow) into the VNC. SMDs were visualized with $P_{glr\text{-}1}$*::gfp* (ventral view) and PLN, SDQR, and SDQL were visualized with $P_{lad\text{-}2}$*::gfp* (lateral view). Bar, 50 μm. (J) Quantitation of defective axons in wild-type, *lad-2(hd31)*, *lad-2(tm3056)*, and *lad-2(tm3040)* animals. These defects can be rescued by $P_{lad\text{-}2}$*::lad-2* as seen in three independent transgenic lines, the first of which is shown. The quantitation of axon defects in the additional two transgenic lines are as follows: SMD, 5.1 ± 1.3% (line 2) and 6.4 ± 3.0% (line 3); PLN, 4.0 ± 2.1% (line 2) and 5.7 ± 2.9% (line 3); SDQR, 8.2 ± 1.5% (line 2) and 9.5 ± 2.0% (line 3); and SDQL, 9.4 ± 2.6% (line 2) and 8.6 ± 1.8% (line 3). Error bars show the standard error of the proportion of three sample sets, where in each set n = 93–112 (SMD); n = 103–135 (PLN); n = 79–108 (SDQR); and n = 76–128 (SDQL). **, $P < 0.01$ compared with wild-type animals.

Subsequent to our phenotypic analysis of *lad-2(hd31)* and genetic study of *lad-2* in relation to previously identified axon guidance pathways (see Figs. 5 and 6), we obtained from the Japanese National Bioresource Project two additional *lad-2* alleles, *tm3040* and *tm3056*. The *tm3056* mutation is a 1,064-bp out-of-frame deletion that is predicted to result in a premature

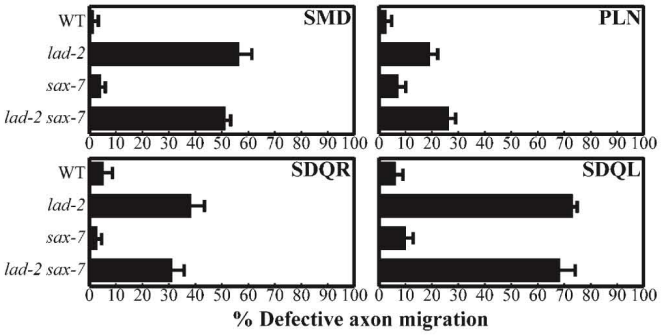

Figure 4. **sax-7 does not participate in lad-2-related axon guidance.** Quantitation of axon defects in *lad-2(hd31)*, *sax-7(eq1)*, and *lad-2(hd31) sax-7(eq1)* animals. Error bars indicate the standard error of proportion of three sample sets, where in each set, $n = 103–118$ (SMD); $n = 99–133$ (PLN); $n = 84–108$ (SDQR); and $n = 85–128$ (SDQL).

stop after the second Ig motif (Fig. 1 A) and is likely a null allele of *lad-2*, removing both LAD-2L and LAD-2S isoforms. Consistent with this prediction, we did not detect any LAD-2 staining in whole-mount antibody staining of *tm3056* animals with anti–LAD-2 antibodies (Fig. S1). *lad-2(tm3056)* animals exhibit similar axon defects with similar penetrance as *lad-2(hd31)* animals (Fig. 3 J). Collectively, these data strongly support our findings, which suggest that *lad-2(hd31)* is a null allele and that LAD-2S does not have functions independent of LAD-2L. In contrast to *hd31* and *tm3056*, *tm3040* acts as a hypomorphic allele. Indeed, low levels of LAD-2 immunostaining can be detected in *lad-2(tm3040)* animals (Fig. S1) despite the fact that the *tm3040* mutation is a 327-bp deletion that is predicted to result in a premature stop after the second Ig motif (Fig. 1 A). Moreover, the penetrance of the axon defects exhibited by *tm3040* animals is lower than those seen in *lad-2(hd31)* and *lad-2(tm3056)* (Fig. 3 J).

lad-2 function in axon guidance is *sax-7* independent

Neurons that express *lad-2* also express *sax-7* (Chen et al., 2001; unpublished data). Because the axon defects in *lad-2* animals are not fully penetrant, we asked whether *sax-7* might function redundantly with *lad-2*. We determined that *lad-2*–expressing neurons in the genetic null *sax-7(eq1)* animals do not exhibit abnormal axon trajectories (Fig. 4). Moreover, the penetrance of the axon defects exhibited by *lad-2* animals does not increase in *lad-2 sax-7* double mutant animals (Fig. 4). These results indicate that *sax-7* does not function in axon guidance in *lad-2*–expressing neurons. Similarly, *lad-2* does not enhance *sax-7* defects (unpublished data). Collectively, these results suggest that *lad-2* and *sax-7* do not have redundant functions.

mab-20 and *plx-2* participate in the same pathway in SDQL axon pathfinding

Guidance cues that direct axon migration include netrins, slits, and semaphorins, among others (for review see Chilton, 2006). We examined animals that are mutants for the *unc-6* netrin, *slt-1* slit, or *mab-20* Sema2 genes for axon defects resembling those seen in *lad-2* animals. Only *mab-20* mutant animals exhibited *lad-2*–like axon defects. Specifically, SDQL axons in 41% of animals homozygous for the putative *mab-20* null allele *ev574* (Roy et al., 2000) displayed aberrant ventral projections into the VNC (Fig. 5, A and C) as well as bipolar axon outgrowths (Fig. 5 B). *mab-20* animals also show modest SMD and SDQR axon defects (Fig. 5 C). These results indicate that, like *lad-2*, *mab-20* participates in SMD, SDQR, and SDQL axon guidance.

Plexins act as semaphorin receptors in both vertebrates and invertebrates (for review see Kruger et al., 2005). Previous genetic analysis revealed that *plx-2* functions in the same pathway as *mab-20* in *C. elegans* epidermal morphogenesis (Ikegami et al., 2004). To determine if *plx-2* also functions together with *mab-20* in axon migration, we examined animals homozygous for the putative *plx-2* null allele *ev773* for axon guidance defects (Fig. 5 C). SDQL neurons in 40% of *plx-2(ev773)* animals exhibit similar guidance and bipolar axon phenotypes observed in *mab-20* and *lad-2* animals (Fig. 5 C), whereas SMD, PLN, and SDQR axons showed more modest defects. These phenotypes are not enhanced in *mab-20;plx-2* double mutant animals (Fig. 5 C), which suggests that *mab-20* and *plx-2* function in the same pathway to direct axon migration.

Examination of *smp-1(ev715)* and *smp-2(ev709)* animals did not reveal axon defects in *lad-2*–expressing neurons, which suggests that the membrane-bound Sema1 proteins are not essential for SMD, SDQR, SDQL, and PLN axon guidance (unpublished data). The PLX-1 plexin functions as a receptor for SMP-1 and SMP-2 semaphorins in epidermal and vulval morphogenesis (Fujii et al., 2002; Dalpe et al., 2004, 2005). As expected, *plx-1(ev724)* animals also do not exhibit the described axon defects (unpublished data).

LAD-2 mediates axon guidance via MAB-20, which acts as a repulsive cue

The axon phenotypes shared by *lad-2*, *mab-20*, and *plx-2* animals suggest that *lad-2* may control SMD, SDQR, and SDQL

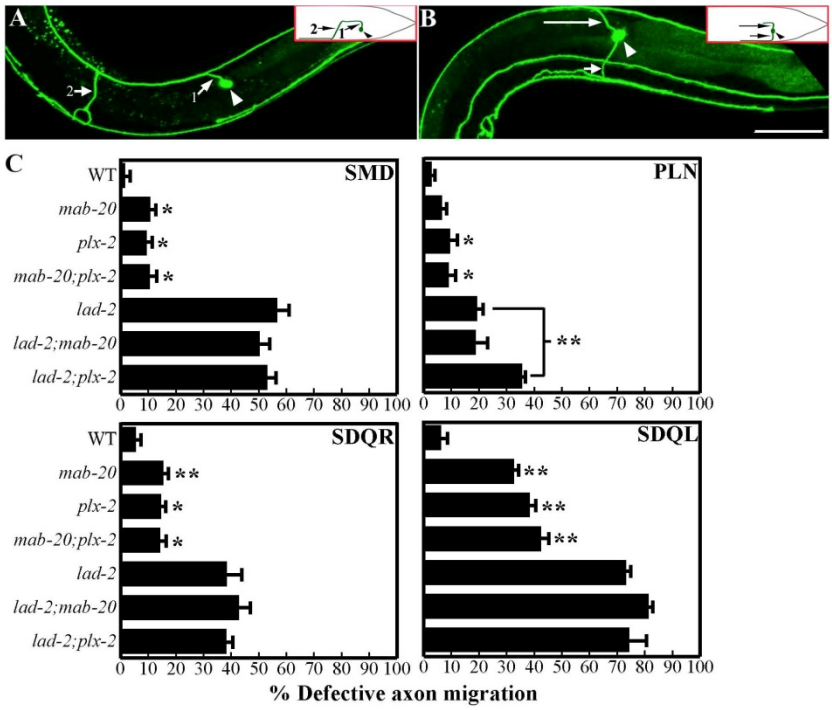

Figure 5. ***mab-20* and *plx-2* function in SDQL axon pathfinding.** (A and B) Confocal micrographs of the SDQL neuron (arrowhead points to cell body) in *mab-20(ev574)* animals as visualized by P_{lad-2}*::gfp* showing abnormal ventral axon migration (A, numbered arrows show sequential progression of axon migration) and a bipolar phenotype (B) with one dorsal process (long arrow) and one ventral process (short arrow). Insets show a schematic of the corresponding phenotype. Bar, 50 µm. (C) Quantitation of axon migration defects. *hd31* was the *lad-2* allele used in this analysis. Interestingly, PLN defects are enhanced in *lad-2;plx-2* animals ($P < 0.01$ compared with *lad-2* animals). Error bars show standard error of the proportions of three sample sets where in each set $n = 103–118$ (SMD); $n = 103–140$ (PLN); $n = 81–108$ (SDQR); and $n = 82–128$ (SDQL). *, $P < 0.05$; **, $P < 0.01$ as compared with wild-type animals.

axon guidance via the *mab-20–plx-2* pathway. Consistent with this hypothesis, defects in these neurons are not enhanced in *lad-2;mab-20* or *lad-2;plx-2* double mutant animals (Fig. 5 C). Interestingly, PLN defects are enhanced in *lad-2;plx-2* but not *lad-2;mab-20* or *mab-20;plx-2* animals (Fig. 5 C). These results imply that *plx-2* may function in PLN axon guidance in a pathway that is distinct from *lad-2* and independent of *mab-20*.

Semaphorins can function both as attractive and repulsive cues (Kruger et al., 2005). The broad embryonic expression of *mab-20*, as inferred by the *Pmab-20::gfp* transcriptional reporter (Roy et al., 2000), does not reveal whether MAB-20 acts as an attractant or a repellent. Of the neurons described that display axon guidance defects in *mab-20* animals, SDQL shows the most penetrant defects. We thus used SDQL as a system to determine how MAB-20 functions. If MAB-20 acts as a repulsive cue, the abnormal ventral trajectory of the SDQL axon in *mab-20* animals would suggest a MAB-20 gradient in wild-type animals with higher ventral and lower dorsal levels of MAB-20. Ventral expression of *mab-20* would thus be expected to rescue the defective ventral migration of the SDQL axon in *mab-20* animals. To test this prediction, we used the *mec-7* promoter (Kim et al., 1999) to express high, sustained levels of MAB-20 in the mechanosensory neurons in *mab-20* animals. Of these neurons, PLM and PVM extend axons past and ventral to the SDQL cell body and axon (Fig. 6 A; White et al., 1986). Importantly, the postembryonically derived SDQL neuron is born after the embryonically derived PLM has completed axon extension so that ectopically expressed MAB-20 that is ventral to the SDQL neuron should be established by the time an SDQL is born and starts extending its axon. Consistent with the notion that MAB-20 acts as a repulsive cue to the SDQL axon, P_{mec-7}*::mab-20* expression partially rescues the SDQL axon guidance defect of *mab-20* animals (Fig. 6 B). This ectopic MAB-20 expression in wild-type animals does not affect SDQL axon migration (Fig. 6 B).

To further test the hypothesis that MAB-20 acts as a repellent to SDQL, we assayed whether ectopic dorsal *mab-20* expression would induce aberrant ventral migration of the SDQL axon. We used the *mir-48* promoter (Li et al., 2005) to express sustained levels of *mab-20* in the embryonically derived RID neuron, which extends a posteriorly directed axon dorsal to SDQL (Fig. 6 A). The *mab-20* expression in the RID neuron and associated axon is expected to establish a dorsal *mab-20* gradient by the time SDQL is born and starts extending its axon.

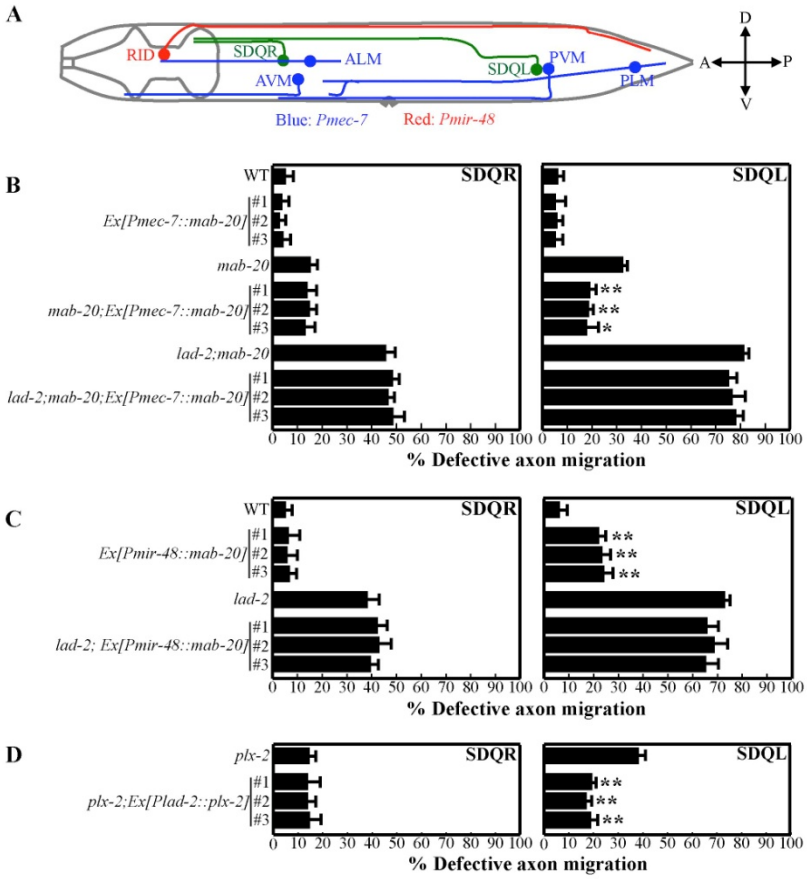

Figure 6. **The effects of ectopic *mab-20* expression require *lad-2* function.** (A) A diagram showing the positions of SDQR and SDQL relative to the neurons and associated axons that ectopically express *mab-20* as driven by P_{mec-7} (AVM, ALM, PVM, and PLM neurons, blue) or P_{mir-48} (RID neuron, red); lateral view. (B–D) Quantitation of SDQR and SDQL defects in animals of the respective genotypes. Error bars show standard error of the proportion of three sample sets where in each set $n = 77–93$ (SDQR) and $n = 77–103$ (SDQL). (B) Ectopic ventral expression of *mab-20* with P_{mec-7}::*mab-20* can rescue SDQL defects in *mab-20*(*ev574*) but not *lad-2*(*hd31*);*mab-20*(*ev574*) animals. *, $P < 0.05$; **, $P < 0.01$ as compared with parent *mab-20*(*ev574*) animals. The percentage of those rescued was 41% (line 1), 43% (line 2), and 45% (line 3). (C) Ectopic dorsal expression of *mab-20* with P_{mir-48}::*mab-20* induces the aberrant ventral migration of the SDQL axon in wild-type animals but does not enhance the SDQL defects already present in *lad-2*(*hd31*) animals. **, $P < 0.01$ as compared with parent wild-type animals. (D) *plx-2* expression in the SDQL neuron with P_{lad-2}::*plx-2*, can partially rescue SDQL axon defects in *plx-2*(*ev773*) animals. **, $P < 0.01$ compared with parent *plx-2*(*ev773*) animals.

Ectopic dorsal *mab-20* expression in wild-type animals induced ventral migration defects in 17% of SDQL axons (Fig. 6 C). This result supports the hypothesis that MAB-20 acts as a repulsive cue to guide the SDQL axon to make dorsal turns at choice points to reach the dorsal sublateral nerve cord. The fact that SDQR axon migration was not affected by this ectopic MAB-20 expression is not too surprising, as SDQR defects are minimal in *mab-20* animals.

If MAB-20 acts as a repellent, dorsal expression of *mab-20* is predicted to enhance the SDQL phenotype in *lad-2* animals unless *lad-2* is required to mediate *mab-20* function. Ectopic dorsal expression of *mab-20* did not enhance SDQL defects in *lad-2* animals (Fig. 6 C), which is consistent with our genetic data suggesting that *lad-2* is required for *mab-20*–mediated SDQL axon pathfinding. As further support of *lad-2* functioning together with *mab-20* and *plx*-2, expression of PLX-2 in the SDQL neuron with the *lad-2* promoter can partially rescue SDQL axon defects in *plx-2* animals (Fig. 6 D), indicating that PLX-2 function is required in the same cell as LAD-2.

LAD-2 secures MAB-20/Sema2 coupling to PLX-2 plexin in a protein complex

L1 was previously shown to physically interact with neuropilin to regulate Sema3A function in mice (Castellani et al., 2000). *C. elegans* lacks a neuropilin. To address how LAD-2 mediates MAB-20 function in SDQL axon guidance, we assayed

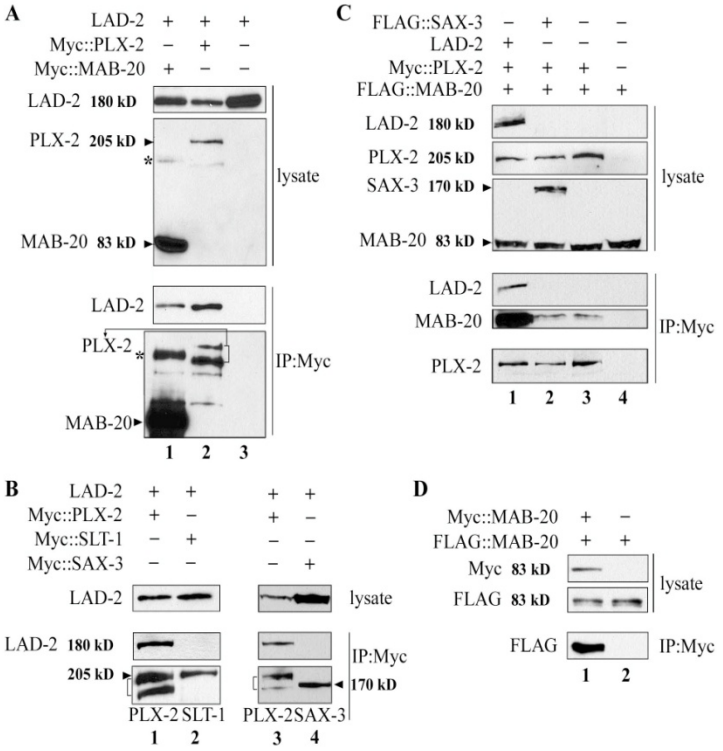

Figure 7. **LAD-2 can enhance coupling of MAB-20 to PLX-2 as determined by Co-IP assays performed using anti-Myc antibodies.** (A) LAD-2 interacts with MAB-20 and PLX-2 independently. Co-IP assays were performed on lysates of HEK293T cells coexpressing LAD-2 with Myc::MAB-20 (lane 1), Myc::PLX-2 (lane 2), and a control Myc vector (lane 3). The top two panels are Western blot analyses of the respective proteins in each lysate and the bottom panels are the Western blot of the Co-IP results. The asterisk points to a 170-kD band seen in lane 1 that may correspond to putative MAB-20 dimers. The bracketed bands in lane 2 are PLX-2 products; the lower band is a putative degradation product of PLX-2. (B) LAD-2 does not interact with SLT-1 or SAX-3. Co-IP assays were performed on cells coexpressing LAD-2 with Myc::PLX-2 (lanes 1 and 3), Myc::SLT-1 (lane 2), and Myc::SAX-3 (lane 4). The top shows LAD-2 in each lysate as assayed by Western blotting; the bottom shows the Western blot analyses of the Co-IP results showing LAD-2 coimmunoprecipitates with PLX-2 (bracketed bands in lane 1 and 3) but not SLT-1 or SAX-3. (C) LAD-2 but not SAX-3 can enhance a weak interaction between mab-20 and PLX-2 as determined by Co-IP assays performed on cells coexpressing FLAG::MAB-20 together with Myc::PLX-2 and LAD-2 (lane 1), Myc::PLX-2 and FLAG::SAX-3 (lane 2), Myc::PLX-2 (lane 3), or a control Myc vector (lane 4). Western blot analyses of the respective proteins in each lysate and Co-IP results are shown. Note that the low levels of FLAG::MAB-20 CoIPs with Myc::PLX-2 (lane 3) increases dramatically in the presence of LAD-2 (lane 1) but remains unchanged in the presence of SAX-3 (lane 2). (D) MAB-20 can form homodimers. Co-IP assays were performed on cells coexpressing FLAG::MAB-20 with Myc::MAB-20 (lane 1) and control Myc vector (lane 2). The top two panels are Western blot analyses of the respective proteins expressed in each lysate; the bottom shows Western blot analyses of the Co-IP results.

for biochemical interactions among LAD-2, MAB-20, and PLX-2. We cotransfected HEK293T cells with LAD-2 and either Myc::MAB-20 or Myc::PLX-2 and performed anti-Myc immunoprecipitations on the cell lysates. We detected the presence of LAD-2 in each immunoprecipitate by Western blot analysis using anti–LAD-2 antibodies (Fig. 7 A, lanes 1 and 2). In contrast, LAD-2 was not detected in immunoprecipitates performed on cells cotransfected with a control Myc vector (Fig. 7 A, lane 3). To test that these LAD-2 interactions with MAB-20 and PLX-2 are not caused by nonspecific binding, we assayed for LAD-2 interaction with another axon guidance cue, SLT-1 slit, and the SAX-3 receptor (Huber et al., 2003). No LAD-2 was detected in the anti-Myc immunoprecipitates of cells coexpressing LAD-2 with either Myc::SLT-1 or Myc::SAX-3 (Fig. 7 B). Thus, we conclude that LAD-2 can interact with MAB-20 and PLX-2, although these results cannot distinguish whether LAD-2 binds MAB-20 and PLX-2 in a common complex.

To determine whether MAB-20 and PLX-2 can interact, we performed similar anti-Myc immunoprecipitations on cells cotransfected with FLAG::MAB-20 and Myc::PLX-2. We observed low levels of FLAG::MAB-20 in the anti-Myc immunoprecipitates, indicating that MAB-20 and PLX-2 can weakly interact (Fig. 7 C, lane 3). However, levels of FLAG::MAB-20 dramatically increased in anti-Myc immunoprecipitates when LAD-2 was coexpressed in combination with FLAG::MAB-20 and Myc::PLX-2 (Fig. 7 C, lane 1), which indicates that LAD-2 enhances the coupling of MAB-20 and PLX-2. To further confirm the specificity of these LAD-2 interactions, we assayed for the ability of SAX-3, a transmembrane protein similar to LAD-2 in structure with multiple Ig and FNIII motifs (Zallen et al., 1998), to similarly enhance MAB-20–PLX-2 interactions. We did not detect increased levels of FLAG::MAB-20 in anti-Myc immunoprecipitates of cells coexpressing FLAG::SAX-3 with FLAG::MAB-20 and Myc::PLX-2 (Fig. 7 C, lane 2). These results suggest that LAD-2 secures coupling of MAB-20 and PLX-2 in a larger protein complex.

Homodimerization of many vertebrate semaphorins appear to be important for their function in axon repulsion (Klostermann et al., 1998; Koppel and Raper, 1998). In our Western blots of Myc::MAB-20, we detected an additional faint band, the size of which was consistent with Myc::MAB-20 dimers. To determine whether MAB-20 can form dimers, we performed anti-Myc immunoprecipitations on cells cotransfected with Myc::MAB-20 and FLAG::MAB-20. We detected FLAG::MAB-20 in the immunoprecipitates by Western blot analysis using anti-FLAG antibody, which indicates that MAB-20 can oligomerize (Fig. 7 D, lane 1). This interaction is specific, as MAB-20::FLAG was not immunoprecipitated in a similar pull-down assay with an anti-Myc antibody from cells expressing a control Myc vector (Fig. 7 D, lane 2).

Discussion

Significance of the restricted *lad-2* expression

L1CAMs are highly conserved adhesion molecules that function in nervous system development. The *C. elegans* L1CAMs SAX-7 and LAD-2 have unique features in protein structure, expression, and function. SAX-7, which has the structural hallmarks of vertebrate L1CAMs, is widely expressed and required for maintaining neuronal positioning (Chen et al., 2001; Sasakura et al., 2005; Wang et al., 2005). In contrast, LAD-2 has a short and divergent cytoplasmic tail and is expressed in only 14 neurons.

It is striking that LAD-2 has such a restricted expression pattern. A common feature of these *lad-2*–expressing neurons is that their associated axons do not fasciculate with the major ventral and dorsal nerve cords. Instead, they migrate, either individually or together with a few other axons, along the "roads less traveled" by axons, i.e., the lateral midline or sublateral axon cords. Another common feature of these neurons is that axon outgrowth occurs postembryonically. The SDQL, SDQR, PLN, and ALN neurons are born postembryonically. The SMD neurons, although embryonically derived, have axons that extend and migrate throughout all larval stages. These characteristics of the *lad-2*–expressing neurons raise the possibility that LAD-2 may be required to keep these late-extending axons distinct and prevent them from merging with the main nerve cords. The functions of these neurons are not clear, although a recent study demonstrated that SDQL, SDQR, PLN, and ALN function in hyperoxia avoidance (A. Chang et al., 2006a). It is currently unknown whether hyperoxia avoidance is affected in *lad-2* animals, which do not exhibit an obvious movement phenotype and are indistinguishable from wild-type animals apart from axon migration defects.

MAB-20/Sema2, which acts as a repellent, participates in axon guidance together with PLX-2

The inhibitory action of the Sema3 class of secreted semaphorins on axon outgrowth has been well demonstrated on multiple cultured vertebrate neurons. Yet, disruption of the Sema3 genes affects only a limited number of neuronal systems in vivo but revealed nonneuronal functions for Sema3 proteins that include vascular and heart development (for reviews see Nakamura et al., 2000; Kruger et al., 2005). Similarly, the *C. elegans* secreted semaphorin MAB-20/Sema2 appears to have a more prominent role in epidermal morphogenesis compared with axon guidance, which was described for certain motor neurons (Roy et al., 2000). Based on the *mab-20* phenotypes, it was postulated that MAB-20 may function as a repellent. Our ectopic *mab-20* expression experiments provide in vivo evidence that SDQL responds to MAB-20 as a repulsive cue or, alternatively, an inhibitor of an attractive cue with respect to axon pathfinding. These data also suggest that there may be a more localized ventral-to-dorsal MAB-20 gradient relative to the SDQL neuron that is not apparent according to the previously reported expression of *mab-20::gfp* reporters (Roy et al., 2000).

Previous genetic studies revealed that *plx-2* functions with *mab-20* in epidermal morphogenesis of the male tail but a role in axon guidance had not been described (Ikegami et al., 2004). Our study shows that *plx-2* does indeed function in axon pathfinding together with *mab-20*, which supports the idea that plexins function as semaphorin receptors. In contrast, *plx-1* does not function with *mab-20*, which is consistent with a previous study showing that PLX-1 is the receptor for the membrane-bound Sema1 proteins SMP-1 and SMP-2 (Fujii et al., 2002).

That *lad-2* functions with both *mab-20* and *plx-2* appears to be restricted to axon guidance. Examination of *lad-2* animals did not reveal any morphogenetic defects in embryos or in the male tail (unpublished data), phenotypes that are prominent in *mab-20* and *plx-2* animals.

SDQL exhibits a bipolar axon phenotype in *lad-2*, *mab-20*, and *plx-2* mutant animals

It is intriguing that the SDQL neuron can extend two axons that migrate in opposite directions in *lad-2*, *mab-20*, or *plx-2* animals. This multipolar axon phenotype is similar to that seen in neurons overexpressing the actin regulatory pleckstrin homology domain protein MIG-10/lamellipodin in the absence of UNC-6 netrin and SLT-1 (Quinn et al., 2006). These studies point to guidance cues, such as slit and netrin, in orienting MIG-10 localization to the part of the neuron that will extend an axon (Adler et al., 2006; C. Chang et al., 2006; Quinn et al., 2006). Based on these MIG-10 studies, we hypothesize that in the absence of MAB-20 signaling, SDQL still responds to other guidance cues. However, the integration of these cues is deregulated, which results in a neuron that is in a "confused" state so that polarized MIG-10 localization is disrupted, leading to multiple processes growing out.

LAD-2 mediates axon guidance via *mab-20*–independent pathways

Consistent with the notion that SDQL axon guidance relies on multiple cues in addition to MAB-20, the SDQL defects in *lad-2*, *mab-20*, and *plx-2* animals are not fully penetrant. Moreover, we hypothesize that LAD-2 also mediates SDQL axon guidance via a MAB-20–independent pathway, as the penetrance of the SDQL axon pathfinding defect in *lad-2* mutant animals is significantly higher than in *mab-20* and *plx-2* mutants. In fact, our data indicates that LAD-2 mediates axon guidance via MAB-20–independent pathways in SMD, PLN, and SDQR. This raises the possibility that L1CAMs in vertebrates may also mediate axon guidance via semaphorin-independent pathways that may include L1 functioning as a direct receptor to a guidance cue or as a regulatory protein in the guidance pathways.

LAD-2 functions as a coreceptor to MAB-20/Sema2 to mediate axon repulsion

Our study provides in vivo evidence that an L1CAM in *C. elegans* participates in axon guidance by mediating the action of secreted semaphorins. In vertebrates, L1 is shown to bind neuropilin to mediate axon guidance via the secreted semaphorin Sema3A (Fig. 8; Castellani et al., 2004). Neuropilin is not conserved in *D. melanogaster* or *C. elegans*, which suggests that this coreceptor is a recent addition to the evolutionarily older semaphorin guidance system. Our biochemical data suggest that

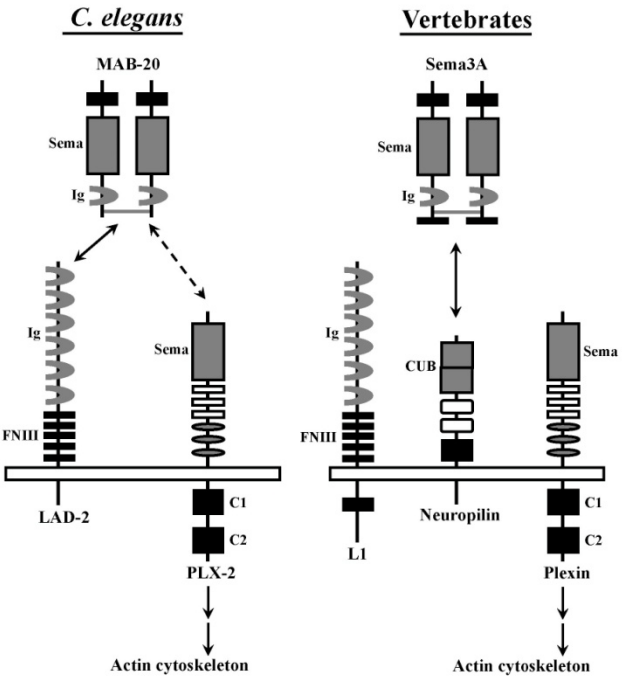

Figure 8. **A model of how LAD-2 functions as a MAB-20 coreceptor to mediate axon guidance.** In *C. elegans*, mab-20/Sema2 acts as a diffusible, repulsive guidance cue in vivo to guide the dorsal migration of the SDQL axon. We hypothesize that LAD-2 binds MAB-20 homodimers and PLX-2 to a secure coupling of MAB-20 and PLX-2, which can interact weakly by themselves. This protein complex initiates a signal transduction cascade to induce actin cytoskeletal changes that lead to axon repulsion. L1CAMs are also implicated in semaphorin-dependent axon repulsion in vertebrates. However, neuropilin instead of L1 is the obligate semaphorin receptor that couples Sema3 to plexin. We hypothesize that in vertebrates, the functions of LAD-2 are executed by L1 and neuropilin, potentially providing an additional level of regulation. The depicted conserved motifs are as follows: Sema, Sema domain; Ig, Ig domain; FNIII, fibronectin type III repeat; C1, conserved region 1; C2, conserved region 2; CUB, complement binding domain.

L1CAMs may be the original coreceptors for secreted semaphorins controlling axon navigation. Our results show that MAB-20 and PLX-2 can weakly interact, which is consistent with a recent published study that found that the ability for MAB-20 to bind to the surface of HEK293T cells requires PLX-2 expression in the cells (Nakao et al., 2007). Our results further show that the weak MAB-20–PLX-2 interaction is dramatically enhanced in the presence of LAD-2, which can form protein complexes independently with MAB-20 and PLX-2. These results suggest that LAD-2 functions as a MAB-20 coreceptor that anchors MAB-20 to PLX-2 to mediate MAB-20 signaling (Fig. 8). Consistent with this hypothesis, expression of PLX-2 in the SDQL neuron in the *plx-2* animal can partially rescue the SDQL axon defects (Fig. 6 D), indicating that PLX-2 function is required in the same cell as LAD-2.

It is intriguing that the LAD-2 cytoplasmic tail is not only divergent from that of canonical L1CAMs but is also short. Strikingly, the LAD-2 and neuropilin cytoplasmic tails are both 40 amino acids long, although they do not share significant sequence homology, which is consistent with neuropilin being a recently evolved protein. Underscoring this notion is the fact that the neuropilin cytoplasmic tail does not appear to be required in Sema3 signaling (for review see Bielenberg et al., 2006); the requirement for the LAD-2 cytoplasmic tail has yet to be determined. It is conceivable that the function of LAD-2 as an L1CAM and possible semaphorin receptor may have evolved in vertebrates into two separate proteins, neuropilin and L1, which may provide an additional layer of regulation required in navigating axon migration in a more complex nervous system.

This study has revealed that the role of L1CAM in axon guidance is conserved in both *C. elegans* and vertebrates. We have shown that LAD-2 mediates axon guidance via both semaphorin-dependent and -independent pathways. Additional studies to determine the semaphorin-independent pathways LAD-2 mediates or whether LAD-2S functions with LAD-2L in axon pathfinding will further reveal L1CAM mechanisms in the process of axon navigation. Loss of LAD-2 results in abnormal ventral migration of the SDQL axon, revealing a default guidance pathway that is concealed by semaphorin signaling. This phenotype is not fully penetrant in *lad-2* animals, which indicates an additional pathway that compensates for the loss of MAB-20 signaling. Future studies will use the SDQL as a simple yet powerful genetic system to elucidate how the different guidance pathways crosstalk and dissect the process by which a neuron integrates the signals of different guidance cues to execute axon steering.

Materials and methods

Strains

C. elegans strains were grown on nematode growth medium plates at 20°C as described by Brenner (1974). N2 bristol served as the wild-type strain. The alleles used are listed by linkage groups as follows. LGI: *mab-20(ev574)* (Roy et al., 2000), *smp-1(ev715)*, and *smp-2(ev709)* (Ginzburg et al., 2002); LGII: *plx-2(ev773)* (Ikegami et al., 2004) and *muls32(P$_{mec-7}$::gfp)* (Pujol et al., 2000); LGIII: *rhIs4(P$_{glr-1}$::gfp)* (Lim et al., 1999); LGIV: *lad-2(hd31)*, *lad-2(tm3040)*, *lad-2(tm3056)*, *sax-7(eq1)* (Wang et al., 2005), and *eri-1(mg360)* (Sieburth et al., 2005). *lad-2(tm3040)* and *lad-2(tm3056)* were backcrossed twice to remove secondary mutations. LGX: *lin-15(n744)* (Sieburth et al., 2005), *slt-1(eh15)* (Hao et al., 2001), *unc-6(ev400)* (Kim et al., 1999), and *oxIs12(P$_{unc-47}$::gfp)* (McIntire et al., 1997); and extrachromosomal GFP marker *otEx331(P$_{lad-2}$::gfp; pha-1[+])* (Aurelio et al., 2002).

C. elegans expression vectors

***P*$_{lad\text{-}2}$*::lad-2* (*lad-2* genomic DNA, pLC358).** The *lad-2* promoter (7.3 kb upstream of the start codon) and *lad-2* genomic DNA (14 kb) were cloned from YAC Y54G2A (Coulson et al., 1988) in pWKS30 (Wang and Kushner, 1991) between SacII and ApaI.

***P*$_{mir\text{-}48}$*::mab-20* (pLC401).** *mab-20* cDNA was amplified from E1SIIN.F (a gift from J. Culotti, Mt. Sinai Hospital, Toronto, Canada; Roy et al., 2000) and subcloned between the 1-kb promoter fragment of the *mir-48* gene (Li et al., 2005) and the *unc-54* 3′ untranslated region in pBluescript backbone (Stratagene).

***P*$_{mec\text{-}7}$*::mab-20* (pLC402).** *mab-20* cDNA with an intron inserted at the SmaI site was amplified from pLC401 and subcloned into pPD96.41 (a gift from A. Fire, Stanford University School of Medicine, Palo Alto, CA) between KpnI and XhoI.

***P*$_{lad\text{-}2}$*::plx-2* (pLC456).** *plx-2* genomic DNA was cloned under the *lad-2* promoter in pBluescript.

Mammalian cell expression vectors

***P*$_{cmv}$*::lad-2* (pLC424).** *lad-2* cDNA was amplified from yk394b9 (a gift from Y. Kohara, National Institute of Genetics, Mishima, Japan) and subcloned into pcDNA3.1(−) (Invitrogen) between BamHI and KpnI.

***P*$_{cmv}$*::FLAG::mab-20* (pLC448).** *mab-20* cDNA was amplified from E1SIIN.F and subcloned into p3XFLAG-CMV-7.1 (Sigma-Aldrich) between NotI and KpnI.

***P*$_{cmv}$*::FLAG::sax-3* (pLC517).** *sax-3* cDNA was cloned by RT-PCR from N2 total RNA and subcloned into p3XFLAG-CMV-7.1 KpnI and XbaI.

***P*$_{cmv}$*:: Myc::mab-20* (pLC433).** *mab-20* cDNA was amplified from E1SIIN.F and subcloned into pcDNA3.1/MycHis B (Invitrogen) between KpnI and XhoI.

***P*$_{cmv}$*:: Myc::slt-1* (pLC505).** *slt-1* cDNA was provided by C. Bargmann (The Rockefeller University, New York, NY; Hao et al., 2001) and subcloned into pcDNA3.1/Myc-His B between KpnI and BamHI.

***P*$_{cmv}$*::sax-3::Myc* (pLC518).** *sax-3* cDNA was cloned by RT-PCR from N2 total RNA and subcloned into pcDNA3.1/Myc-His B between KpnI and XbaI. The *Myc-plx-2* expression vector was kindly provided by S. Takagi (Nagoya University, Nagoya, Japan; Fujii et al., 2002).

Isolation of *lad-2(hd31)*

An ethyl methanesulfonate–induced deletion library of animals (Jansen et al., 1997; Liu et al., 1999) was screened with the following *lad-2*–specific primers, resulting in the identification and isolation of the *hd31* mutation: Y54_dx1 (GAAAGCTCAAAAACATGGTTCC) and Y54_dx2 (CACTTTTCACGACAGCTTTTTG). The isolated *lad-2(hd31)* strain was backcrossed eight times to remove secondary mutations.

Generation of LAD-2 antibodies

Guinea pigs were immunized with LAD-2 cytoplasmic tail expressed in bacteria in frame with glutathione *S*-transferase in a pGEX vector (GE Healthcare). Sera were preadsorbed over a glutathione *S*-transferase column (GE Healthcare) and affinity purified using an antigen fusion protein column. The resulting purified antibodies, 1622 and 1623, are specific to LAD-2L and effective in whole-mount staining (Figs. 2 E and S1). LAD-2 was not detected in whole animal lysate by Western blot analysis, probably because of low levels of LAD-2, which was present in only 14 cells. Indeed, these antibodies are effective on Western blots on HEK293T cells expressing LAD-2 (Fig. 7).

Whole-mount immunofluorescence

Animals were fixed and stained for indirect immunofluorescence using protocols adapted from Finney and Ruvkun (1990). Fixed animals were washed, incubated with 1622 or 1623 (1:100 dilution) at 4°C overnight, washed again, and incubated in secondary antibody (Alexa Fluor 568 goat anti–guinea pig IgG; Invitrogen) for 2 h at room temperature. After washing, worms were mounted and examined using an Axioplan 2 microscope (Carl Zeiss, Inc.). Images were acquired using an AxioCam MRm and AxioVision 4.5 software (Carl Zeiss, Inc.). The numerical aperture of the 63× and 100× objective lenses is 1.40 and 1.45, respectively.

lad-2 rescue and ectopic *mab-20* expression

***lad-2* rescue.** 10 ng/µl pLC358 was injected with 70 ng/µl pRF4 (*rol-6[su1006]*) into *lad-2(hd31);otEx331* to generate transgenic array *Ex(P*$_{lad\text{-}2}$*::lad-2;rol-6[su1006])*.

Ectopic *mab-20* expression. 10 ng/µl pLC402 was injected with 70 ng/µl pRF4(*rol-6[su1006]*) into *otEx331*, *mab-20(ev574);otEx331*, and *lad-2(hd31);mab-20(ev574);otEx331* to generate *Ex(P*$_{mec\text{-}7}$*::mab-20;rol-6[su1006])*. 10 ng/µl pLC401 was injected with 70 ng/µl pRF4(*rol-6[su1006]*) into *otEx331* and *lad-2(hd31);otEx331* to generate *Ex(P*$_{mir\text{-}48}$*::mab-20;rol-6[su1006])*.

***plx-2* rescue.** 10 ng/µl pLC456 was injected with 70 ng/µl pRF4(*rol-6[su1006]*) into *plx-2(ev773);otEx331* to generate *Ex(P*$_{lad\text{-}2}$*::plx-2)*.

Phenotypic analysis of SMD, PLN, SDQR, and SDQL axons

Young adult animals were mounted on 2% agarose pads and scored for axon defects using fluorescence microscopy. SMD axonal migration was observed using the integrated *P*$_{glr\text{-}1}$*::gfp* transgene *rhIs4[lil]*. The SMD axon was scored as a mutant if it failed to extend posteriorly in a direct path. PLN, SDQR, and SDQL axons were observed using the extrachromosomal *P*$_{lad\text{-}2}$*::gfp* transgene *otEx331*. The PLN axon was scored as a mutant if it migrated back toward the posterior end of the animal; the SDQR axon was scored as a mutant if it migrated ventrally; and the SDQL axon was scored as a mutant if it migrated ventrally or exhibited a bipolar phenotype. Three sample sets were analyzed for each genetic strain, where, on average, n = 100 for each sample set (see corresponding legends for specifics on n for each experiment). Statistical significance was calculated using the t test to compare the proportion of abnormalities between two genetic strains. Images of all the axon guidance phenotypes were taken with a confocal microscope (Eclipse E800; Nikon) and processed with the EZ-C1 viewer Gold 3.2 software (Nikon). The numerical aperture of the 40× objective lens is 1.30.

Cell culture and transfection

HEK293T cells were maintained in DME (Mediatech, Inc.) with 10% newborn bovine serum. HEK293T cells were transfected with LipofectAMINE 2000 (Invitrogen) according to the standard procedure provided by the manufacturer. 40 h after transfection, cells were collected and washed with PBS.

Coimmunoprecipitation (Co-IP) assays

200–500 µl of cell lysate was incubated with NETN buffer (20 mmol/liter Tris, pH 8, 100 mmol/liter NaCl, 1 mmol/liter EDTA, and 0.5% NP-40) containing a Myc antibody at 4°C for 4 h followed by an incubation with 20 µl of protein A/G beads (Santa Cruz Biotechnology, Inc.) for 2 h or overnight. The beads were washed three times with NETN lysis buffer.

Western blot analysis and reagents

Cell lysates were prepared in NETN buffer containing 1 mmol/liter NaF, 2.5 mmol/liter β-glycerophosphate, and a protease inhibitor cocktail (Roche). Protein concentrations were determined with the Bio-Rad protein assay (Bio-Rad Laboratories). Cell lysates were resolved by SDS-PAGE and electrophoretically transferred to nitrocellulose membrane. Membranes were blocked in PBST (137 mmol/liter NaCl, 2.7 mmol/liter KCl, 10 mmol/liter Na_2HPO_4, 2 mmol/liter KH_2PO_4, and 0.1% Tween 20) containing 5% milk for at least 40 min. Blots were probed with primary antibodies followed by horseradish peroxidase–conjugated anti–mouse or anti–rabbit secondary antibody (Jackson ImmunoResearch Laboratories). Blots were then developed on film using an enhanced chemiluminescence kit (Thermo Fisher Scientific) according to the manufacturer's instructions. The primary antibodies used included anti-FLAG M2 (Sigma-Aldrich), anti-Myc (9E10; Covance), and anti-LAD-2 (1622).

lad-2 RNAi

dsRNA *lad-2* RNA was generated by in vitro transcription (MEGAscript kit; Ambion) using yk394b9 as a template. 5′ dsRNA corresponds to 206–1,002 bp of *lad-2L* cDNA; 3′ dsRNA corresponds to 2,715–3,523 bp of *lad-2L* cDNA. dsRNAs were injected at a concentration of 1 mg/ml in young adult animals of respective genetic backgrounds and their progenies were scored.

Analyzing *lad-2L* transcripts

Total RNA was purified from animals of the following backgrounds: wild-type, *lad-2(hd31)*, *eri-1;lin-15;lad-2(RNAi5′)*, and *eri-1 lad-2(hd31);lin-15;lad-2 (RNAi5′)*. Reverse transcription was performed with 2 µg RNA using Superscript II reverse transcription (Invitrogen) using *lad-2*– and ama-1–specific primers. PCR was performed with the *lad-2* primers LC523 and LC524, which flank the *hd31* deletion, and the *ama-1* primers A3 and B2 as a control (Spike et al., 2001). The sequence for LC523 is 5′-CAGAATGAGAAAAACGAAACC-3′ and the sequence for LC524 is 5′-CTCAAACAATGCACTTTATATTAATG-3′.

PCR products were gel purified and sequenced to confirm that they were *lad-2L* transcripts. To compare levels of *lad-2L* transcripts among wild-type, *lad-2(hd31)*, and *lad-2(RNAi)* animals, RT-PCR was performed with the same primers with increasing cycle numbers (from 25 to 30 cycles) to evaluate the linearity of the reactions.

Online supplemental material
Fig. S1 shows LAD-2 staining with LAD-2 antibody 1622 in wild-type and *lad-2* animals. Fig. S2 shows that *RNAi*-hypersensitive animals in an otherwise wild-type or *lad-2(hd31)* background that, when treated with *lad-2(RNAi)*, display phenotypes of similar penetrance as untreated *lad-2(hd31)* animals. Online supplemental material is available at http://www.jcb.org/cgi/content/full/jcb.200704178/DC1.

We thank Alan Coulson, Yoji Kohara, Joseph Culotti, and Shin Takagi for various reagents, including cDNAs and strains; the Japanese National Bioresource Project for *lad-2* alleles; the Caenorhabditis Genetic Center for strains used in this study; and the University of Minnesota *C. elegans* community for intellectual exchange. We thank John Yochem, Ann Rougvie, and David Greenstein in particular for experimental and editorial advice.

W. Zhang is supported by the University of Minnesota grant-in-aid award (20631). This work was supported in part by the Max Planck Society, a Deutsche Forschungsgemeinschaft grant (within Sonderforschungsbereich 488) to H. Hutter, a Natural Science and Engineering Research Council of Canada grant (RGPIN/312498-2006) to H. Hutter, and a National Institutes of Health grant (R01-NS045873) to L. Chen.

Submitted: 30 April 2007
Accepted: 5 December 2007

References

Adler, C.E., R.D. Fetter, and C.I. Bargmann. 2006. UNC-6/Netrin induces neuronal asymmetry and defines the site of axon formation. *Nat. Neurosci.* 9:511–518.

Aurelio, O., D.H. Hall, and O. Hobert. 2002. Immunoglobulin-domain proteins required for maintenance of ventral nerve cord organization. *Science.* 295:686–690.

Bielenberg, D.R., C.A. Pettaway, S. Takashima, and M. Klagsbrun. 2006. Neuropilins in neoplasms: expression, regulation, and function. *Exp. Cell Res.* 312:584–593.

Brenner, S. 1974. The genetics of *Caenorhabditis elegans*. *Genetics.* 77:71–94.

Castellani, V., A. Chedotal, M. Schachner, C. Faivre-Sarrailh, and G. Rougon. 2000. Analysis of the L1-deficient mouse phenotype reveals cross-talk between Sema3A and L1 signaling pathways in axonal guidance. *Neuron.* 27:237–249.

Castellani, V., J. Falk, and G. Rougon. 2004. Semaphorin3A-induced receptor endocytosis during axon guidance responses is mediated by L1 CAM. *Mol. Cell. Neurosci.* 26:89–100.

Chang, A.J., N. Chronis, D.S. Karow, M.A. Marletta, and C.I. Bargmann. 2006. A distributed chemosensory circuit for oxygen preference in *C. elegans*. *PLoS Biol.* 4:e274.

Chang, C., C.E. Adler, M. Krause, S.G. Clark, F.B. Gertler, M. Tessier-Lavigne, and C.I. Bargmann. 2006. MIG-10/lamellipodin and AGE-1/PI3K promote axon guidance and outgrowth in response to slit and netrin. *Curr. Biol.* 16:854–862.

Chen, L., B. Ong, and V. Bennett. 2001. LAD-1, the *Caenorhabditis elegans* L1CAM homologue, participates in embryonic and gonadal morphogenesis and is a substrate for fibroblast growth factor receptor pathway–dependent phosphotyrosine-based signaling. *J. Cell Biol.* 154:841–855.

Chilton, J.K. 2006. Molecular mechanisms of axon guidance. *Dev. Biol.* 292:13–24.

Cohen, N.R., J.S. Taylor, L.B. Scott, R.W. Guillery, P. Soriano, and A.J. Furley. 1998. Errors in corticospinal axon guidance in mice lacking the neural cell adhesion molecule L1. *Curr. Biol.* 8:26–33.

Coulson, A., R.H. Waterston, J.E. Kiff, J.E. Sulston, and Y. Kohara. 1988. Genome linking with yeast artificial chromosomes. *Nature.* 335:184–186.

Dalpe, G., L.W. Zhang, H. Zheng, and J.G. Culotti. 2004. Conversion of cell movement responses to Semaphorin-1 and Plexin-1 from attraction to repulsion by lowered levels of specific RAC GTPases in *C. elegans*. *Development.* 131:2073–2088.

Dalpe, G., L. Brown, and J.G. Culotti. 2005. Vulva morphogenesis involves attraction of plexin1-expressing primordial vulva cells to semaphorin 1a sequentially expressed at the vulva midline. *Development.* 132:1387–1400.

Falk, J., A. Bechara, R. Fiore, H. Nawabi, H. Zhou, C. Hoyo-Becerra, M. Bozon, G. Rougon, M. Grumet, A.W. Puschel, et al. 2005. Dual functional activity of semaphorin 3B is required for positioning the anterior commissure. *Neuron.* 48:63–75.

Finney, M., and G.B. Ruvkun. 1990. The *unc-86* gene product couples cell lineage and cell identity in *C.elegans*. *Cell.* 63:895–905.

Fujii, T., F. Nakao, Y. Shibata, G. Shioi, E. Kodama, H. Fujisawa, and S. Takagi. 2002. *Caenorhabditis elegans* PlexinA, PLX-1, interacts with transmembrane semaphorins and regulates epidermal morphogenesis. *Development.* 129:2053–2063.

Ginzburg, V.E., P.J. Roy, and J.G. Culotti. 2002. Semaphorin 1a and semaphorin 1b are required for correct epidermal cell positioning and adhesion during morphogenesis in *C. elegans*. *Development.* 129:2065–2078.

Hao, J.C., T.W. Yu, K. Fujisawa, J.G. Culotti, K. Gengyo-Ando, S. Mitani, G. Moulder, R. Barstead, M. Tessier-Lavigne, and C.I. Bargmann. 2001. *C. elegans* slit acts in midline, dorsal-ventral, and anterior-posterior guidance via the SAX-3/Robo receptor. *Neuron.* 32:25–38.

Huber, A.B., A.L. Kolodkin, D.D. Ginty, and J.F. Cloutier. 2003. Signaling at the growth cone: ligand-receptor complexes and the control of axon growth and guidance. *Annu. Rev. Neurosci.* 26:509–563.

Ikegami, R., H. Zheng, S.H. Ong, and J. Culotti. 2004. Integration of semaphorin-2A/MAB-20, ephrin-4, and UNC-129 TGF-beta signaling pathways regulates sorting of distinct sensory rays in *C. elegans*. *Dev. Cell.* 6:383–395.

Jansen, G., E. Hazendonk, K.L. Thijssen, and R.H. Plasterk. 1997. Reverse genetics by chemical mutagenesis in *Caenorhabditis elegans*. *Nat. Genet.* 17:119–121.

Kenwrick, S., A. Watkins, and E. De Angelis. 2000. Neural cell recognition molecule L1: relating biological complexity to human disease mutations. *Hum. Mol. Genet.* 9:879–886.

Kim, S., X.C. Ren, E. Fox, and W.G. Wadsworth. 1999. SDQR migrations in *Caenorhabditis elegans* are controlled by multiple guidance cues and changing responses to netrin UNC-6. *Development.* 126:3881–3890.

Klostermann, A., M. Lohrum, R.H. Adams, and A.W. Puschel. 1998. The chemorepulsive activity of the axonal guidance signal semaphorin D requires dimerization. *J. Biol. Chem.* 273:7326–7331.

Koppel, A.M., and J.A. Raper. 1998. Collapsin-1 covalently dimerizes, and dimerization is necessary for collapsing activity. *J. Biol. Chem.* 273:15708–15713.

Kruger, R.P., J. Aurandt, and K.L. Guan. 2005. Semaphorins command cells to move. *Nat. Rev. Mol. Cell Biol.* 6:789–800.

Li, M., M.W. Jones-Rhoades, N.C. Lau, D.P. Bartel, and A.E. Rougvie. 2005. Regulatory mutations of mir-48, a *C. elegans* let-7 family MicroRNA, cause developmental timing defects. *Dev. Cell.* 9:415–422.

Lim, Y.S., S. Mallapur, G. Kao, X.C. Ren, and W.G. Wadsworth. 1999. Netrin UNC-6 and the regulation of branching and extension of motoneuron axons from the ventral nerve cord of *Caenorhabditis elegans*. *J. Neurosci.* 19:7048–7056.

Liu, L.X., J.M. Spoerke, E.L. Mulligan, J. Chen, B. Reardon, B. Westlund, L. Sun, K. Abel, B. Armstron, G. Hardiman, et al. 1999. High-throughput isolation of *Caenorhabditis elegans* deletion mutants. *Genome Res.* 9:859–867.

McIntire, S.L., R.J. Reimer, K. Schuske, R.H. Edwards, and E.M. Jorgensen. 1997. Identification and characterization of the vesicular GABA transporter. *Nature.* 389:870–876.

Nakamura, F., R.G. Kalb, and S.M. Strittmatter. 2000. Molecular basis of semaphorin-mediated axon guidance. *J. Neurobiol.* 44:219–229.

Nakao, F., M.L. Hudson, M. Suzuki, Z. Peckler, R. Kurokawa, Z. Liu, K. Gengyo-Ando, A. Nukazuka, T. Fujii, F. Suto, et al. 2007. The PLEXIN PLX-2 and the ephrin EFN-4 have distinct roles in MAB-20/Semaphorin 2A signaling in *Caenorhabditis elegans* morphogenesis. *Genetics.* 176:1591–1607.

Pujol, N., P. Torregrossa, J.J. Ewbank, and J.F. Brunet. 2000. The homeodomain protein CePHOX2/CEH-17 controls antero-posterior axonal growth in *C. elegans*. *Development.* 127:3361–3371.

Quinn, C.C., D.S. Pfeil, E. Chen, E.L. Stovall, M.V. Harden, M.K. Gavin, W.C. Forrester, E.F. Ryder, M.C. Soto, and W.G. Wadsworth. 2006. UNC-6/netrin and SLT-1/slit guidance cues orient axon outgrowth mediated by MIG-10/RIAM/lamellipodin. *Curr. Biol.* 16:845–853.

Roy, P.J., H. Zheng, C.E. Warren, and J.G. Culotti. 2000. *mab-20* encodes Semaphorin-2a and is required to prevent ectopic cell contacts during epidermal morphogenesis in *Caenorhabditis elegans*. *Development.* 127:755–767.

Sasakura, H., H. Inada, A. Kuhara, E. Fusaoka, D. Takemoto, K. Takeuchi, and I. Mori. 2005. Maintenance of neuronal positions in organized ganglia by SAX-7, a *Caenorhabditis elegans* homologue of L1. *EMBO J.* 24:1477–1488.

Sieburth, D., Q. Ch'ng, M. Dybbs, M. Tavazoie, S. Kennedy, D. Wang, D. Dupuy, J.F. Rual, D.E. Hill, M. Vidal, et al. 2005. Systematic analysis of genes required for synapse structure and function. *Nature.* 436:510–517.

Spike, C.A., J.E. Shaw, and R.K. Herman. 2001. Analysis of *sm-1*, a gene that regulates the alternative splicing of *unc-52* pre-mRNA in *Caenorhabditis elegans*. *Mol. Cell. Biol.* 21:4985–4995.

Sulston, J.E., and H.R. Horvitz. 1977. Post-embryonic cell lineages of the nematode, *Caenorhabditis elegans*. *Dev. Biol.* 56:110–156.

Sulston, J.E., E. Schierenberg, J.G. White, and J.N. Thomson. 1983. The embryonic cell lineage of the nematode *Caenorhabditis elegans*. *Dev. Biol.* 100:64–119.

Wang, R.F., and S.R. Kushner. 1991. Construction of versatile low-copy-number vectors for cloning, sequencing and gene expression in *Escherichia coli*. *Gene*. 100:195–199.

Wang, X., J. Kweon, S. Larson, and L. Chen. 2005. A role for the *C. elegans* L1CAM homologue *lad-1/sax-7* in maintaining tissue attachment. *Dev. Biol.* 284:273–291.

White, J.G., E. Southgate, J.N. Thomson, and S. Brenner. 1986. The structure of the nervous system of the nematode *Caenorhabditis elegans*. *Philosophical Transactions of the Royal Society of London. Series B, Biological Sciences*. 314:1–340.

Zallen, J.A., B.A. Yi, and C.I. Bargmann. 1998. The conserved immunoglobulin superfamily member SAX-3/Robo directs multiple aspects of axon guidance in *C. elegans*. *Cell*. 92:217–227.